Impact of ERK signaling and its spatial regulation on cisplatin sensitivity in ovarian cancer cells

Dissertation

zur

Erlangung des Doktorgrades (Dr. rer. nat.)

der

Mathematisch-Naturwissenschaftlichen Fakultät

der

Rheinischen Friedrich-Wilhelms-Universität Bonn

vorgelegt von

Shahana Dilruba

aus

Dhaka, Bangladesch

Bonn 2019

Angefertigt mit Genehmigung der Mathematisch-Naturwissenschaftlichen Fakultät der
Rheinischen Friedrich-Wilhelms-Universität Bonn

Erstgutachter: PD Dr. Ganna Vasylivna Staal geb. Kalayda
Zweitgutachter: Prof. Dr. Ulrich Jaehde

Tag der Promotion: 16.07.2019
Erscheinungsjahr: 2019

Acknowledgement

It is a pleasure for me to have this opportunity to express my sincere thanks to those who have contributed to this doctoral thesis in various ways. First, I would like to thank Prof. Dr. Ulrich Jaehde for giving me the opportunity to work in his vibrant group. It was an amazing experience to work in this group. Discussing with him I could always find a solution to my problems on scientific and technical issues, which helped me to progress my work successfully.

My special gratitude to PD Dr. Ganna Staal nee, Kalayda for accepting me as her PhD student. I especially thank her for her dedicated supervision throughout the thesis work. Her door was always open to guide me even within her busy schedule. I thank her for her invaluable advice and support in various scientific and technical aspects, which was a great encouragement for me to continue my work. Her input and comments on the documentation obviously improved the quality of my writing.

I would like to thank PD Dr. Anke Schiedel for showing her interest in my work, helping me always whenever I required during my PhD work and also Prof. Christa E. Müller for giving me the permission to use her lab facilities. I am grateful to Dr. Anke Schiedel for her acceptance to act as co-examiner of my PhD examination.

I would like to thank Prof. Dr. Dieter Fürst for his acceptance to act as an external co-examiner in my PhD examination committee.

I am grateful to BMBF-BIGS-Drugs for giving me the one-year scholarship for my PhD research.

I would like to thank Dr. Navin Sarin and Dr. Maximilian Kullmann for their support in lab during the beginning of my PhD thesis. My special thanks to the three master students Tharsii Kirschmann, Vanessa Buffa and Alessia Grondana. Working with them in lab and knowing them personally was an amazing experience. I would like to thank Anna Krüger and Sophie Möltgen for their support, whenever I required. Thanks to my office mates Corinna Jansen and Dr. Melanie Kulick for always being nice and friendly.

My special thanks to Dr. Elisabetta De Filippo and Dr. Dominik Thimm for their help and support regarding the retroviral transfection.

My sincere gratitude to Prof. Dr. Naoto T. Ueno of MD Anderson Cancer Center, Houston, Texas for giving me the chance to visit his working group, the time he gave me during my visit to MD Anderson, his prompt reply to all my emails and for his valuable

suggestions regarding my project. I would like to thank Dr. Xuemei Xie for her continuous support and help during my stay in USA and our ever-lasting friendship made within a very short period of time.

I would like to thank the whole AK Jaehde for giving me a comfortable and friendly environment to work.

I am grateful to all my family members for always being there for me and my beloved husband Rizvi for continuous mental support and my son Rodoleen for all his sacrifices that he made unknowingly for my work and giving me the exact idea of my strength and energy level.

For my Mother

Beware of anything which is not approved by your conscience

Leo Tolstoy

Table of Contents

Abbreviations

A2780	Human ovarian carcinoma cell line
A2780cis	Cisplatin-resistant human ovarian carcinoma cell line
ANOVA	Analysis of variance
ARE	Anti-oxidant response element
ATM	Ataxia telangiectasia mutated
ATP	Adenosine triphosphate
ATP7A	Copper-transporting P-type adenosine triphosphatase 7A
ATP7B	Copper-transporting P-type adenosine triphosphatase 7B
BCA	Bicinchoninic acid
BSA	Bovine serum albumin
CaMKII	Calmodulin kinase II
CRC	Colorectal carcinoma
CSC	Cancer stem cell
CTR1	Copper transporter 1
DAPI	4´, 6-diamidino-2-phenylindole
DAPK	Death-associated protein kinase
DED	Death effector domain
DISC	Death-inducing signaling complex
DMSO	Dimethyl sulfoxide
DANN	Deoxyribonucleic acid
DTT	Dithiothreitol
EC_{50}	50% of effective concentration
ERK1/2	Extracellular signal-regulated kinase 1/2
FADD	Fas-associated death domain protein
FCS	Fetal calf serum
GAPDH	Glyceraldehyde 3-phosphate dehydrogenase
GNB1	Guanine nucleotide binding protein β1
GPCR	G-protein-coupled receptor
GSH	Glutathione
HA	Influenza hemagglutinin
HCC	Hepatocellular carcinoma cell
HCl	Hydrochloric acid
HRP	Horseradish peroxidase
LB	Lysogeny broth
MAPK	Mitogen-activated protein kinase

MEK1/2	Mitogen-activated protein kinase kinase 1/2
MMR	Mismatch repair
mRNA	Messenger RNA
MRP2	Multidrug resistance protein
MTT	3-(4,5-Dimethylthiazol-2-yl)-2,5-diphenyltetrazolium bromide
N	Number of replicates
NER	Nucleotide excision repair
NES	Nuclear export signal
Nrf2	Nuclear factor erythroid 2-related factor 2
n.s.	Not significant
PCR	Polymerase chain reaction
p-ERK1/2	Phosphorylated extracellular signal-regulated kinase 1/2
PKC	Protein kinase C
PLD1	Phospholipase D1
PVDF	Polyvinylidene fluoride
QC	Quality control
RISC	RNA-induced silencing complex
RNA	Ribonucleic acid
RNAi	RNA interference
SCLIP	SCG10-like protein
SDS	Sodium dodecyl sulfate
SDS-PAGE	Sodium dodecyl sulfate polyacrylamide gel electrophoresis
SEM	Standard error of the mean
siRNA	Small-interfering RNA
SKOV-3	Human ovarian adenocarcinoma cell line
TBS	Tris-buffered saline
TBS-T	Tris-buffered saline with Tween®-20
TEMED	Tetramethylethylenediamine
TNF-α	Tumor necrosis factor-α
TRAIL	TNF-α-related apoptosis-inducing ligand
UGT1A	UDP-glucuronosyltransferase superfamily 1A

1. Introduction

1.1 Ovarian cancer

Ovarian cancer is the leading cause of death from gynecological malignancies with estimated 65,697 new cases and 41,448 deaths per year in Europe [1]. Patients with early-stage ovarian cancer have an 80–95 % survival rate, but the survival rate drops dramatically to 10–30% in patients with advanced-stage ovarian cancer [2]. Because very few ovarian cancers are detectable at an early stage, understanding the molecular mechanisms of tumor development is crucial for the design of more efficient treatment. Epithelial ovarian cancer is the most common type, accounting for 85% to 90% of all ovarian cancers. Currently, no specific biomarkers have been identified for an early detection of ovarian cancer; the only known biomarker currently in use is CA125, a protein produced in large amounts in 80% of ovarian cancer cases, having a drawback that it is also produced in benign conditions such as endometriosis, pregnancy, and liver disease [3].

1.2 Ovarian cancer treatment

The standard of care for patients with advanced ovarian cancer comprises primary maximal debulking surgery and a platinum-based chemotherapy. While most patients initially respond to treatment and achieve a clinical remission, nearly 80% die within five years. Platinum-based drugs have been used to treat ovarian cancer since the late 1970s and cisplatin- followed by carboplatin-based combinations has been the standard of care for over 15 years. The combination of cisplatin with paclitaxel was shown to be more efficient than cisplatin and cyclophosphamide [4] and by 2003, it was evident that carboplatin and paclitaxel were equivalent to cisplatin and paclitaxel [5,6]. As most patients relapse and ultimately succumb to ovarian cancer, new strategies are urgently required to improve survival. Ongoing research includes gene therapy, immunotherapy, targeted therapy, and novel chemotherapeutic agents. Since the prevalence of ovarian cancer stem cells (CSCs) is associated with recurrence in early-stage ovarian cancer [7], these approaches not only aim at the bulk population but also at the CSCs.

1.3 Cisplatin: mechanisms of action and drug resistance (modified from Dilruba et al., 2016, [8])

Cisplatin is one of the most potent antitumor agents known to date, which has a strong effect against a wide variety of solid tumors including ovarian cancer. Its cytotoxicity is believed to be mediated by its interaction with DNA to form DNA adducts, primarily intrastrand crosslink adducts, which initiate several signal transduction pathways, among others involving Ataxia Telangiectasia Mutated (ATM) protein, p53, p73, and mitogen activated protein kinases (MAPK), and terminate in the initiation of apoptosis. DNA damage-mediated apoptotic signals can be diminished, and the resistance that follows is a major restraint of cisplatin-based chemotherapy [9].

The mechanisms of cisplatin resistance have been classified into pre-target (i.e., those interfering with cisplatin transport prior to DNA binding), on-target (repair of Pt-DNA lesions), post-target (cellular events taking place after DNA platination) and off-target (alterations in signaling pathways not directly engaged by cisplatin but interfering with cisplatin-induced proapoptotic events) [10].

Cisplatin had been long presumed to enter the cells by passive diffusion as its uptake is concentration-dependent and non-saturable. However, copper transporter 1 (CTR1), was found to play an important role in the uptake of cisplatin as well. CTR1 is a transmembrane protein involved in copper homeostasis [11,12]. $Ctr1^{-/-}$ (CTR1-deficient) mouse embryonic fibroblasts accumulated much less cisplatin than their wild-type variants and were several times more resistant to the drug [13]. Downregulation of CTR1 is frequently observed in cisplatin-resistant cells [14]. Low levels of CTR1 correlated with poor therapeutic response in non-small cell lung cancer patients [15]. On the other hand, copper-extruding P-type ATPases, ATP7A and ATP7B, were found to contribute to cisplatin transport as well. Detailed studies showed that ATP7A sequesters cisplatin in vesicular structures inhibiting further distribution of the drug, while ATP7B is responsible for cisplatin efflux [12,16]. These transporters were reported to be upregulated in cisplatin-resistant cancer cells [17], and patients with high levels of ATP7A and ATP7B had significantly poor overall survival [15, 18]. Other transporters were found to be involved, too. For instance, inhibition of Na^+,K^+-ATPase leads to a decrease in cisplatin accumulation, and the transporter is downregulated in cisplatin-resistant ovarian cancer cells [19]. Recently, the loss of LRRC8A and LRRC8D subunits of the heteromeric volume-regulated anion channels (VRACs) was shown to be linked with resistance to cisplatin [20].

Once inside the cells, where the chloride concentration is much lower (4-20 mM) than in the bloodstream (100 mM), cisplatin is hydrolyzed yielding monoaqua $[Pt(NH_3)_2Cl(H_2O)]^+$ and diaqua complexes $[Pt(NH_3)_2(H_2O)_2]^{2+}$ [21]. Cytoplasmic nucleophiles such as glutathione (GSH), metallothioneins and other cysteine-rich proteins bind to these reactive species. Consequently, cytoplasmic antioxidant reserves decrease resulting in the oxidative stress in cells. The amount of available reactive cisplatin depletes due to these nucleophilic scavengers, thus contributing to cisplatin resistance. High levels of glutathione or glutathione-S-transferase, an enzyme facilitating cisplatin coupling to GSH, were observed in cisplatin-resistant cells [10]. Platinum-glutathione conjugates are readily excreted out of the cells by multidrug resistance protein MRP2, a member of the ABC family ATPases. Thus, MRP2 also mediates cisplatin resistance by upregulating the efflux of drug [22] (Figure 1).

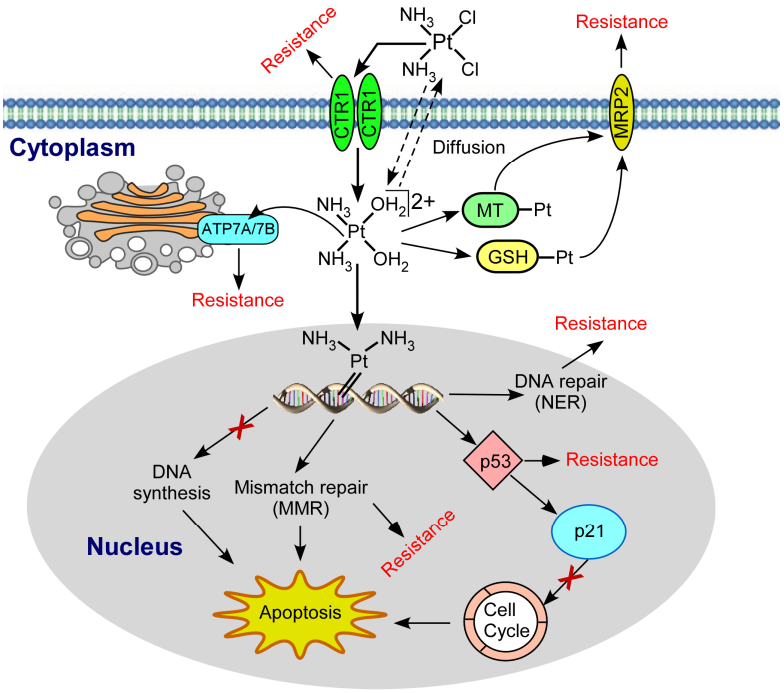

Figure 1: Representation of the mechanisms of action of cisplatin and the resistance against this drug [8].

The reactive platinum species also interact with nucleophilic centers on purine bases of DNA, in particular, N7 positions of guanosine and adenosine residues. The two reactive sites of the active platinum species permit the formation of a cross-link between two adjacent guanines. In addition, platinum can coordinate to guanine bases of different DNA strands to form interstrand cross-links. The intrastrand 1,2-d(GpG) cross-linking

induces a significant distortion in the DNA double helix [23]. This DNA lesion, which is assumed to largely account for cisplatin cytotoxicity, is recognized by cellular proteins leading to the repair, replication bypass or initiation of apoptosis. Several protein families are involved in the recognition of Pt-DNA adducts including non-histone chromosomal high-mobility group proteins 1 and 2 (HMG1 and HMG2), nucleotide excision repair (NER) proteins and mismatch repair (MMR) proteins. HMG proteins are mainly involved in gene regulation and chromatin structure. HMG1 and HMG2 recognize intrastrand DNA adducts between adjacent guanines changing cell cycle events and subsequently inducing apoptosis [24]. HMG proteins also contribute to cisplatin cytotoxicity by shielding platinum-DNA adducts from repair [25]. On the contrary, NER is the pathway employed by cancer cells for removal of platinum-DNA adducts and for DNA damage repair. A cellular defect in this pathway resulted in hypersensitivity to cisplatin and the restoration of this pathway reversed the process [26]. On the other hand, enhanced NER activity is associated with cisplatin resistance [10]. Mismatch repair (MMR) protein complex tries to repair DNA damage, but after failing to do so, it induces apoptosis. Downregulation or mutation of MMR genes is consistently documented in the context of cisplatin resistance [27]. Another protein family, poly (ADP-ribosylated proteins) (PARP), involved in base excision repair, is getting attention, as PARP are highly expressed and constitutively hyperactivated in cisplatin-resistant cells [28].

DNA damage initiates the signal transduction pathways that eventually lead to apoptosis. Post-target resistance develops from defects in the signaling pathways as well as from problems with the cell death execution machinery itself. Among a plethora of signaling pathways triggered by DNA damage, mitogen-activated protein kinases (MAPK) are of particular interest for its diverse function in modulating cell death machineries. MAPK are a family of structurally-related serine/threonine protein kinases that coordinate various extracellular stimuli to regulate cell growth and survival [29-31]. There are three major subfamilies of MAPK: extracellular signal-regulated kinase (ERK1 and 2), stress-activated protein kinase (SAPK)/c-Jun N-terminal kinase (JNK) and p38 MAPK.

The inactivation of tumor suppressor p53 plays a pivotal role in the mechanisms of post-target resistance, as it is the case in half of the human neoplasms [32]. HMG1 and HMG2 facilitate the binding of p53 to DNA to induce the transactivation of several target genes involved in cell cycle progression (p21), DNA repair and apoptosis (Bax). Ovarian cancer patients with a wild-type p53 have a higher probability of recovering following cisplatin-based therapy than the patients with mutations in this protein [33].

Moreover, testicular neoplasms are particularly sensitive to cisplatin since they almost lack mutated p53 [34]. The impact of the off-target mechanisms to cisplatin resistance is increasingly recognized. For example, overexpression of the ERBB2 protooncogene (also known as HER-2) encoding a member of epidermal growth factor receptor (EGFR) family was found to be associated with resistance to cisplatin in non-small cell lung cancer patients [10].

1.4 Extracellular signal-regulated kinase 1/2 (ERK1/2)

Extracellular stimuli such as growth factors, cytokines, mitogens, hormones and oxidative or heat stress [35] trigger a signal by interacting with a multimolecular complex of receptors such as receptor tyrosine kinases (RTKs) and G protein-coupled receptors (GPCRs). EGFR receptors transmit the signals, activate Ras and initiate the interaction with a wide range of downstream effector proteins, including isoforms of the serine/threonine kinase Raf [36]. The binding of Ras to Raf, a MAPK kinase kinase (MAPKKK), results in a conformational change of Raf increasing its kinase activity or providing the proper environment for Raf signaling [37-39]. Once activated, MAPKs primarily phosphorylate a multitude of target substrates on serine or threonine residues followed by a proline residue, and regulate cellular activities ranging from gene expression, mitosis, embryogenesis, cell differentiation, movement, metabolism and programmed cell death.

MEK1/2 activation by Raf leads to the phosphorylation of threonine and tyrosine residues of ERK1 and ERK2 (referred to as ERK1/2) with the recognition sites Thr-Glu-Tyr (TEY) [40-43]. ERK1 and ERK2 are homologous isoforms that share the same substrate specificity in vitro [44-46]. These 44- and 42-kDa proteins that phosphorylate a multitude of protein substrates [47, 48] share 85% of amino acid identity with much greater similarity in the core regions and are expressed in almost all tissues [49]. Owing to a high sequence homology, the MEK1 and MEK2 kinases, as well as ERK1 and ERK2, have been considered as redundant isoforms [50]. However, these proteins can also carry out specific functions [51]. For example, a predominant role of MEK1 over MEK2 and ERK2 over ERK1 was highlighted by gene inactivation experiment in mice. MEK1 or ERK2 knockout is lethal at the embryonic stage of mice development, while MEK2$^{-/-}$ or ERK1$^{-/-}$ mice are viable, fertile and appear normal [52-55]. A specific function of MEK1 and ERK2 in the proliferation of various cancer cell lines, including HCC cells was also shown by RNA interference experiments [56-59]. It has been hypothesized that both isoforms ERK1 and ERK2 could participate in cell

proliferation, but at different rates, related to their expression level [60, 61]. The relative level of protein expression between the two isoforms could thus account for the apparent specificity of the kinase in some cell lines [62].

In resting conditions, ERK is anchored in the cytoplasm by its association with MEK [63], the microtubule network [64] or with phosphatases, which contain a nuclear export signal (NES) [65]. Upon stimulation, ERK1/2 becomes phosphorylated at threonine and tyrosine residues and the latter results in the separation of ERK1/2 from MEK1/2. Then ERK1/2 translocates to the nucleus by passive diffusion of the monomer [66], active transport of the dimer [67], or by a direct interaction of ERK1/2 with the nuclear pore complex [68-70]. Upon translocation to the nucleus, activated ERK1/2 phosphorylates the ternary complex factors Elk-1, Sap-1a, and TIF-IA [71-73]. Phosphorylation of Elk-1 enhances transcription of growth-related proteins, such as c-Fos [74].

The first protein to be identified as cytoplasmic sequesters of ERK1/2 was its upstream activator MEK1/2 [63]. However, this protein is not the only retaining molecule, because the number of MEK molecules is significantly lower than that of ERK molecules in most cells. ERK1/2 is retained in the cytoplasm by a large number of scaffold proteins such as Sef1, MAPK phosphatases (MKP1), PEA-15 and tubulin. Sef resides on the Golgi apparatus, it binds the MEK/ERK complex and permits signaling to cytosolic substrates but not nuclear targets [75]. PEA-15 binds ERK1/2, stops its nuclear translocation, and blocks the phosphorylation of Elk-1 [76]. MKP1 contains a nuclear export signal and retains nonstimulated ERK1/2 in the cytoplasm [65]. Death-associated protein kinase (DAPK) was isolated from HeLa cells as a mediator of interferon-gamma (IFNγ) induced cell death [77]. DAPK sequesters ERK1/2 in the cytoplasm by interacting with it. DAPK-ERK interplay promotes the proapoptotic function of DAPK [78] (Figure 2).

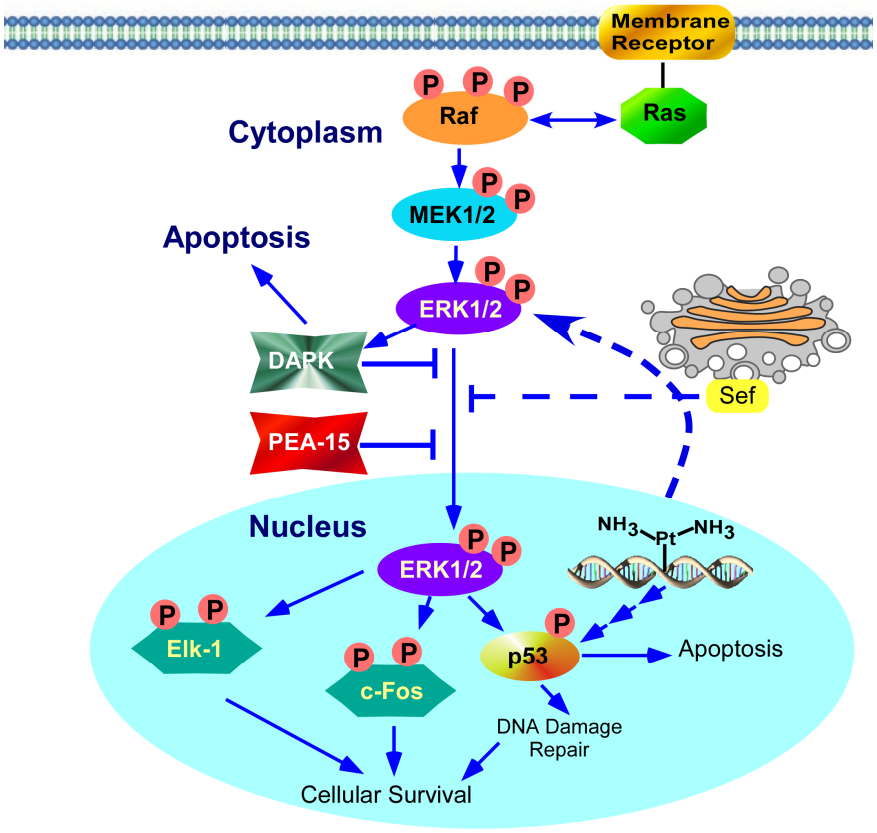

Figure 2: Mechanism of cisplatin-mediated ERK1/2 activation and overview of its subcellular localization.

Cisplatin binds to DNA and forms inter- and intrastrand cross-links, which inhibit DNA replication. ERK1/2 is activated in response to DNA and cellular damage. Upon activation ERK1/2 translocates to the nucleus to activate the survival genes e.g. Elk-1 and c-fos. ERK1/2 also have cytoplasmic targets e.g. DAPK, Bcl2-associated death promoter (BAD). However, ERK1/2 can also be retained in the cytoplasm by binding to scaffold proteins e.g. Sef, PEA-15, DAPK.

p53 plays a pivotal role in the regulation of cell cycle and initiation of apoptosis. One study reported that ERK directly phosphorylates p53 on Ser-15 [79]. Another study showed that overexpression of wild-type p53 results in ERK activation [80] with ATM kinase activation induced by the DNA damage response pathway as the possible underlying mechanism. ATM kinase could in turn lead to ERK activation, conforming with the observation that ERK activation depends on ATM after DNA damage [81].

1.5 ERK1/2 activation and cell proliferation

Cisplatin has been shown to cause activation of ERK in several cell types despite the controversies whether activation of ERK prevents or contributes to cisplatin-induced cell death [82-88]. ERK is assumed to function as a prosurvival protein in ovarian cancer [79], melanoma [89], cervical cancer SiHA [90], human myeloid leukemic [91], and gastric cancer [92] cells. In ovarian cancer inhibition of ERK1/2 by PD98059 (a chemical inhibitor of MEK1/2) was shown to inhibit the phosphorylation of Ser 15 of p53, thereby the accumulation of p53 was reduced, which is required for cellular survival upon cisplatin exposure [79]. In cervical cancer cells (SiHA) inhibition of MEK/ERK pathway by PD98059 enhanced the activation of cisplatin-mediated NF-κB, leading to decreased cisplatin sensitivity [90]. Inhibition of ERK1/2 by U0126 led to diminished cisplatin-DNA adducts formation and intracellular peroxide accumulation in human myeloid cells [91]. ERK1/2 inhibitor PD98059 attenuated the expression of glutathione-S-transferase-pi (GSTP1) in human gastric carcinoma cells. GSTP1 belongs to the superfamily of detoxifying enzymes involved in the repair of DNA damage and responsible for developing cisplatin resistance in many cell lines [92].

Cisplatin activated ERK2 in both OVCAR-3 and OVCAR-3/CDDP cells. High basal phospho-ERK2 (p-ERK2) was detected in the nuclei of OVCAR-3/CDDP cells. P-ERK2 accumulated at the early stage of cisplatin treatment in OVCAR-3/CDDP cells, while in the nuclei of OVCAR-3 cells p-ERK2 was marginally detected. Pre-treatment of OVCAR-3 cells with phorbol 12-myristate 13-acetate (PMA), an activator of ERK1/2, diminished cisplatin sensitivity. Pre-treatment of OVCAR-3/CDDP cells with U0126, increased the sensitivity to cisplatin, which rationalized the fact that high basal nuclear p-ERK2 is associated with cisplatin resistance of ovarian cancer OVCAR-3 cells [93].

Upon activation by the MAPK kinase MEK1 and/or MEK2, the MAPK ERK1 and ERK2 are translocated into the nucleus and phosphorylate a plethora of downstream targets determining cell fate. MEK1, MEK2 and ERK1 and ERK2 are no longer considered as redundant forms due to their high sequence homology. They were proved to have specific functions in cells [51]. Guégan et al. showed that ERK1 plays a predominant role over ERK2 in determining cisplatin-mediated cell death in hepatocellular carcinoma cells (Huh-7). Silencing ERK1 protected cells from clinically relevant dose of cisplatin by downregulating Noxa expression. Noxa is a critical mediator of cisplatin cytotoxicity. ERK2 silencing increased cisplatin sensitivity by enhancing

ERK1 expression [94]. However, in this work only cisplatin sensitive cells were examined, so the role of ERK1 and ERK2 in cisplatin resistance remains unclear.

1.6 Regulation of PEA-15 protein

Phosphoprotein Enriched in Astrocytes PEA-15 is a small cytosolic protein, ubiquitously expressed and highly conserved among mammals [95-97], further referred to as PEA-15. It is involved in the regulation of several cellular functions, including glucose metabolism, cell proliferation, apoptosis and survival [98]. It has an N-terminal death effector domain (DED) and a C-terminal tail with irregular structure. PEA-15 lacks enzymatic activity and serves as a molecular adaptor [99]. PEA-15 is a scaffold protein, modulating signaling pathways relevant to many human diseases such as cancer and type 2 diabetes [100, 101]. Its expression is elevated in different tumors, including human glioma and mammary carcinomas [102, 103] and in several tumor cell lines derived from human larynx, cervix and skin tumors [104, 103]. PEA-15 functions either as a tumor promoter or as a tumor suppressor, regulating both proliferation and apoptosis [105].

PEA-15 has two phosphorylation sites at Ser104 and Ser116 and is preferentially phosphorylated by protein kinase C (PKC) at Ser104 or by calcium/calmodulin-dependent protein kinase II (CaMKII) or Akt at Ser116 [106, 96, 107] (Figure 3). Phospholipase Cγ1 activates both PKC and CaMKII. PEA-15 acts as an anchor of ERK1/2 by sequestering it in the cytoplasm, preventing subsequent translocation into the nucleus. PEA-15 can bind both ERK1/2 and phosphorylated ERK1/2 with equal affinity [108]. PEA-15 phosphorylation releases ERK1/2 resulting in its translocation to the nucleus and activation of the nuclear transcription factor, Elk-1, as well as other transcription factors which promotes proliferation of the cell. PEA-15 contains a death effector domain (DED), which upon phosphorylation at Ser116 by CaMKII or Akt stimulates the binding of Fas-associated death domain protein (FADD) [109,110]. The binding of PEA-15 and FADD prevents FADD-mediated activation of caspases and the formation of the death-inducing signaling complex (DISC) [109, 111-113] resulting in an inhibition of apoptosis (Figure 3).

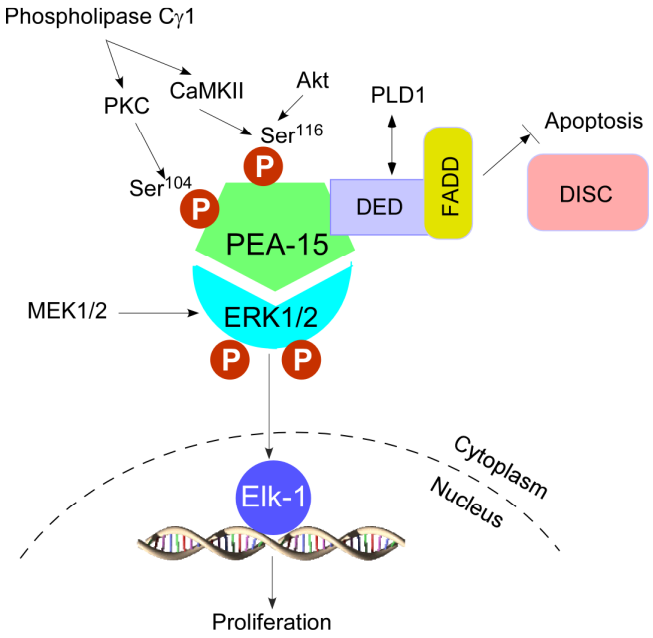

Figure 3: PEA-15 plays a pivotal role in proliferation and apoptosis (modified from Greig et al., 2014) [114].

The DED of PEA-15 also interacts with phospholipase D1 (PLD1). PLD1 phosphorylates phosphatidylcholine to phosphatidic acid. DED can block the extracellular signal-regulated kinase 1/2 (ERK1/2)-mediated H-Ras suppression of integrin activation [97] (Figure 3).

One of the major cellular functions of PEA-15 is its action as a cytoplasmic “anchor” for ERK1/2 [76]. PEA-15 regulates the outcome of ERK1/2 signaling by binding to and sequestering it in the cytoplasm. As PEA-15 has a nuclear export sequence, it is almost exclusively confined to the cytoplasm [76]. PEA-15-mediated sequestration of ERK1/2 in cytoplasm suppresses tumorigenicity in ovarian cancer by diminishing the activity of Elk-1 [115]. In another study conducted by Bartholomeusz et al, PEA-15 was overexpressed in low-PEA-15-expressing cells and the expression of PEA-15 was analyzed in an annotated tissue microarray of tumor samples from primary epithelial ovarian cancer. The analysis revealed that PEA-15 expression inhibited cell proliferation by autophagy involving ERK1/2 activation and that women with high-PEA-15-expressing tumors survived longer than those with low-PEA-15-expressing tumors [116].

Bartholomeusz et al. investigated the role of PEA-15 in ERK-targeted therapy in clear cell carcinoma (CCC). EGFR tyrosine kinase inhibitor erlotinib and MEK inhibitor selumetinib (AZD6244) individually inhibit cell proliferation of EGFR-overexpressing CCC cell lines through partial dependence on the MEK/ERK pathway [117]. Silencing

PEA-15 expression rendered selumetinib-sensitive cells resistant, implying that PEA-15 contributes to selumetinib sensitivity.

PEA-15 function was also investigated in malignant glioma cells and colorectal carcinoma (CRC) cells. In malignant glioma cells, PEA-15 induced the activation of ERK1/2 and JNK. JNK activation was mediated by the phosphorylated PEA-15 only. JNK increased autophagy in glioma cells and rendered the cells more resistant to adverse stimuli like starvation or ionizing radiation [118]. Funke et al. found that PEA-15 positive colorectal carcinoma patients have longer tumor specific survival time. Overexpression of PEA-15 in several CRC cells resulted in reduced clonogenecity, proliferation and invasiveness. These effects were mediated by a PEA-15-dependent down-regulation of integrin $\alpha v\beta 5$ as well as by elevated levels of the phosphorylated MAP kinase ERK1/2. Moreover, PEA-15 overexpression protected cells from cytotoxic drugs like 5-fluorouracil, cisplatin via the death ligand called TNF-α related apoptosis inducing ligand (TRAIL) [119].

The functions of PEA-15 are tightly regulated by its phosphorylation status [98]. The impact of PEA-15 phosphorylation was investigated by Lee et al. [120] in ovarian cancer tissue samples revealing that tissues from patients with ovarian cancer were significantly more likely than adjacent normal tissues to express PEA-15 phosphorylated at both sites. The authors used the phosphomimetic and non-phosphorylatable PEA-15 mutants where the two serine residues of PEA-15 at 104 and 116 positions were replaced by two aspartic acid (PEA-15DD) and two alanine (PEA-15AA) residues, respectively. PEA-15AA was found to have more antitumorigenic effect in ovarian cancer than did phosphomimetic PEA-15. PEA-15AA inhibited the migration capacity of cells and angiogenesis in vivo by inhibiting the expression and nuclear translocation of β-catenin [120].

To study the influence of PEA-15 phosphorylation on paclitaxel sensitivity in ovarian cancer, PEA-15AA and PEA-15DD were overexpressed in SKOV-3.ip1, OVTOKO and HEY cells. All of the cells showed enhanced sensitivity to paclitaxel when phosphomimetic PEA-15DD was overexpressed, while nonphosphorylatable PEA-15AA augmented resistance to paclitaxel. cDNA microarray analysis revealed that SCLIP (SCG-10 like protein), a microtubule destabilizing protein, is involved in PEA-15DD-mediated paclitaxel sensitization in ovarian cancer cells. PEA-15DD overexpression instigated reduced expression and posttranslational modification of SCLIP following paclitaxel treatment. This phenomenon impaired the microtubule-

destabilizing effect of SCLIP, thereby promoting induction of mitotic arrest and apoptosis by paclitaxel [121]. The influence of PEA-15 on cisplatin sensitivity in ovarian cancer cells has not been studied to date. The phosphorylation status of PEA-15, which is a key regulating factor of PEA-15 function has also not been explored in the context of cisplatin sensitivity yet.

2. Aims and objectives

Development of resistance to cisplatin is a big obstacle in the treatment of ovarian cancer. MAPK is an important multidimensional signaling pathway activated by cisplatin within the cell and influences the wide variety of downstream signaling targets contributing to apoptosis or cellular survival. One way to potentiate cisplatin effect and to combat the development of drug resistance is a combination therapy targeting cellular signaling pathways involved in drug action.

The aim of this work has been to investigate the influence of MAPK signaling, in particular ERK1/2, in the context of cisplatin sensitivity and resistance to the drug in ovarian cancer cells and to explore the prospect of a small scaffold protein PEA-15 as a cytoplasmic anchor of ERK1/2 in sensitizing ovarian carcinoma to cisplatin in vitro. For this purpose, the following objectives were perused:

1. Inhibition of MEK1/2 with a chemical inhibitor U0126 and investigating its effect on cisplatin sensitivity in ovarian cancer cells;
2. Silencing ERK1 and ERK2 individually in cisplatin-resistant cells by siRNA-mediated knockdown and assessing its effect on cisplatin sensitivity;
3. Studying the influence of phosphorylation status of PEA-15 protein on cisplatin sensitivity in ovarian cancer cells;
4. Analyzing the genes influenced by the overexpression of different mutant forms of PEA-15 in SKOV-3 cells in order to rationalize the impact of PEA-15 phosphorylation status in the context of cisplatin sensitivity.

3. Materials and methods

3.1. Chemicals, reagents and kits

Chemicals	Company
30% Acrylamide	Carl Roth GmbH & Co. KG, Karlsruhe, Germany
All-trans-retinoic acid	Sigma-Aldrich GmbH, Steinheim, Germany
Ammonium persulfate (APS)	Carl Roth GmbH & Co. KG, Karlsruhe, Germany
Benzamidine	AppliChem GmbH, Darmstadt, Germany
BCA protein assay kit (Novagen®)	Merck KGaA, Darmstadt, Germany
Bromophenol blue	AppliChem GmbH, Darmstadt, Germany
CASY® ton, isotonic diluting solution	Schärfe System, Reutlingen, Germany
Clariom™ S assay, human	Thermo Fisher Scientific, Darmstadt, Germany
Cispaltin	Sigma-Aldrich GmbH, Steinheim, Germany
4′,6-diamidino-2-phenylindole (DAPI)	Thermo Fisher Scientific, Darmstadt, Germany
Dimethylsulfoxide (DMSO)	Sigma-Aldrich GmbH, Steinheim, Germany
Disodium hydrogen phosphate dihydrate	Honeywell GmbH, Seelze, Germany
Dithiothreitol (DTT)	Thermo Fisher Scientific, Darmstadt, Germany
ERK1 antibody (Rabbit polyclonal)	Santa Cruz Biotechnology, Heidelberg, Germany
ERK1/2 antibody (Rabbit polyclonal)	Santa Cruz Biotechnology, Heidelberg, Germany
Ethanol 96-100 % (V/V)	VWR International, Radnor, USA
Fetal calf serum (FCS)	PAN-Biotech™ GmbH, Aidenbach, Germany
Fluoromount™ aqueous mounting medium	Sigma-Aldrich GmbH, Steinheim, Germany
GAPDH antibody (rabbit polyclonal)	Genetex, Irvine, CA, USA
GNB1 antibody (mouse monoclonal)	Santa Cruz Biotechnology, Heidelberg, Germany
Goat anti-rabbit antibody (IgG-HRP)	Southern Biotech, Birmingham, AL, USA
Goat anti-mouse antibody (IgG-HRP)	Jackson ImmunoResearch Europe Ltd., Cambridgeshire, UK
Glycerol	AppliChem GmbH, Darmstadt, Germany
Glycerolphosphate	AppliChem GmbH, Darmstadt, Germany
Glycine	AppliChem GmbH, Darmstadt, Germany

Chemicals	Company
HA antibody (mouse monoclonal)	Covance Inc., Denver, PA, USA
HiPure Plasmid Filter Midiprep kit	Invitrogen, Darmstadt, Germany
Hydrochloric acid 37% (m/V)	Merck KGaA, Darmstadt, Germany
Isopropanol 100 % (V/V)	Merck KGaA, Darmstadt, Germany
K2® Transfection system	Biontex Laboratories GmbH, Munich, Germany
Leupeptin hemisulfate	Sigma-Aldrich GmbH, Steinheim, Germany
MEK1/2 inhibitor (U0126)	Selleckchem, Munich, Germany
Milk powder	Carl Roth GmbH & Co. KG, Karlsruhe, Germany
Methanol	Merck KGaA, Darmstadt, Germany
3-(4,5-dimethylthiazol-2-yl)-2,5-diphenyltetrazolium bromide (MTT)	AppliChem GmbH, Darmstadt, Germany
my-Budget RNA mini kit	Bio-Budget Technologies GmbH, Krefeld, Germany
NRF2 antibody (rabbit polyclonal)	Santa Cruz Biotechnology, Heidelberg, Germany
Nuclear/cytosol fractionation kit	Biovision Inc., Milpitas, CA, USA
PEA-15 antibody (mouse monoclonal)	Santa Cruz Biotechnology, Heidelberg, Germany
p-ERK1/2 antibody (rabbit monoclonal)	Cell Signaling Technology, Danvers, MA, USA
Penicillin-streptomycin solution	PAN-Biotech™ GmbH, Aidenbach, Germany
Pepstatin A	Sigma-Aldrich GmbH, Steinheim, Germany
PeqGOLD protein marker V	PEQLAB GmbH, Erlangen, Germany
Phenylmethylsulfonyl fluoride (PMSF)	AppliChem GmbH, Darmstadt, Germany
Pierce™ ECL Western blotting substrate	Thermo Fisher Scientific, Darmstadt, Germany
Plasmid Miniprep-Classic kit	Zymo Research, Freiburg, Germany
Potassium chloride	Sigma-Aldrich GmbH, Steinheim, Germany
Potassium dihydrogen phosphate	AppliChem GmbH, Darmstadt, Germany
RNAse-free water	Qiagen, Hilden, Germany
RPMI 1640 medium	PAN-Biotech™ GmbH, Aidenbach, Germany
Sodium azide	Merck KGaA, Darmstadt, Germany
Sodium chloride (NaCl)	Th. Geyer GmbH, Renningen, Germany
Sodium dodecyl phosphate (SDS)	Roth GmbH & Co., Karlsruhe, Germany
Sodium deoxycholate	AppliChem GmbH, Darmstadt, Germany
Sodium fluoride (NaF)	AppliChem GmbH, Darmstadt, Germany

Chemicals	Company
Sodium hydroxide (NaOH)	Sigma-Aldrich GmbH, Steinheim, Germany
Sodium orthovanadate(Na_3VO_4)	AppliChem GmbH, Darmstadt, Germany
Tetramethylethylendiamine (TEMED)	AppliChem GmbH, Darmstadt, Germany
Triton®X-100	AppliChem GmbH, Darmstadt, Germany
Tris base	AppliChem GmbH, Darmstadt, Germany
Tris hydrochloride (Tris HCl)	AppliChem GmbH, Darmstadt, Germany
Trypsin-EDTA solution	Sigma-Aldrich GmbH, Steinheim, Germany
Tween®-20	AppliChem GmbH, Darmstadt, Germany
UGT1A antibody (Mouse monoclonal)	Santa Cruz Biotechnology, Heidelberg, Germany
Ultrapure water	Pure lab Plus™ system, Elga Lab water, Celle, Germany

3.2 Composition of media, buffers, and solutions

3.2.1 RPMI medium

	Volume added
RPMI	500 ml
Fetal Calf Serum (FCS)	50 ml
Penicillin/ Streptomycin	5 ml

3.2.2 Phosphate buffered saline (PBS)

NaCl	8 g
KCl	0.2 g
$Na_2HPO_4 \times 2H_2O$	1.4 g
KH_2PO_4	0.2 g
Ultrapure water	up to 1000.0 ml
pH adjusted to 7.4 using hydrochloric acid or sodium hydroxide	

3.2.3 Cisplatin stock solution

Cisplatin	1.5 mg
Sterile Sodium Chloride solution (0.9%)	1.0 ml

3.2.4 MTT solution [5 mg/mL]

MTT	10 mg
PBS	2.0 ml

3.2.5 Cell lysis buffer

Chemicals	Amount added	Final concentration
NaCl	0.876 g	150 mM
Tris-HCl	0.788 g	50 mM
SDS	1 ml (10% SDS)	0.1%
NaF	4.2 mg	1 mM
PMSF	8.71 mg	0.5 mM
Sodium orthovanadate	0.0368 g	2 mM
NP-40 (70%)	1.429 ml	1%
Sodium deoxycholate	0.5 g	0.5%
Benzamidine	0.075 g	6.24 mM
Ultrapure water	up to 100 ml	

3.2.6 siRNA stock solution [20 µM]

siRNA against ERK1, ERK2, PEA-15	5 nmol (as provided by the supplier)
RNase-free water	250 µl

3.2.7 Solutions required for gel electrophoresis and Western blot

3.2.7.1 Ammonium persulfate (APS) solution [10%]

APS	1.0 g
Ultrapure water	1 ml

3.2.7.2 Dithiothreitol (DTT) solution [3.2 M]

DTT	49.4 g
Ultrapure water	1 ml

3.2.7.3 Loading buffer (5x)

Stacking gel buffer	2.5 ml
Glycerol	5 ml
Sodium dodecyl sulfate	0.4 g
Bromophenol blue	0.025 g

3.2.7.4 Sodium dodecyl sulfate (SDS) solution [10%]

SDS	1.0 g
Ultrapure water	10.0 ml

3.2.7.5 Stacking gel buffer (pH 6.8)

Tris base	12.11 g
Ultrapure water	100.0 ml
pH adjusted to 6.8 with concentrated hydrochloric acid	

3.2.7.6 Separating gel buffer (pH 8.8)

Tris base	12.11 g
Ultrapure water	100.0 ml
pH adjusted to 8.8 with concentrated hydrochloric acid	

3.2.7.7 Electrophoresis buffer buffer

Glycine	14.4 g
Tris base	3 g
SDS	1 g
Ultrapure water	100.0 ml

3.2.7.8 Tris-buffered saline (TBS)

NaCl	4 g
Tris base	0.6 g
Ultrapure water	500.0 ml
pH adjusted to 7.3 using concentrated hydrochloric acid	

3.2.7.9 Tris-buffered saline with Tween®-20 (TBS-T) solution

Tween®-20	1.6 ml
TBS	800.0 ml

3.2.7.10 Blocking solution

Milk powder	5 g
TBS-T solution	100.0 ml

3.2.7.11 Transfer buffer

Glycine	14.4 g
Tris base	3 g
Ultrapure water	100.0 ml
pH adjusted to 8.2 to 8.4 with concentrated hydrochloric acid	

3.2.7.12 Primary antibody dilution

Sodium azide	5 mg
BSA	400 mg
antibody (mouse/rabbit polyclonal IgG)	according to the required dilution
TBS-T solution	10.0 ml

3.2.7.13 Secondary anti-mouse/rabbit antibody solution

Milk powder	0.5 g
Anti-mouse/rabbit IgG horseradish peroxidase-conjugated antibody	according to the required dilution
TBS-T solution	10.0 ml

3.3 Important devices and instruments

Devices	Company
CASY® cell counter, Model TT	Schärfe System, Reutlingen, Germany
Centrifuge Universal 32R	Hettich GmbH & Co. KG, Tuttlingen, Germany
Centrifuge Mikro 200R	Hettich GmbH & Co. KG, Tuttlingen, Germany
Gel electrophoresis chamber	Bio-Rad Laboratories GmbH, Munich, Germany
Incubator Thermo	Thermo Electron GmbH, Dreieich, Germany
InoLab® pH level 2 pH meter	WTW GmbH, Weilheim, Germany
Innova 4200, bacterial shaker	New Brunswick Scientific, Nürtingen, Germany
Kern 770 analytical balance	Kern & Sohn GmbH, Balingen-Frommern, Germany
Kern EW analytical balance	Kern & Sohn GmbH, Balingen-Frommern, Germany
Laminar air flow work bench	Heraeus Holding GmbH, Hanau, Germany
Mini Trans-Blot® Cell	Bio-Rad Laboratories GmbH, Munich, Germany
MT Classic AB135-S analytical balance	Mettler-Toledo GmbH, Giessen, Germany
Multiskan Ascent® microplate reader	Thermo Electron GmbH, Dreieich, Germany
NanoDropTM N-1000	Thermo Fisher Scientific, Oberhausen, Germany
Nikon A1 Eclipse Ti® confocal microscope	Nikon, Kingston, UK
Purelab Plus™ system	ELGA LabWater, Celle, Germany
Shaker KS 15 control	Edmund Bühler GmbH, Hechingen, Germany
Sonicator Bandelin HD2070/UW2070	Bandelin electronic GmbH, Berlin, Germany
Thermomixer comfort	Eppendorf, Hamburg, Germany
Ultrasonic bath Sonorex® Super RK 103 H	Bandelin electronic GmbH, Berlin, Germany
Chemidoc™ XRS+ Imaging System	Bio-Rad Laboratories GmbH, Munich, Germany

3.4 Consumables

Consumables	Company
Blotting paper, 7 x 10 cm	Sigma-Aldrich GmbH, Steinheim, Germany
CASY® tubes	Schärfe System, Reutlingen, Germany
Cell culture flasks 25, 75, 175 cm^2	Sarstedt AG & Co., Nümbrecht, Germany
Cell scraper	Sarstedt AG & Co., Nümbrecht, Germany
Conical centrifuge tubes 15, 50 ml	Sarstedt AG & Co., Nümbrecht, Germany
Cover slips (round, square)	Carl Roth GmbH & Co., Karlsruhe, Germany
Cryovials	Sarstedt AG & Co., Nümbrecht, Germany
Disposable syringe (10 ml)	B. Braun Melsungen AG, Melsungen, Germany
Glass pipettes	Labomedic GmbH, Bonn, Germany
Microscope slides	Carl Roth GmbH & Co., Karlsruhe, Germany
Pasteur pipettes	Brand GmbH & Co., Wertheim, Germany
Petri dishes	Greiner Labortechnik, Frickenhausen, Germany
Pipette tips	Mettler-Toledo GmbH, Giessen, Germany
Polyvinylidene fluoride (PVDF) membrane	Carl Roth GmbH & Co.KG, Karlsruhe, Germany
Eppendorf reaction tubes (0.5, 1.5, 2 ml)	Greiner Labortechnik, Frickenhausen, Germany
Tissue culture plates, 96 wells	Sarstedt AG & Co., Nümbrecht, Germany
Tissue culture plates, 6 wells	Sarstedt AG & Co., Nümbrecht, Germany

3.5 Software

Software	Company
Ascent software (Multiskan Ex®)	Thermo Electron GmbH, Dreieich, Germany
GraphPad Prism® 6.0	GraphPad Software, San Diego, CA, USA
Image Lab® 5.1	Bio-Rad Laboratories, Munich, Germany
Microsoft Excel® 2010	Microsoft Corporation, Redmond, WA, USA
Transcriptome Analysis Console 4.1 (TAC 4.1)	Thermo Fisher Scientific, Darmstadt, Germany

3.6 Cell culture

3.6.1 Cell lines and cultivation

The ovarian carcinoma cell line A2780 and the cisplatin-resistant variant A2780cis cells were obtained from the European Collection of Cell Cultures, United Kingdom (ECCC, UK). The SKOV-3 cell line was from ATCC and was provided by Prof. Martin Michaelis (University of Kent, UK) and Prof. Jindrich Cinatl (Goethe University Hospital, Frankfurt, Germany).

Cell culture work was performed under a laminar flow bench, which was cleaned with a disinfectant before and after use. Media and solutions were pre-warmed at 37 °C prior to use. The cells were cultured in an incubator at standard conditions (37 °C with saturated humidity, 95% air and 5% CO_2). The cells were regularly investigated microscopically for contamination. Cells were cultivated to about 90% confluence and then sub-cultivated or used in experiments. Backups of each cell line suspended in FCS containing 10% DMSO were stored in liquid nitrogen. After using cells over a period of at most 12 passages they were discarded and a new backup was thawed. If a distinct number of cells was needed for an experiment, cells in a cell suspension were counted by electronic pulse area analysis using a CASY® cell counter. Distributions of cell volume and cell aggregation were assessed at the same time.

3.6.2 Mycoplasma test

A problem in cell culture is the possible contamination of cells with mycoplasma bacteria that may influence experimental results. Mycoplasma can grow on mammalian cell culture and are resistant to common antibiotics used. Cells were regularly screened for mycoplasma infections using 4′,6-diamidino-2-phenylindole (DAPI). Mycoplasma does not have a cell wall. Therefore, DAPI binds directly to the DNA of mycoplasma and can be seen in mammalian cells under a fluorescence microscope.

For a mycoplasma test, cells were seeded on microscope slides in a petri dish. After two to three days the medium was removed and the slides were washed with 5 ml of cold PBS. Then, cells were incubated with 80 µl of DAPI working solution (5 µg/ml) in 2 ml methanol for 5 minutes. Subsequently, the slide was washed with 2 ml methanol and dried in the dark. Cover slips were fixed on the slides using mounting medium. Cells were analyzed using a Nikon A1 Eclipse Ti® confocal microscope. Positively stained cells show a blue shade surrounding nuclei, indicating the stained mycoplasma DNA. No mycoplasma contaminations were detected in cell culture.

3.7 Cytotoxicity assay

The cytotoxicity of compounds was determined in different cell lines by the MTT assay. MTT is a colorimetric assay for assessing cell metabolic activity. The assay is based on the reduction of 3-(4,5-dimethylthiazol-2-yl)-2,5-diphenyltetrazolium bromide (MTT), a yellow tetrazole, to a purple formazan by mitochondrial dehydrogenases of living cells. Thus, the amount of formazan formed is proportional to the number of living cells.

For an MTT test, cells were seeded in 96-well plates at a density of 1 x 10^4 cells per well (A2780, A2780cis, SKOV-3) in 100 µl cell culture medium and allowed to attach overnight (37 °C, 5% CO_2). As protection against evaporation, the outer wells of the 96-well plate were filled with PBS only. After 24 hours, the medium was discarded and 100 µl compound (cisplatin, retinoic acid or U0126) dilutions in medium at different concentrations were added to each well. For treating the cells with two compounds, e.g. cisplatin and U0126 or cisplatin and retinoic acid, a certain dilution of the compound (20 µM U0126, 20 µM retinoic acid) was prepared in medium first. Then this medium was used for making cisplatin dilutions. Each dilution was added to cells in triplicates. The plates were incubated at 37 °C for 72 hours or 48 hours (as indicated in Result section). Then 20 µl of MTT solution (5 mg/ml) in PBS per well were added and the plates were kept in an incubator for one hour. Afterwards the supernatant was discarded and the formazan crystals were lysed by adding 100 µl DMSO per well. The plates were shaken and UV absorbance at 570 nm with background subtraction at 690 nm was measured using a Multiskan Ascent® micro titer plate reader.

The procedure described above was adapted from Mueller et al. [122] with a slight modification (formazan lysis with DMSO instead of 1:1 isopropanol and 1M HCl as described by Alley et al. [123]). Dose-effect curves were generated by non-linear regression with sigmoidal dose response, variable slope model using GraphPad Prism® (settings: no comparison, constraint: 'BOTTOM must be greater than 0.0, no weighing, consider each replicate Y value as an individual point). Effective concentration (EC_{50}: concentrations that provoke 50% of the maximal response) was calculated using GraphPad Prism®.

3.8 Protein quantification

In order to determine protein concentration in cell lysates the bicinchoninic acid assay (BCA) was used. The assay is based on the reduction of Cu^{2+} to Cu^{+} by proteins under alkaline conditions. In this assay, a purple chelate complex is formed by the

reaction of two molecules of bicinchoninic acid (BCA) with one Cu^+ ion. The absorbance of the purple chelate complex at 570 nm was determined using a UV microtiter plate reader. Protein concentration was calculated using a calibration curve.

3.8.1 Standards and quality control solutions for protein quantification

Standards and quality control (QC) solutions were made by diluting the 2mg/ml stock solution of bovine serum albumin (BSA) provided by the manufacturer (Table 1).

Table 1: Standards and quality control solutions for BCA assay

	BSA stock solution, volume (µl)	Water, volume (µl)	Protein concentration (µg/ml)
Standard solutions			
S1	50	1950	50
S2	75	1925	75
S3	100	1900	100
S4	200	1800	200
S5	300	1700	300
S6	400	1600	400
Quality Control solutions			
Q1	150	1850	150
Q2	250	1750	250
Q3	350	1650	350

3.8.2 BCA assay

Samples were analyzed according to the manufacturer's protocol. After dilution of samples to fit into the calibration range, 20 µl of standard solutions in triplicates, quality controls in duplicates, and samples in duplicates were pipetted into a 96-well plate. Then a mixture of 50 parts BCA working reagent A (containing BCA) and 1 part BCA working reagent B (containing $CuSO_4$) was prepared. 200 µl of this mixture was added to each well and the plate was incubated for 15 minutes at 60 °C. After 5 min of cooling down to room temperature the UV absorbance at 570 nm was determined using a Multiskan Ascent® microtiter plate reader. Linear regression of standard solution's absorbance values was performed using Microsoft Excel® 2010 and sample concentrations were calculated based on the calibration curve. The calibration was considered valid if at least four out of six standard solutions did not deviate more than 15% from the nominal value

(20% at the lower limit of quantification) and two of the three QC samples did not deviate more than 15% of the nominal value. The correlation co-efficient of the linear regression of the standard curve was accepted only when $R^2 \geq 0.99$.

3.9 siRNA-mediated transient knockdown

In order to investigate the function of a protein, silencing the gene expression is a common technique nowadays through RNA interference (RNAi). The active components of the RNAi are small interfering RNAs (siRNAs), 21-22 nucleotides long double stranded (dsRNA). These short RNAs are naturally produced by Dicer-mediated cleavage of larger dsRNAs and they contain 2 nucleotide (nt) overhang at the 3´ end, a 5´ phosphate and a 3´-hydroxyl group [124, 125]. Synthetic siRNAs (double-stranded RNA consisting of 21-25 base pairs) is inserted in to the cell by lipofection. RNAi works in two steps in cytoplasm. At first, the double stranded RNA is cleaved by the RNase II enzymes Dicer and Drosha and forms small interfering RNA (siRNA). In the second step, siRNA is loaded onto the RISC (RNA-induced silencing complex) complex. The RISC complex unwinds siRNA and the single strand siRNA then hybridizes with target mRNA. The targeted mRNA is degraded by the RNAse H enzyme (Slicer) released from RISC.

For siRNA mediated knockdown, A2780, A2780cis and SKOV-3 cells were seeded in 6-well plates at a density of 2.5×10^5 cells/well in 1 ml antibiotic-free medium. After 24 hours, siRNA directed against the protein of interest was added via lipofection. In order to evaluate the effect of the transfection procedure itself on protein expression a negative/control knockdown was performed for each experiment with a scrambled siRNA (Table 2), not targeting any specific mRNA.

Table 2: List of siRNA used for knockdown experiments

Target protein	Product name	Catalogue number	Company
ERK1	ON-TARGETplus Human MAPK3 (5595) siRNA SMARTpool	L-003592-00-0005	Dharmacon™, GE Healthcare Europe GmbH, Freiburg, Germany
ERK2	Flexitube siRNA	1027417	Qiagen, Hilden, Germany
PEA-15	ON-TARGETplus Human PEA15 (8682) siRNA SMARTpool	L-010553-00-0005	Dharmacon™, GE Healthcare Europe GmbH, Freiburg, Germany
Negative Control siRNA	siGENOME Non-Targeting siRNA	D-001210-01-05	Dharmacon™, GE Healthcare Europe GmbH, Freiburg, Germany

For mixing the siRNA and the K2® transfection reagent, medium without serum and antibiotics was used. For two wells of a 6-well plate, 10 µl of siRNA stock (20 µM) was mixed with 125 µl medium in a pre-sterilized Eppendorf tube. In another tube, 13.5 µl of transfection reagent was mixed with 125 µl of medium. Then the siRNA was mixed with the transfection reagent and incubated at room temperature for 15 minutes. The plate was gently swayed to ensure the equal distribution of the transfection complex. After 24 hours incubation at room temperature, the medium was exchanged for normal medium containing serum and antibiotics. After another 24 hours or 48 hours, the transfected cells were used for MTT tests or cell lysate preparation for Western blot.

3.10 Plasmid transfection for protein overexpression

Plasmids are small circular DNA molecules that bacteria use to transfer their genetic information. The mechanism of adding DNA plasmid to mammalian cells is known as plasmid transfection. Plasmid DNA, which is negatively charged, is complexed with cationic lipids, to efficiently deliver it to the nucleus of mammalian cells.

Lipofectamine-mediated transfection of a plasmid encoding a specific protein in mammalian cells is a widely used process for analyzing the impact of the abundance of that specific protein on cell fate in different (disease) conditions.

3.10.1 PEA-15 plasmids

Three DNA constructs of pcDNA3-HAR36 containing two mutated PEA-15 protein versions and the empty vector were received from the lab of Prof. Naoto T. Ueno (Breast Medical Oncology, MD Anderson Cancer Center, University of Texas, Houston, USA). The constructs were originally made by Prof. Dr. Joe W. Ramos [97]. The two mutated versions of PEA-15 protein were the PEA-15AA, in which two serine residues at 104 and 116 positions were replaced by two alanine (A) residues, the PEA-15DD in which the same two serine residues were replaced with aspartic acid (D). The plasmids were received as dried on filter paper from Prof. Ueno's lab. These plasmids were taken out of the filter paper by soaking with 100 µl of sterilized water. In order to produce enough plasmid DNA for transfection, plasmid DNA was amplified by chemocompetent bacteria.

3.10.2 Transformation of chemocompetent bacteria

Aliquots of chemocompetent Top 10 *E. coli* bacteria were thawed from -80 °C on ice for 30 minutes. 10-50 ng of plasmid DNA were added to the bacterial suspension, carefully mixed and incubated for 30 minutes on ice. The heat shock to produce rearrangements in the bacterial membrane was performed at 42 °C for 30 seconds and then back on ice for 2 minutes. 200 µl of LB medium were then added and the bacterial suspension was incubated for one hour at 37 °C on a shaker (300 rpm) in order to let the bacteria recover. The complete mixture was transferred on an agar plate containing the selective antibiotic and incubated overnight at 37 °C.

3.10.3 Colony screening and MiniPreps

One day after the bacteria transformation with plasmid DNA, grown clones on the agar plates were checked for the right insertion. Several colonies were randomly picked up from the agar plate and cultivated in 4 ml of LB medium supplemented with the ampicillin antibiotic overnight at 37 °C on a shaker. The next day plasmids were isolated from the bacterial culture using Plasmid Miniprep Classic kit according to the manufacturer's instruction. The isolated plasmids were then loaded on an agarose gel together with a negative control (vector without insert) to check their size. The negative control band should have a lower molecular weight than the vector ligated with the insert. The positive plasmids were then digested with the same restriction enzymes used for the insertion of the PCR product into the vector. The digestion mix is afterwards loaded into a second agarose gel where the insert should be cut out from the vector. Sequencing of the positive clones was then performed by GATC Biotech, provider of DNA

sequencing and bioinformatics for industry and academic research. The sequence obtained from GATC was examined by nucleotide BLAST. The sequences completely aligned with the source protein's (PEA-15 from Chinese Hamster Ovary) nucleotide sequence and the mutations at 104 and 116 positions remained intact.

3.10.4 Plasmid preparation by Midipreps

When high amount of plasmid DNA is required (i.e. for mammalian cell transfection), a large scale plasmid isolation needs to be performed. 50 µl of bacterial or glycerol culture was inoculated in 4 ml of LB medium with the selective antibiotic and incubated for 6-7 hours at 37 °C on the shaker. The bacterial culture was then amplified to a 100 ml culture and cultivated overnight. The next day MidiPreps were performed using HiPure Plasmid Filter MidiPrep kit according to manufacturer's protocol.

3.10.5 PEA-15 plasmids transfection in SKOV-3 cells

The plasmids were transfected into SKOV-3 cells by the following procedure. First, the concentrations of the plasmids were determined using a Nano drop analyzer. 2.5 x 10^5 cells per well in a 6-well plate were seeded in 2 ml antibiotic free medium. After 24 hours, cells were treated with 45 µL of K2® Multiplier, 2 hours before plasmid DNA transfection. The multiplier was mixed well with the medium by gently swirling the plates. The plasmids were diluted in medium without serum and antibiotics. This diluted DNA was added to the dilution of K2® transfection reagent in medium, mixed by pipetting once and incubated for 15 minutes. 270 µl of this mixture was added to each well (Table 3). Again, plates were gently swirled to assure a uniform distribution of transfection reagent. After 24 hours, the medium was replaced with the complete medium. After 48 hours, efficiency of overexpression was assessed by Western Blot. In case of an MTT test with the transfected cells, the cells were trypsinized 24 hours after the transfection, counted and seeded in a 96-well plate with a density of 1 x 10^4 cells per well in 50 µl medium. Then 50 µl of different dilutions of compounds to be tested in medium were added to each well. MTT test was performed after incubation with test compound.

Table 3: Transfection of PEA-15 plasmid DNA with K2® transfection reagent

For one well of a 6-well plate		
Medium without FCS and antibiotics	135	µl
K2® transfection reagent	10.8	µl
Medium without FCS and antibiotics	135	µl
Plasmid pcDNA3-HA/ pcDNA3-PEA-15AA/ pcDNA3-PEA-15DD	2.7	µg
Diluted DNA	135	µl
Diluted K2® Transfection reagent	135	µl
Amount Plasmid DNA used per well	2.7	µg

3.11 Cell fractionation

Nuclear/cytosol fractionation kit from BioVision was used for separating the cytosolic and the nuclear fractions of the transfected cells according to the manufacturer's protocol. All steps of the fractionation were performed on ice. To analyze the efficiency of the fractionation, Western blot was performed for each fraction (nuclear or cytosolic). As a marker for the cytosolic fraction, GAPDH was used. For nuclear fraction, Lamin B1 was used as an indicator of the purity of the fraction. Cross-contamination was assumed when the indicator was detected in the wrong fraction.

3.12 Gel electrophoresis and Western blot

Western blot was used for protein expression analysis. For Western blot, first the proteins are separated by electrophoresis through a gel matrix. Smaller proteins move faster due to the less resistance of the gel matrix. SDS (sodium dodecyl sulfate) is a detergent with a strong protein denaturing effect and binds to proteins at a constant molar ratio. In the presence of SDS and a reducing agent that cleaves disulfide bonds important for proper protein folding, proteins unfold into linear chains with negative charge proportional to the polypeptide chain length. Thus, in SDS-PAGE (sodium dodecyl sulfate polyacrylamide gel electrophoresis), SDS-treated proteins are separated based on their polypeptide length. After the separation of proteins by SDS gel electrophoresis, they are transferred to a polyvinylidene fluoride (PVDF) membrane. After the transfer, specific proteins were detected by using a primary antibody targeted for that specific protein. For visualization of the target protein, a secondary antibody against the primary antibody was used. The secondary antibody is conjugated to a

horseradish peroxidase (HRP). Proteins are detected after incubation of the membrane with luminol. HRP oxidizes luminol to produce a chemiluminescent signal. The signal is then detected by the Chemidoc™ XRS+ imaging system of BioRad. The signal is proportional to the amount of the certain protein in a sample. The analysis was performed with Image Lab™ software. Protein expressions in experiments were normalized to the expression of GAPDH, which was used as a housekeeping protein.

3.12.1 Sample preparation for SDS-PAGE

For analysis of protein expression in cells, cells were seeded in a 6-well plate at densities from 2.5 x 10^5 to 5.0 x 10^5 cells per well depending on the subsequent incubation period. Cells were treated at least 24 hours after seeding, so that the cells are all attached to the surface of the plates. After treatment, cells were washed with ice-cold PBS twice, then cell lysis buffer was added and the cells were collected with a cell scrapper. The cell suspensions were incubated on ice for 30 minutes, then sonicated with a sonicator with settings: 60% power, 5 seconds pulse, 30 seconds interval, 3 shots. After the sonication, lysates were centrifuged at 16000 rpm for 5 minutes at 4 °C. The supernatant was collected in a fresh Eppendorf tube and stored at -80 °C for later use.

3.12.2 SDS-PAGE and Western blot

Proteins were separated according to size by SDS-PAGE. Stacking and separating gels were made according to Table 4. At first the separating gel with a fixed amount of acrylamide (10% or 12%) was poured into the gel casting apparatus. The gel was overlaid immediately with 70% isopropanol. After 15 minutes, the isopropanol was discarded and stacking gel was poured on the top of the separating gel. Wells for sample loading were prepared on the top of stacking gel using a comb. After 30 minutes, the fixture containing the gels was put into the electrophoresis chamber. Then electrophoresis buffer was poured into the chamber until the gels were fully submerged in water. The combs were removed and the wells were washed with buffer. The samples were diluted with the loading buffer to a concentration range of 10-50 µg total protein in 10 µl. Samples were boiled in a heat block for 5 minutes at 95 °C for denaturation of proteins. Afterwards, the protein samples and protein marker were loaded on gel. The proteins were separated at 200 Volts for approximately 50 minutes or until the sample front reach near the end of the gel. Then the gels were taken out of the apparatus using a spatula and equilibrated in transfer buffer for 5 minutes.

Table 4: Preparation of separating gel and stacking gel

	Separating gel 10%	Separating gel 12%	Stacking gel 5%
Acrylamide [30%]	3.30 ml	3.97 ml	833 µl
Separating gel buffer	3.75 ml	3.75 ml	-
Stacking gel buffer	-	-	625 µl
Ultrapure water	2.76 ml	2.10 ml	3.445 ml
SDS [10%]	100 µl	100 µl	50 µl
TEMED*	18 µl	18 µl	5 µl
Ammonium peroxodisulfate (APS) (10%)*	70 µl	70 µl	20.8 µl

*Added shortly before casting the gel in order to initiate polymerization

PVDF membranes were activated in methanol for 20 seconds and then equilibrated in transfer buffer for 5 minutes. Afterwards the gels and the membranes were clipped in tight fixture. Electric current (100 volts for one hour) was applied to the fixture for transferring the proteins from gel to the membrane. In order to visualize several proteins on one membrane blots were cut according to the size of the proteins of interest. The membrane parts were subsequently treated with the respective antibodies.

3.12.3 Visualization of proteins

To minimize the background signals, membranes were blocked with 5% non-fat dry milk in TBS-T for one hour. Subsequently, the membranes were washed three times for 5 minutes with TBS-T. Then the primary antibody against the protein of interest (with dilutions as mentioned in Table 5) was added to the membrane and incubated overnight at 4 °C. The next day, blots were washed three times with TBS-T and a secondary antibody against the primary antibody was added. The secondary antibody was incubated for 1.5 hours, and then membrane was washed twice with TBS-T. For visualization, Pierce™ ECL Western blotting substrate was used according to the manufacturer's protocol. 500 µl of the substrate was evenly distributed on the membrane and incubated for 2 minutes at room temperature. Then the substrate was removed and the blot was placed inside the Chemidoc™ XRS+ Imaging System producing a digital image, which was densitometrically analyzed with Image Lab® software.

Table 5: Dilution of antibodies used in Western blot

Antibody	Dilution	Catalogue number
CTR1	1:1000	NB-100-402
ERK1 (G-8)	1:500	SC-271269
GAPDH	1:20000	GTX-100118
GNB1 (F-2)	1:1000	SC-515764
Goat anti-rabbit-Horseradish peroxidase (HRP) conjugate	1:2000	4030-05
HA.11 monoclonal antibody	1:500	MMS-101P
Lamin B1	1:1000	GTX-103292
Nrf2 (C-20)	1:500	SC-722
PEA-15 (H-3)	1:500	SC-166678
p-ERK1/2 (Thr202/Tyr204)	1:1000	9101
Peroxidase AffiniPure Goat Anti-Mouse IgG (H+L)	1:5000	115-035-003
UGT1A (B-4)	1:1000	SC-271268

3.13 Clariom™ S assay

Clariom™ S assay is a gene-level whole-transcriptome expression profiling assay provided by the Applied Biosystems™ [126] for a fast, simple and scalable path to determine gene level expression across the transcriptome. The assay measures gene-level expression from > 20,000 well-annotated genes. For Clariom™ S assay, SKOV-3 cells were first transfected with PEA-15 siRNA as described above to suppress all the intrinsic PEA-15 expression in SKOV-3 cells. 24 hours after siRNA transfection, the cells were washed twice with the antibiotic-free medium and transfected with PEA-15HA (empty vector, EV), PEA-15AA or PEA-15DD containing plasmids, respectively. 24 hours after transfection, cells were treated with 15 µM cisplatin (EC_{50} of cisplatin for EV-transfected cells over 48 hours) for 24 hours and then the total RNA of the cells was extracted using my-Budget RNA mini kit following the instructions provided by the manufacturer. Clariom™ S assay was performed by Life and Brain GmbH, Bonn.

The raw data of the array were collected as CEL files and analyzed using the Transcriptome Analysis Console (TAC 4.1) software. The gene expression was analyzed with the Gene Level SST-RMA (Signal Space Transformation-Robust Multi-Chip Analysis) summarization method. Data obtained from the microarrays were normalized by the robust multiarray average method [127]. A probe set was considered expressed

if ≥ 50% samples had DABG (Detected Above Background) values below DABG threshold ($p < 0.05$). Statistical significances of the differences in gene expression was analyzed using Limma [128]. Differential expression was assumed at a p-value < 0.05 and a fold change in expression > 2 or < -2.

3.14 Statistical analysis

The mean value of at least three independent experiments was determined (biological replicates). The results are presented as mean (x) and with the standard error of the mean (SEM). EC_{50} data describing the cytotoxic effect were assumed to be log-normally distributed [129]. Therefore, the negative logarithm of the EC_{50} (pEC_{50}) value was calculated. Afterwards, mean and standard error of the mean (SEM) were determined. The significance of differences was analyzed using an unpaired t-test in this case. For siRNA experiments, statistical comparisons between groups were carried out using a one-way analysis of variance (ANOVA). If a significant difference was found the Holm-Sidak post-test was used to determine which means differed. Differences were considered statistically significant in the case of $p < 0.05$.

4. Results

4.1 Effect of cisplatin on ERK1/2 signaling in ovarian cancer cells

Both ERK1 and ERK2 are activated in response to cisplatin treatment in sensitive A2780 and cisplatin-resistant A2780cis cells. In A2780 cells, p-ERK1 level increased with cisplatin concentration and had its peak after 6 hour-incubation (Figure 4A). In A2780cis cells, the increase in ERK1 phosphorylation followed a similar trend in time but was independent of concentration. The level of p-ERK1 in A2780cis cells was lower than that of A2780 cells for all experimental conditions (Figure 4A). For p-ERK2, the scenario was the opposite. That is, the p-ERK2 level was higher in A2780cis cells than in A2780 cells (Figure 4B). Also in this case, the phosphorylation extent was the highest after 6 hours in both cell lines.

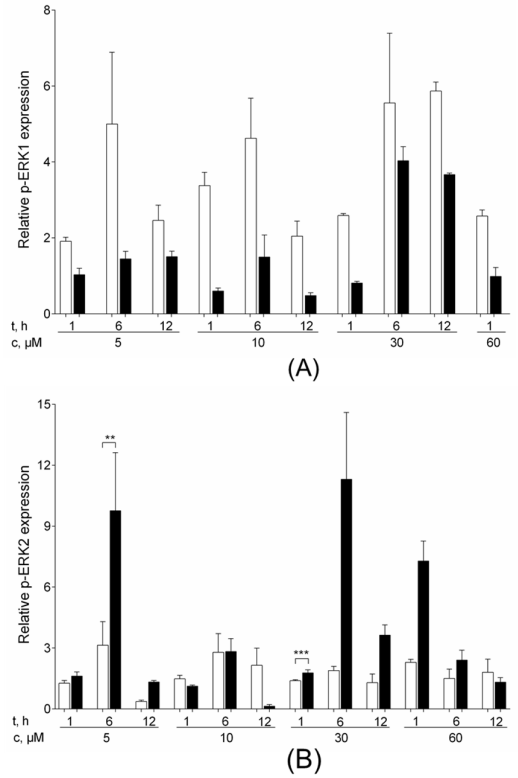

Figure 4: Densitometric analysis of p-ERK1 (A) and p-ERK2 (B) expression in A2780 (white columns) and A2780cis (black columns) cells after treating them with 5 µM, 10 µM, 30 µM, or 60 µM cisplatin for 1 hour, 6 hours, or 12 hours. GAPDH was used as loading control (mean ± SEM, n = 4). *p < 0.05, **p < 0.01, ***p < 0.001.

4.2 ERK1/2 inhibition in ovarian cancer cells

4.2.1 Inhibition of ERK1/2 activation in A2780 and A2780cis cells

As shown above, ERK1/2 is activated in response to cisplatin treatment in A2780 and A2780cis cells. In order to investigate whether the activation of ERK1/2 was required for cellular survival or apoptosis, ERK1/2 was inhibited by U0126, a potent chemical inhibitor of MEK1 and MEK2. The concentration of U0126 was chosen as 20 µM for ERK1/2 inhibition, based on the literature [130]. The efficiency of U0126 inhibition of ERK1/2 phosphorylation was assessed by Western blot. The results showed a significant decrease of p-ERK1/2 level in A2780 cells after treatment with U0126 alone compared to the untreated controls. Exposure to cisplatin increased the expression significantly, while the combination of cisplatin and U0126 reduced the level of p-ERK1/2 significantly compared to the cells treated only with cisplatin (Figure 5). In A2780cis cells, the basal level of p-ERK1/2 was very low, and although, treatment with U0126 alone led to the decrease in p-ERK1/2 level compared to the untreated controls, this difference was not statistically significant. Cisplatin exposure increased the p-ERK1/2 level in A2780cis cells significantly compared to the untreated control cells, while the combination of cisplatin and U0126 resulted in a significant reduction of ERK1/2 activation in comparison to the samples treated with cisplatin alone, as was also the case with A2780 cells (Figure 5).

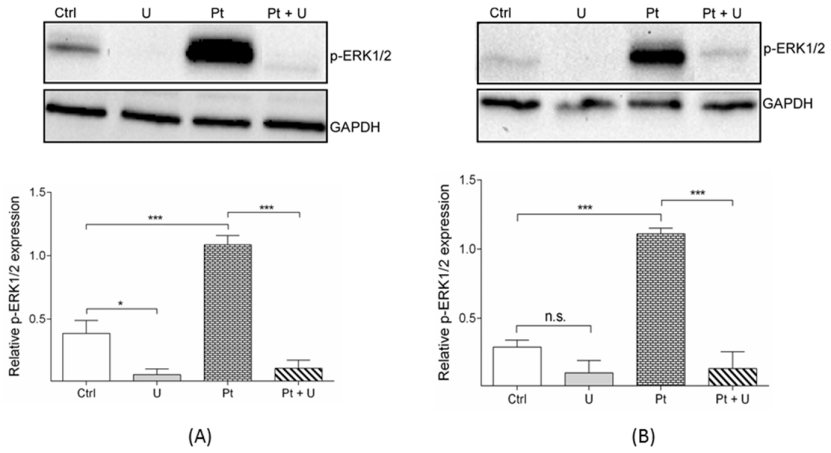

Figure 5: Representative Western blot and corresponding densitometric analysis of relative p-ERK1/2 expression (mean ± SEM, n = 3) in A2780 (A) and A2780cis cells (B): in untreated control cells (Ctrl), after treatment with 20 µM U0126 (U), 33.3 µM cisplatin (Pt), and the combination of 33.3 µM cisplatin and 20 µM U0126 (Pt + U) for 24 hours. GAPDH was used as a loading control. *$p < 0.05$, ***$p < 0.001$, n. s. = not significant.

4.2.2 Effect of MEK1/2 inhibition on cisplatin sensitivity of A2780 and A2780cis cells

U0126 was used in combination with cisplatin in order to assess the role of ERK1/2 activation in cisplatin sensitivity in A2780 and A2780cis cells. As is clear from Figure 6, co-incubation with 20 µM U0126 led to a decrease in cisplatin cytotoxicity in both A2780 (EC_{50} = 3.83 µM) and A2780cis (EC_{50} = 20.7 µM) cells compared to the cisplatin treatment alone (EC_{50} of 0.93 µM and 9.2 µM, respectively). Therefore, it can be concluded that the inhibition of ERK1/2 phosphorylation decreased sensitivity to cisplatin in A2780 and A2780cis cells, which means the activation of ERK1/2 rather contributes to cell death in A2780 and cisplatin-resistant A2780cis cells.

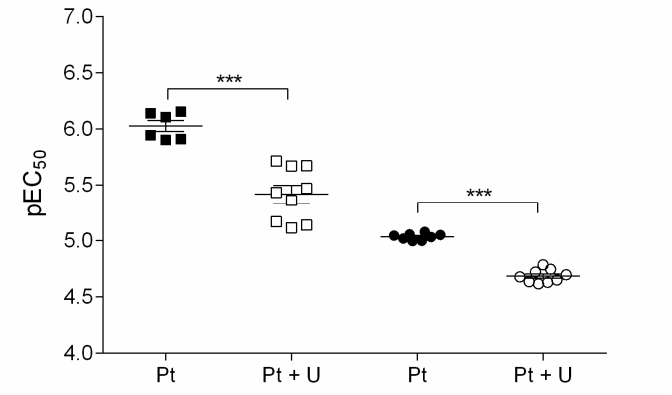

Figure 6: Cytotoxicity (pEC_{50}, mean ± SEM, n = 6-10) of cisplatin in A2780 (squares) and A2780cis (circles) cells was assessed after treating the cells for 72 hours with cisplatin only (Pt, filled symbols) and with the combination of cisplatin and 20 µM U0126 (Pt + U, open symbols). ***$p < 0.001$.

4.2.3 Inhibition of ERK1/2 activation in SKOV-3 cells

In SKOV-3 cells, the basal expression of p-ERK1/2 was very low. Cisplatin treatment for 24 hours increased the phosphorylation of ERK1/2 significantly (Figure 7).

U0126 inhibited the expression of p-ERK1/2, which was not detectable after treatment of cells with U0126 alone. This is likely due to the very low basal expression of p-ERK1/2. When the expression of p-ERK1/2 in cisplatin-treated samples and after exposure to the combination of cisplatin and U0126 was compared, a significant reduction in p-ERK1/2 expression was observed in U0126-containing samples.

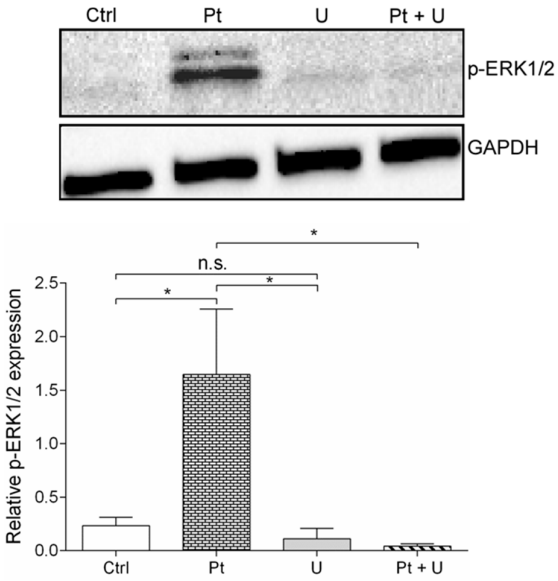

Figure 7: Representative Western blot and densitometric analysis of the relative p-ERK1/2 expression (mean ± SEM, n = 3) in SKOV-3 cells before (Ctrl) and after treatment with 20 µM U0126 (U), 16.5 µM cisplatin (Pt), and the combination of 16.5 µM cisplatin and 20 µM U0126 (Pt + U) for 24 hours. GAPDH was used as a loading control. *p < 0.05, n.s. = not significant.

4.2.4 Effect of MEK1/2 inhibition on cisplatin sensitivity of SKOV-3 cells

Inhibition of ERK1/2 phosphorylation by U0126 reduced the sensitivity to cisplatin in SKOV-3 cells. The EC_{50} value of cisplatin in SKOV-3 cell was 2.9 µM. When the cells were co-incubated with 20 µM of U0126, the EC_{50} of cisplatin increased to 18.2 µM (Figure 8).

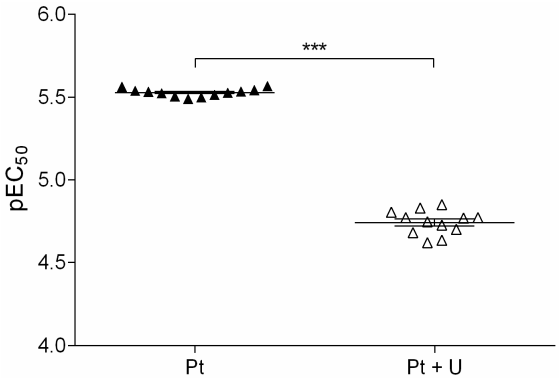

Figure 8: Cytotoxicity (pEC_{50}, mean ± SEM, n = 12) of cisplatin in SKOV-3 cells after treating them for 72 hours with cisplatin only (Pt) and with the combination of cisplatin and 20 µM U0126 (Pt + U). ***p < 0.001.

In order to investigate whether this reduction of cisplatin cytotoxicity was due to possible interaction between cisplatin and U0126, the effect of pre-incubation with U0126 on cell sensitivity to the platinum drug was investigated. Pre-treatment of SKOV-3 cells with 20 µM U0126 for 6 hours significantly increased cisplatin cytotoxicity to 7.9 µM (5.1 ± 0.038, mean $pEC_{50} \pm$ SEM, $n = 4$, $p < 0.001$) showing that the inhibition of ERK1/2 activation itself has a negative impact on cell sensitivity to the drug. It should be noted, however, that the observed reduction is not so pronounced as in the case of co-incubation. On one hand, the inhibitory effect of U0126 may be reversed after drug withdrawal, on the other hand, the interaction between cisplatin and U0126 cannot be completely ruled out.

4.3 Effect of MEK1/2 inhibition on CTR1 expression

Platinum drug resistance is a multifactorial event, which involves decreased drug accumulation, increased intracellular inactivation of platinum species, improved repair of DNA damage, and the failure of apoptotic pathways. Thus, platinum sensitivity and resistance are also regulated by the expression of transport proteins. The uptake of cisplatin was shown to be higher in A2780 cells compared to the A2780cis cells in previous studies [14]. Some transport proteins, such as copper transporter 1 (CTR1) [131], Na^+, K^+-ATPase [132], and volume-regulated anion channels (VRAC) [20] were found to mediate this process. Treatment with 20 µM U0126 over 24 hours was reported to decrease CTR1 expression in A2780 cells, while in A2780cis cells, the reduction in CTR1 expression level following U0126 exposure was not statistically significant [133]. This was associated with the lower basal level of CTR1 in A2780cis cells. Therefore, CTR1 expression was also investigated in SKOV-3 cells to examine whether the CTR1 downregulation was responsible for U0126-mediated lower sensitivity to cisplatin.

In SKOV-3 cells, after treatment with 20 µM U0126 for 24 hours, a decrease in the CTR1 expression was observed (Figure 9), but the decrease was not statistically significant when compared with the untreated cells.

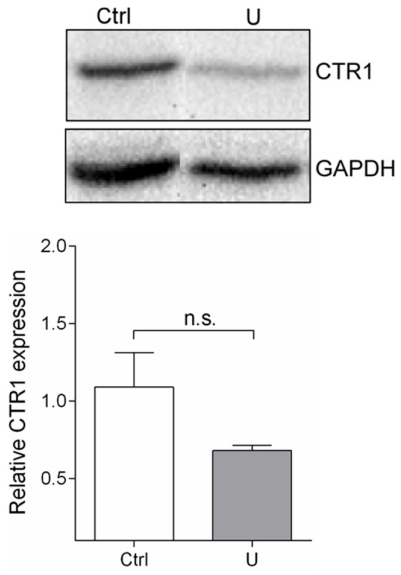

Figure 9: Representative Western blot and densitometric analysis of the CTR1 expression (mean ± SEM, n = 4) in untreated SKOV-3 cells (Ctrl) and after treatment with 20 µM U0126 (U) for 24 hours. GAPDH was used as a loading control. n. s. = not significant.

4.4 Silencing ERK1 and ERK2 in A2780 and A2780cis cells

The inhibition of ERK1/2 reduced the sensitivity to cisplatin in sensitive A2780 and cisplatin-resistant A2780cis cells, as shown above (Figure 6). Therefore, it is clear that ERK1 and ERK2 are both involved in initiating cell death. ERK1 activation in response to cisplatin treatment is stronger in A2780 cells compared to A2780cis cells, while in A2780cis cells, the level of activated ERK2 was found to be higher than that of A2780 cells (Figure 4). Thus, to address the question whether ERK1 plays rather a survival or an apoptotic role compared to ERK2, knockdown of ERK1 and ERK2 was performed independently in A2780 and A2780cis cell lines.

4.4.1 ERK1 knockdown in A2780 and A2780cis cells

The contribution of ERK1 activation to cisplatin sensitivity was assessed after a transient siRNA-mediated silencing of ERK1 in both cell lines. The efficiency of the ERK1 knockdown was evaluated by Western blot. In A2780 cells, the expression of ERK1 was reduced to 74.6% in ERK1-transfected cells compared to that of negative control although a very high concentration of ERK1 siRNA (400 pmol / well) was used for transfection (Figure 10A). ERK1 was successfully silenced into A2780cis cells, the expression level of ERK1 decreased to 35.71% compared to the negative knockdown control (Figure 10B).

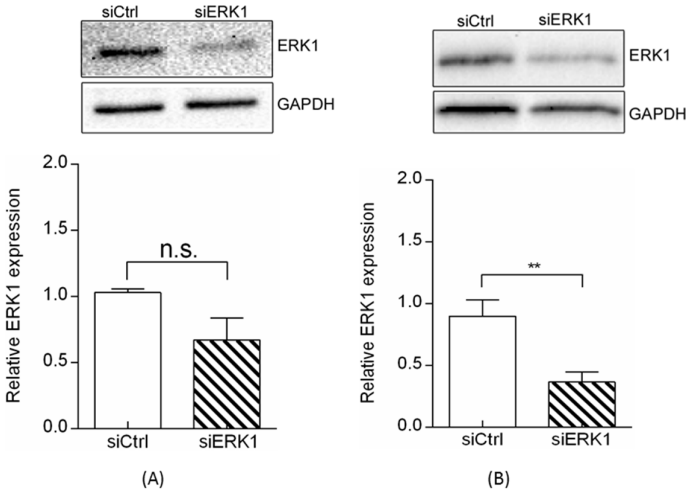

Figure 10: Representative Western blot and corresponding densitometric quantification of ERK1 expression (mean ± SEM, n = 3) in A2780 and A2780cis cells after transient transfection with ERK1 siRNA (siERK1) and negative control siRNA (siCtrl). GAPDH was used as a loading control. **p < 0.01, n.s. = not significant.

4.4.2 Cisplatin cytotoxicity after the ERK1 knockdown in A2780 and A2780cis cells

After knockdown of ERK1 in A2780 and cisplatin-resistant A2780cis cells, cytotoxicity to cisplatin was evaluated by MTT assay. The results revealed no significant difference in sensitivity to cisplatin in A2780 cells after ERK1 knockdown (2.5 µM) and negative knockdown control (2.7 µM) (Figure 11). In A2780cis cells, the EC_{50} value increased significantly after the inhibition of ERK1 expression (32.3 µM) compared to the negative knockdown cells (16 µM). That is, ERK1 inhibition augmented resistance to cisplatin in A2780cis cells (Figure 11).

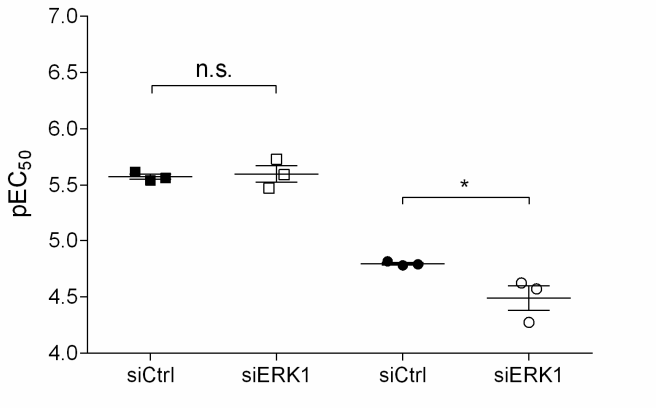

Figure 11: Cytotoxicity (pEC_{50}, mean ± SEM, n = 3-4) of cisplatin in A2780 (squares) and A2780cis cells (circles) after the ERK1 knock down (siERK1, open symbols) and negative knockdown (siCtrl, filled symbols) of cells. *$p < 0.05$, n. s. = not significant.

4.4.3 ERK2 knockdown in A2780 and A2780cis cells

The effect of ERK2 silencing on cisplatin sensitivity was determined after the transient knockdown of ERK2 using siRNA in A2780 and A2780cis cells. The efficiency of the knockdown (Figure 12) was measured by Western blot as was done for ERK1.

In A2780 cells, after knockdown with ERK2 siRNA, the remaining expression of ERK2 was 34.3% compared to that of negative control siRNA transfected cells (Figure 12A). In A2780cis cells, the knockdown of ERK2 decreased the expression to 33.9% compared to the negative control A2780cis cells (Figure 12B).

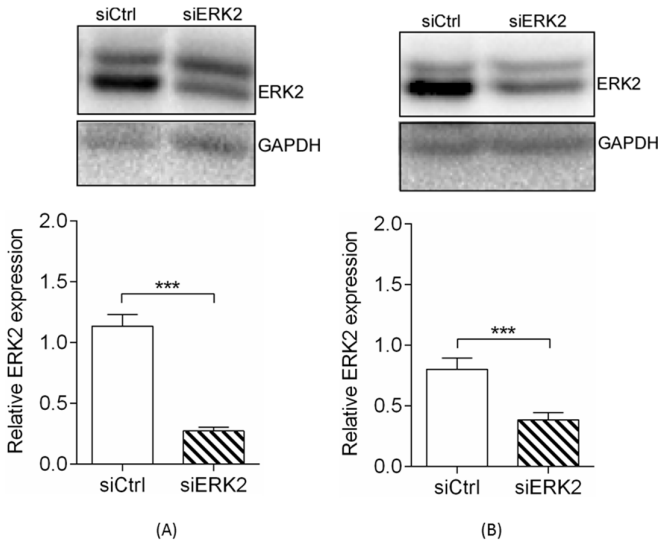

Figure 12: Representative Western blot and corresponding densitometric quantification of ERK2 expression (mean ± SEM, n = 12-15) in A2780 (A) and A2780cis cells (B) after transient transfection with ERK2 siRNA (siERK2) and negative control siRNA (siCtrl). GAPDH was used as a loading control. ***p < 0.001.

4.4.4 Cisplatin cytotoxicity after ERK2 knockdown

The cytotoxicity of cisplatin was measured by MTT assay after successful knockdown of ERK2. The results showed no significant difference in EC_{50} of cisplatin after ERK2 silencing (0.8 µM) compared to negative knockdown (0.8 µM) in A2780 cells (Figure 13). In A2780cis cells, EC_{50} for cisplatin increased to 10.56 µM after ERK2 silencing compared to the negative knockdown cells (9.68 µM). The increase in EC_{50} was statistically significant for A2780cis cells.

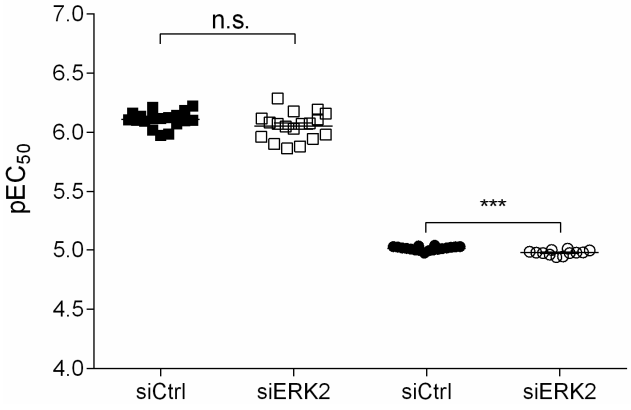

Figure 13: Cytotoxicity (pEC_{50}, mean ± SEM, n = 12-18) of cisplatin in A2780 (squares) and A2780cis cells (circles) after ERK2 knockdown (siERK2, open symbols) and negative knockdown (siCtrl, filled symbols) of cells. ***p < 0.001, n.s. = not significant.

4.5 Effect of PEA-15 protein on cisplatin sensitivity in SKOV-3 cells

Upon activation, ERK1/2 shuttles between different cellular compartments, where it acts on different target molecules [134]. The trafficking of ERK1/2 is partly controlled by a small scaffold protein PEA-15. Depending on its phosphorylation at Ser104 and Ser116, PEA-15 can sequester ERK1/2 in the cytoplasm or promote its nuclear translocation [98]. Therefore, to investigate the relevance of PEA-15 on cisplatin sensitivity, PEA-15 was silenced in SKOV-3 cells. Also, the mutated versions of PEA-15; PEA-15AA (non-phosphorylatable form) and PEA-15DD (phospho-mimetic form) were overexpressed in SKOV-3 cells and cisplatin sensitivity was investigated.

4.5.1 Effect of PEA-15 knockdown in SKOV-3 cells

PEA-15 was silenced in SKOV-3 cells by transfecting them with PEA-15 siRNA. The efficiency of the knockdown was determined by Western blot and compared with that of negative control siRNA transfected cells. After knockdown with PEA-15 siRNA, the expression of PEA-15 was significantly decreased to 22.6% (Figure 14). As is clear from the Figure 16, the sensitivity of SKOV-3 cells to cisplatin increased after knockdown of PEA-15 compared to the cells with a negative knockdown (Figure 15).

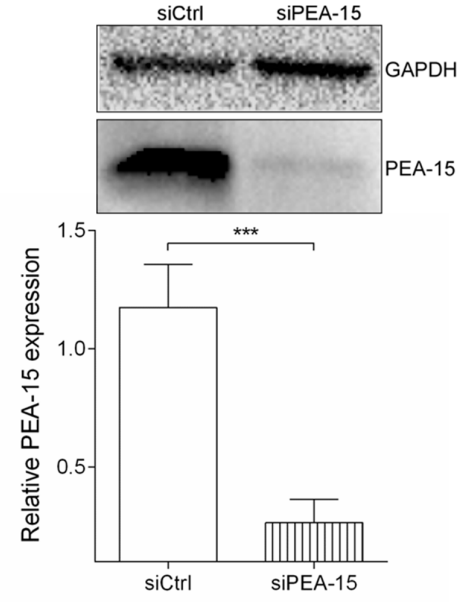

Figure 14: Representative Western blot and corresponding densitometric quantification of PEA-15 expression (mean ± SEM, n = 6-9) in SKOV-3 cells after transient transfection with PEA-15 siRNA (siPEA-15) and negative control siRNA (siCtrl). GAPDH was used as a loading control. ***p <0.001.

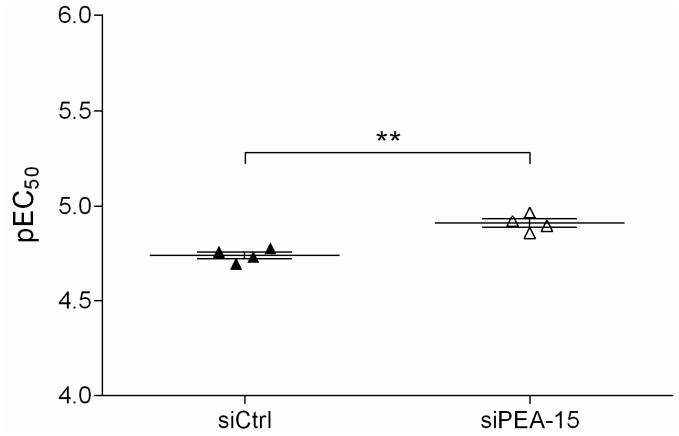

Figure 15: Cytotoxicity (pEC_{50}, mean ± SEM, n = 4) of cisplatin in SKOV-3 cells assessed by MTT test after transient transfection with PEA-15 siRNA (siPEA-15) and negative control siRNA (siCtrl). **p < 0.01.

4.5.2 Overexpressing different forms of PEA-15 protein in SKOV-3 cells

The two mutated forms of PEA-15 proteins: PEA-15AA (further AA) and PEA-15DD (further DD) were overexpressed in SKOV-3 cells by liposome-mediated transient transfection in order to analyze the influence of phosphorylation status of this protein on cisplatin sensitivity of SKOV-3 cells. The control cells were transfected with empty vector (further EV). The efficiency of the transfection was analyzed by Western blot (Figure 16). PEA-15 was knocked down by PEA-15 siRNA prior to the transfection with EV, AA, and DD in order to remove the influence of basal PEA-15. The empty vector has only HA tag without any PEA-15 protein and HA tag is not alone detectable as it has a molecular weight of 1 kDa.

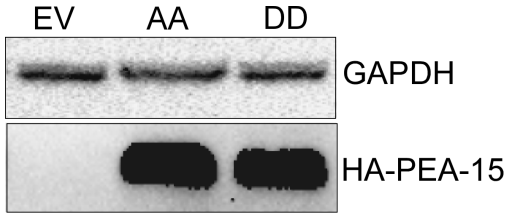

Figure 16: Representative Western blot of the empty vector (EV), PEA-15AA (AA), and PEA-15DD (DD) in the SKOV-3 cells after transient transfection with these proteins as detected by antibody against the influenza hemagglutinin (HA) tag. GAPDH was used as a loading control.

4.5.3 PEA-15AA sensitized the SKOV-3 cells to cisplatin

Following the transfection, cisplatin cytotoxicity was assessed in SKOV-3-EV (transfected with empty vector), SKOV-3-AA (transfected with PEA-15AA), and SKOV-3-DD (transfected with PEA-15DD) cells. The results of the MTT test revealed that PEA-15AA overexpression increased the sensitivity of SKOV-3 cells to cisplatin significantly compared to the empty vector transfected cells (Figure 17). The EC_{50} in SKOV-3-AA cells was decreased (EC_{50} = 9.9 µM) compared to the SKOV-3-EV cells (14.9 µM), while SKOV-3-DD cells (EC_{50} = 14.3 µM) had similar cisplatin sensitivity as the SKOV-3-EV controls.

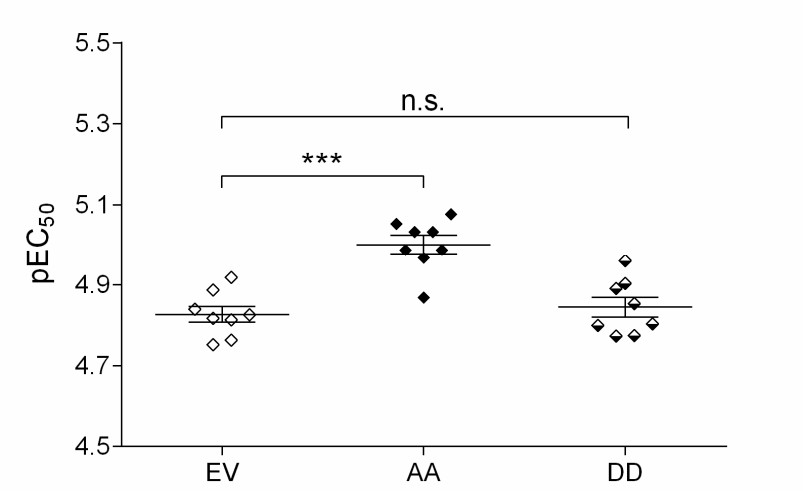

Figure 17: Cytotoxicity (pEC_{50}, mean ± SEM, n = 8) of cisplatin in SKOV-3 cells after transfection with empty vector (EV), PEA-15AA (AA), and PEA-15DD (DD). ***p < 0.001, n.s. = not significant.

4.5.4 The influence of PEA-15 phosphorylation status on ERK1/2 localization

After the successful transfection of the two mutated forms of PEA-15 protein: PEA-15AA and PEA-15DD, the transfected SKOV-3 cells were fractionated to separate the nuclear and cytosolic fractions using the Nuclear/Cytosol fractionation kit. Western blot was performed to detect the expression of p-ERK1/2 in the fractions. The result showed an overall increase of p-ERK1/2 expressions in the PEA-15 transfected cells compared to the empty vector transfected cells. Among the PEA-15 transfected cells, PEA-15AA-expressing cells had higher p-ERK1/2 expression compared to the PEA-15DD-transfected cells (Figure 18).

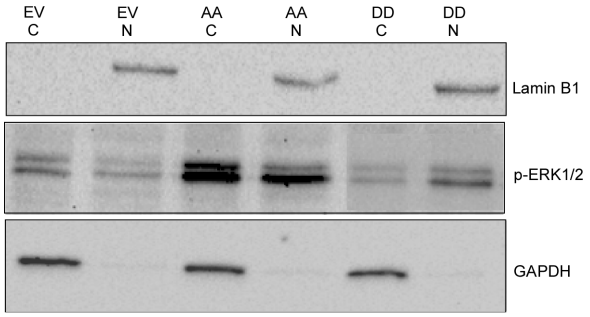

Figure 18: Representative Western blot of p-ERK1/2 expression in nuclear and cytosolic fractions of the SKOV-3 cells transfected with empty vector (EV), PEA-15AA (AA), and PEA-15DD (DD). GAPDH and Lamin B1 were used as the markers and loading controls of cytosolic (C) and nuclear fractions (N), respectively.

In SKOV-3-AA transfected cells, the cytosolic fraction had more p-ERK1/2 than the corresponding nuclear fraction, while in SKOV-3-DD cells the scenario was the opposite, that is, higher p-ERK1/2 levels were found in the nuclear fraction (Figure 18). This is the proof of concept that PEA-15 unphosphorylated at both serine residues (Ser104 and Ser116) retains p-ERK1/2 in the cytoplasm of SKOV-3 cells while the phosphomimetic PEA-15DD does not keep p-ERK1/2 in the cytoplasm, promoting an increase in p-ERK1/2 nuclear accumulation in the SKOV-3-DD cells.

4.5.5 Transcriptome analysis of SKOV-3 cells after PEA-15 transfection

SKOV-3 cells transfected with unphosphorylatable PEA-15 (PEA-15AA) were thus found to be more sensitive to cisplatin. As PEA-15 has many functions other than controlling the ERK1/2 localization e.g. autophagy, glucose metabolism, apoptosis [98]; a transcriptome-wide gene level analysis of the PEA-15-transfected cells was performed to find out the candidate genes responsible for the increased sensitivity of PEA-15AA-tansfected cells to cisplatin.

For doing the gene level whole-transcriptome expression profiling Clariom™ S solutions from Applied Biosystems™ was used [126]. Clariom™ S solutions is a small version of transcriptome wide gene level analysis platform, which covers only the well annotated genes (>20,000 genes). After PEA-15 knockdown, SKOV-3 cells were transfected with empty vector, PEA-15AA and PEA-15DD, then treated with 15 µM cisplatin for 24 hours before harvesting the cells for RNA isolation. We selected 15 µM of cisplatin that would induce cell death (as determined by MTT assay) in 50% of the SKOV-3-EV cells at 48 hours and collected samples earlier, that is, after 24 hours. We reasoned that these conditions would facilitate the study of transcriptional alterations

linked to pre-apoptotic signaling rather than to degradative phenomena that characterize end-stage cell death [10].

4.5.5.1 Differentially expressed genes in transfected cells

Clariom™ S assay was performed to analyze the differences in gene regulation among the three differently transfected SKOV-3 cells: SKOV-3-EV, SKOV-3-15AA, and SKOV-3-15DD, for untreated and cisplatin-treated cells. The genes were considered differentially expressed when the fold change was ≥ 2 and the p-value was < 0.05. The generated heat map of differentially expressed genes shows clear clustering among the differentially expressed genes between different treatment conditions (Figure 19).

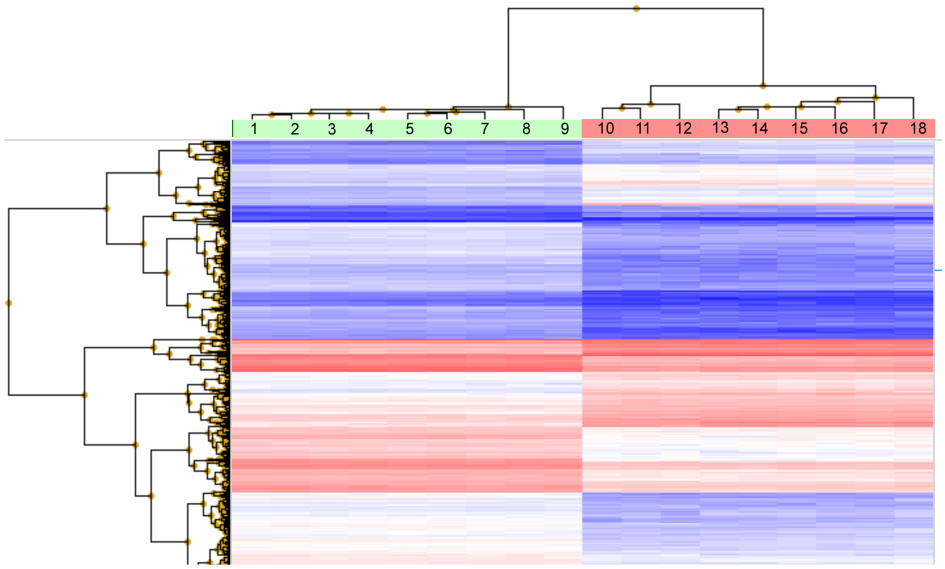

Figure 19: Heat map of the transcriptome-wide Clariom™ S array, with fold change cut-off for differentially regulated genes at 2.0 and a p-value cut-off at 0.05 for all replicates of cisplatin-treated and untreated transfected cells. Numbers above lanes indicate: 1, 3, 4: PEA-15AA-transfected, untreated; 5, 6, 7: EV transfected, untreated; 2, 8, 9: PEA-15DD-transfected, untreated; 10, 11, 17: EV-transfected, treated with 15 µM cisplatin; 12, 16, 18: PEA-15DD-transfected, treated with 15 µM cisplatin, and 13, 14, 15: PEA-15AA-transfected, treated with 15 µM cisplatin.

Little difference between SKOV-3-EV, SKOV-3-AA, SKOV-3-DD was observed, most likely because only different forms of the same protein were overexpressed in the SKOV-3 cell line.

4.5.5.2 Venn diagram of differentially expressed genes by the transfected cells

Table 6 shows the number of differentially expressed genes in EV-, PEA-15AA-, and PEA-15DD- transfected cells after cisplatin exposure and in untreated transfected

cells. Prior to cisplatin exposure, only three genes were differentially regulated between untreated SKOV-3-EV and untreated SKOV-3-AA. Between SKOV-3-EV and SKOV-3-DD, the number of differentially expressed genes were 18, while for SKOV-3-AA and SKOV-3-DD the number was 10. Following cisplatin treatment, 4430 genes were differentially regulated in EV-transfected cells, while in AA- and DD- transfected cells the numbers were 4196 and 4110, respectively (Table 6).

Table 6: Number of differentially expressed genes, compared as treatment condition 1 vs. condition 2 with at least two-fold up- or down-regulation with $p < 0.05$.

Treatment condition 1	**Treatment condition 2**	**Number of differentially expressed genes**
SKOV-3-EV, Untreated	SKOV-3- PEA-15AA, Untreated	3
SKOV-3-EV, Untreated	SKOV-3- PEA-15DD, Untreated	18
SKOV-3-PEA-15AA, Untreated	SKOV-3- PEA-15DD, Untreated	10
SKOV-3-EV, Untreated	SKOV-3-EV, 15 µM Cisplatin, 24h	4430
SKOV-3-PEA-15AA, Untreated	SKOV-3-PEA-15AA, 15 µM Cisplatin, 24h	4197
SKOV-3-PEA-15DD, Untreated	SKOV-3-PEA-15DD, 15 µM Cisplatin, 24h	4110

Venn diagram was created to analyze the exclusively regulated genes in different transfected cells. Among all three types of transfected cells, 3039 genes were differentially regulated (Figure 20). However, 717 genes were exclusively regulated after cisplatin exposure in SKOV-3-EV cells, while in SKOV-3-AA and SKOV-3-DD cells 444 genes and 383 genes respectively were differentially regulated (Figure 20).

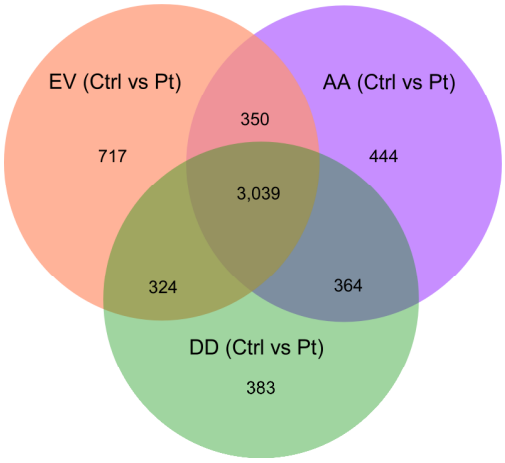

Figure 20: Venn diagram showing the total number of genes affected by cisplatin exposure in the empty vector(EV)-, PEA-15AA(AA)-, and PEA-15DD(DD)-transfected cells.

4.5.5.3 Pathway analysis for the genes exclusively regulated in SKOV-3-AA cells following cisplatin treatment

The overexpression of the non-phosphorylatable PEA-15AA improved the sensitivity of SKOV-3 cells to cisplatin. From the Venn diagram (Figure 20), 444 genes were found to be exclusively differentially regulated in SKOV-3-AA cells upon cisplatin exposure. To investigate the biological pathways, which were affected by these exclusive genes, pathway analysis was done based on Wikipathways. In total, 21 pathways were affected significantly within this set of genes in SKOV-3-AA cells in response to cisplatin treatment (Figure 21).

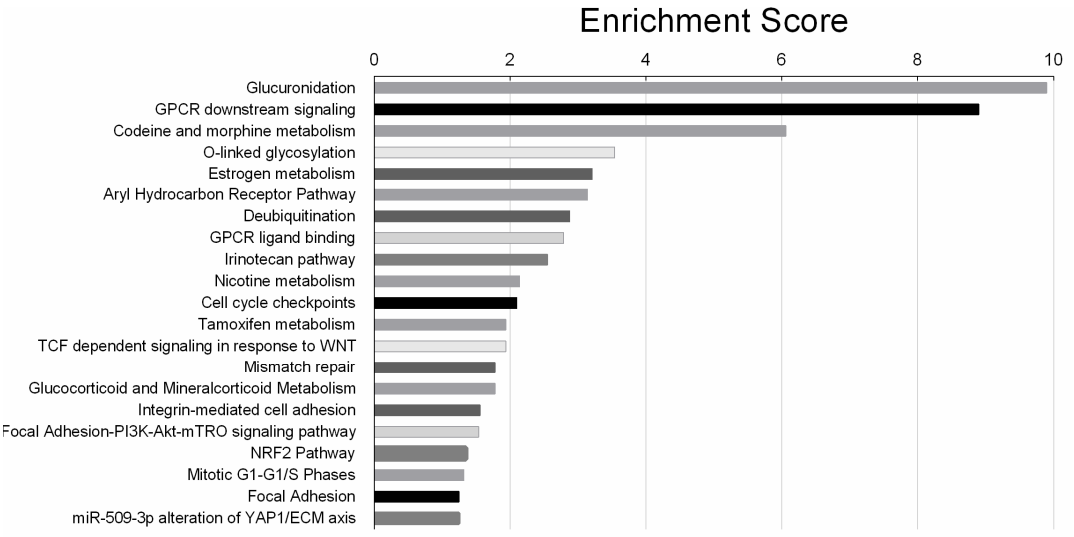

Figure 21: Pathway analysis in PEA-15AA transfected cells after cisplatin exposure. The pathways are listed according to the significance level in a descending order.

The most significantly affected pathway is the glucuronidation pathway with a significance value of 9.9 (log 2 base). Glucuronidation is the process of metabolizing substances such as drugs, pollutants, bilirubin, androgens, estrogens, glucocorticoids, fatty acids and bile acids. In glucuronidation, the glucuronic acid of a uridine diphosphate glucuronic acid is transferred to a substrate by UDP-glucuronyl transferase (UGT). The resulting substrate is called glucuronides and are more soluble in water and are excreted from body by urine and feces. The conjugation of xenobiotic molecule to hydrophilic molecular species is called phase II metabolism. UGTs, a representative member of phase II detoxification enzymes, include two families: UGT1A and UGT2. The UGT1 isoforms in human are encoded by a single gene locus on chromosome 2-q37 [135]. The UGT1A locus encodes nine functional exon cassettes (UGT1A1 and UGT1A3-UGT1A10) that encodes the unique N-terminal domains and approximately two-thirds of the luminal domains of the UGT1A proteins [136]. Among the other significant pathways, nuclear factor erythroid 2-related factor 2 (Nrf2) is of relative importance, as it is an upstream regulator of the UGT1A expression. Also, Nrf2 pathway was found to influence cisplatin sensitivity in cancer cells [137].

4.6 Evaluation of the responsible genes within the affected pathways

4.6.1 UGT1A expression in transfected cells

Glucuronidation was the most significantly affected pathway in SKOV-3-AA cells in response to cisplatin treatment. The genes affected within this pathway all belong to the family of UDP-glucuronyl transferases (UGT1A). The human UGT1 encodes nine UGT1A proteins (UGT1A1, UGT1A3-UGT1A10) that play a prominent role in drug and xenobiotic metabolism [138]. The microarray data showed the downregulation of all ten UGT1A mRNA in SKOV-3-AA cells after cisplatin exposure. Therefore, Western blot analysis was performed in all three different transfected cells to validate the expression of UGT1A family members after cisplatin treatment on protein level. After cisplatin treatment, the expression of UGT1A in EV, PEA-15AA, and PEA-15DD transfected cells decreased to 55.63%, 38.65%, and 48.27% respectively of their basal level in untreated cells (Figure 22).

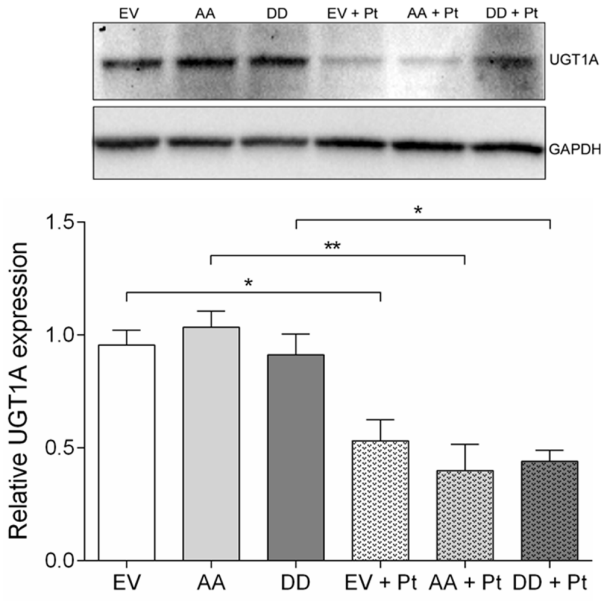

Figure 22: Representative Western blot and corresponding densitometric quantification of the relative UGT1A expression (mean ± SEM, n = 3) in empty vector (EV), PEA-15AA (AA), and PEA-15DD (DD) transfected cells after treating them with 15 µM cisplatin (Pt) for 24 hours and untreated SKOV-3 cells. GAPDH was used as a loading control. *p < 0.05, **p < 0.01.

The expression of UGT1A was most significantly decreased in SKOV-3-AA cells (adjusted p value = 0.0013) upon cisplatin treatment, while in SKOV-3-EV (adjusted p value = 0.02) and SKOV-3-DD (adjusted p value = 0.01) transfected cells the decrease was less significant (Figure 22).

4.6.2 GNB1 expression in transfected cells

The second most significantly affected pathway was the GPCR downstream signaling pathway. The gene differentially regulated within this pathway was the Guanine Nucleotide Binding Protein Beta 1 (GNB1). GNB1 mRNA was significantly downregulated in PEA-15AA-transfected cells after cisplatin treatment. GNB1 was found to play an important role in the mTOR-related anti-apoptotic pathway in breast cancer cells [139]. Therefore, the expression of this gene at protein level was measured to investigate whether the downregulation of GNB1 in SKOV-3-AA contributed to the increased sensitivity to cisplatin. The protein expression of GNB1 did not reveal any significant difference between the transfected cells before and after cisplatin treatment (Figure 23).

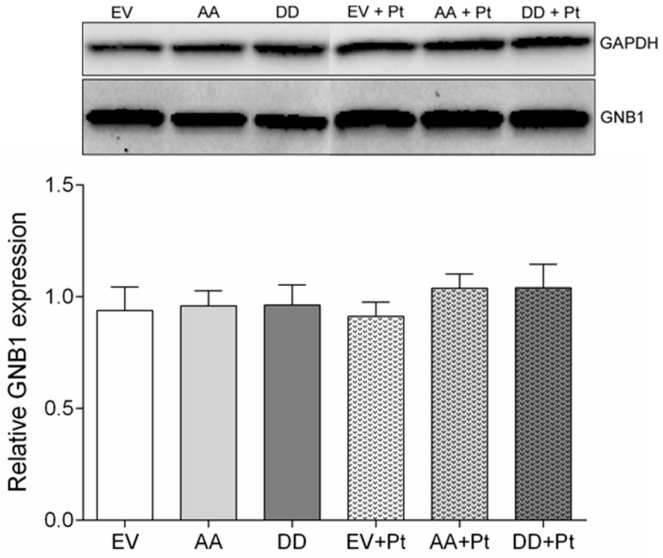

Figure 23: Representative Western blot and corresponding densitometric quantification of the relative GNB1 expression (mean ± SEM, n = 3) in empty vector (EV), PEA-15AA(AA), and PEA-15DD(DD) transfected cells after treating them with 15 µM cisplatin (Pt) for 24 hours and untreated transfected SKOV-3 cells. GAPDH was used as a loading control.

4.6.3 Nrf2 expression in transfected cells

UGT1A family members belong to the group of genes affected within most of the other significantly regulated pathways upon cisplatin treatment in SKOV-3-AA cells, like: Codeine and Morphine metabolism, Estrogen metabolism, constitutive Androstane receptor pathway, Aryl hydrocarbon receptor pathway, Pregnane X receptor pathway, meta-pathway biotransformation Phase I and II, Irinotecan pathway, Nicotine metabolism, Liver steatosis AOP, Arylamine metabolism, Tamoxifen metabolism, Nrf2 pathway. Among them, Nuclear Factor Erythroid derived 2-Related Factor 2 (Nrf2) is the upstream regulator of UGT1A expression. The array did not show any differential regulation of Nrf2 expression, but some downstream genes of Nrf2 were differentially regulated. Therefore, the expression of Nrf2 was analyzed at the protein level by Western blot in transfected cells before and after exposure to cisplatin (Figure 24).

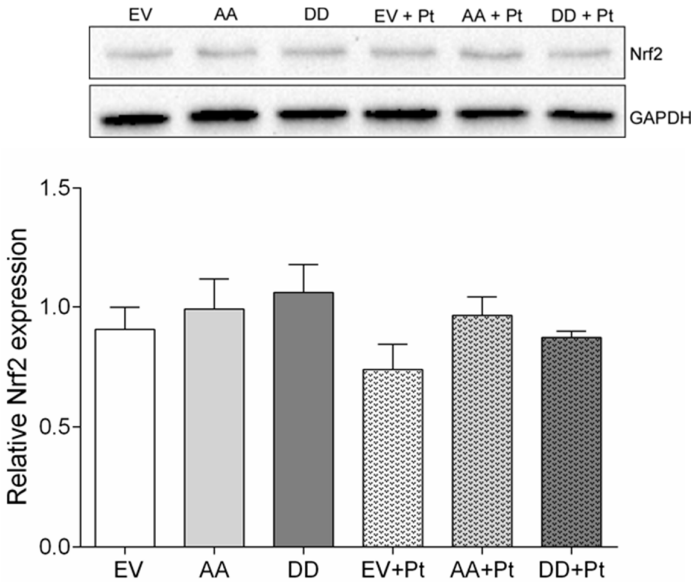

Figure 24: Representative Western blot and corresponding densitometric quantification of the relative Nrf2 expression (mean ± SEM, n = 3) in empty vector(EV)-, PEA-15AA(AA)-, and PEA-15DD(DD)-transfected cells after treating them with 15 µM cisplatin (Pt) for 24 hours and untreated transfected SKOV-3 cells. GAPDH was used as a loading control.

The results of the Western blot showed a slight decrease in overall Nrf2 expression after cisplatin exposure in all types of transfected cells. However, the differences in expression level were not significant in any case conforming with the result of the array.

4.7 Retinoic acid mediated inhibition of Nrf2 and downstream genes

4.7.1 Inhibition of Nrf2 by retinoic acid

All-trans-retinoic acid (further retinoic acid) has a wide range of biological effects. It inhibits tumorigenesis by suppression of cell growth and stimulation of cellular differentiation [140]. Also, retinoic acid promotes apoptosis, which may contribute to its antitumor properties [141,142]. Retinoic acid was found to reduce the Nrf2-mediated induction of Anti-oxidant Response Element (ARE)-driven genes [143]. Therefore, retinoic acid was used to inhibit Nrf2 pathway in parent SKOV-3 cells in order to investigate the influence of Nrf2/ARE signaling on cisplatin sensitivity.

To determine a non-toxic concentration of retinoic acid, MTT test was performed in SKOV-3 cells with varying concentrations of retinoic acid. The EC_{50} value of retinoic acid was 216 µM (pEC_{50} = 3.660 ± 0.003, mean ± SEM, n = 6) over a period of 48 hours. In order to investigate the influence of Nrf2 inhibition on cisplatin cytotoxicity, 20 µM of

retinoic acid was used in combination with cisplatin in SKOV-3 cells. The concentration 20 µM chosen as it was lower than EC_{10} (21.6 µM) for SKOV-3 cells.

The expression of Nrf2 was investigated by Western blot after treatment with cisplatin, retinoic acid and combination of cisplatin and retinoic acid for 24 hours (Figure 25). Nrf2 expression did not show any significant difference compared to the control cells after different treatments mentioned above. That is, retinoic acid did not influence the level of Nrf2 expression.

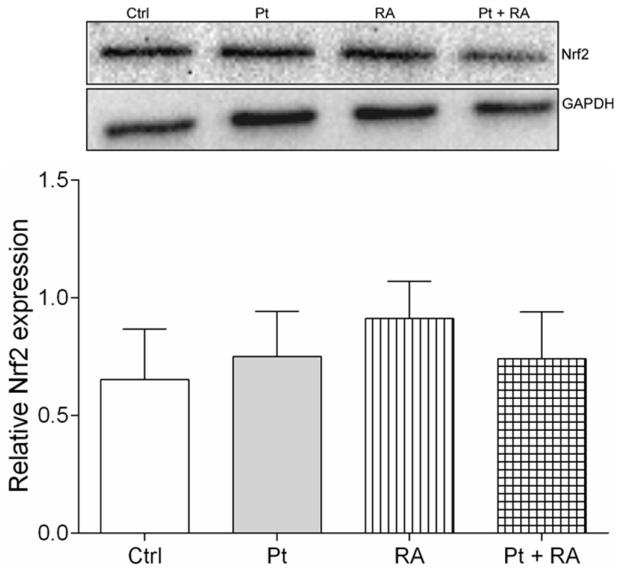

Figure 25: Representative Western blot and corresponding densitometric quantification of the relative Nrf2 expression (mean ± SEM, n = 3) in the untreated cells (Ctrl), after exposure to 15 µM cisplatin (Pt), 20 µM retinoic acid (RA) and co-incubation with 20 µM retinoic acid and 15 µM cisplatin (Pt + RA) for 24 hours in SKOV-3 cells. GAPDH was used as a loading control.

4.7.2 UGT1A expression after retinoic acid treatment

UGT1A is a downstream target of the Nrf2-mediated induction of ARE-driven genes. The expression of UGT1A was thus assessed in SKOV-3 cells after treatment with cisplatin, retinoic acid and the combination of both for 24 hours (Figure 26). Treatment with cisplatin did not have any effect on UGT1A expression compared to control cells. Treatment with 20 µM retinoic acid for 24 hours decreased the expression level of UGT1A significantly.

Also in combination with cisplatin, retinoic acid decreased the UGT1A level significantly compared to samples treated only with cisplatin (Figure 26). Thus Nrf2

inhibition by retinoic acid decreases UGT1A expression confirming their connection in agreement with the result of the array.

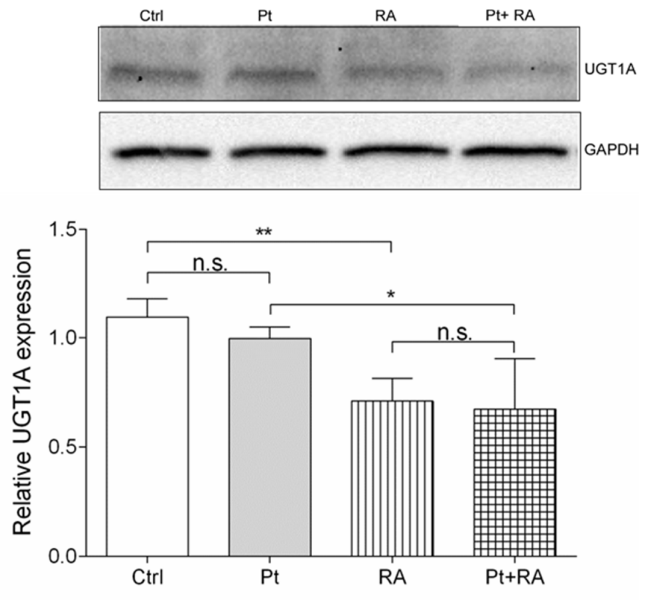

Figure 26: Representative Western blot and corresponding densitometric quantification of the relative UGT1A expression (mean ± SEM, n = 3) in the untreated cells (Ctrl), after exposure to 15 µM cisplatin (Pt), 20 µM retinoic acid (RA) and co-incubation with 20 µM retinoic acid and 15 µM cisplatin (Pt + RA) for 24 hours in SKOV-3 cells. GAPDH was used as a loading control. *$p < 0.05$, n. s. = not significant.

4.7.3 Effect of retinoic acid exposure on cisplatin sensitivity

The influence of retinoic acid on cisplatin sensitivity was assessed by treating the SKOV-3 cells with cisplatin alone and in combination with 20 µM retinoic acid. The results of the cytotoxicity test revealed that retinoic acid significantly sensitized the SKOV-3 cells to cisplatin (Figure 27). The EC_{50} value for cisplatin decreased from 32.6 µM to 13.9 µM upon co-incubation with retinoic acid.

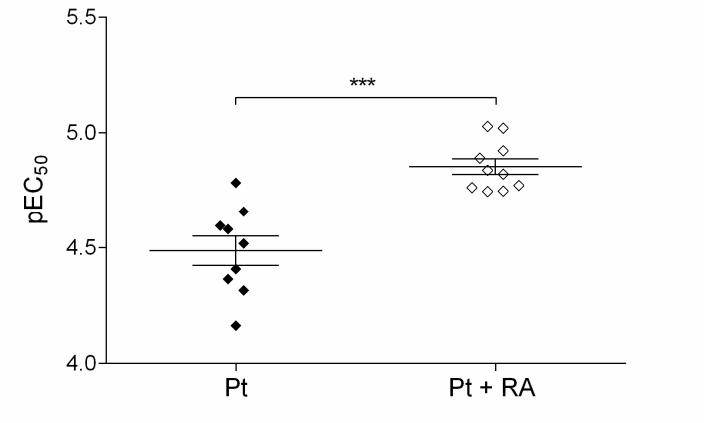

Figure 27: Cytotoxicity (pEC_{50}, mean ± SEM, n = 9-10) of cisplatin alone (Pt), and upon co-incubation with 20 µM retinoic acid (Pt + RA). ***$p < 0.001$.

5. Discussion

5.1 Effect of cisplatin on ERK1/2 signaling in ovarian cancer cells

Cisplatin induces several signaling pathways in ovarian cancer cells. ERK1/2 is activated in response to cisplatin treatment in all human ovarian cancer cell lines studied in this thesis, i.e. A2780, cisplatin-resistant A2780cis and SKOV-3 cells. The activation of ERK1/2 was time- and concentration dependent. As ERK1/2 was activated upon cisplatin exposure, a pharmacological inhibitor of MEK1/2 (U0126) was used to investigate the effect of ERK1/2 inhibition on cisplatin sensitivity. The results showed an increase in cellular survival when the ERK1/2 activation was inhibited. This implies that, ERK1/2 activation is involved in induction of cell death process. Similar results were reported by Wang et al. (2000) with HeLa and A549 cells [83]. In their study, two chemical inhibitors of MEK/ERK signaling pathway PD98059 and U0126 were shown to inhibit cisplatin-induced apoptosis. An activator of ERK pathway (tissue plasminogen activator, TPA) was reported to enhance the sensitivity of HeLa and A549 cells to cisplatin, while suramin, a growth factor receptor antagonist, and an ERK1/2 inhibitor reduced cisplatin sensitivity. Interestingly, resistant HeLa cell variants showed lower level of ERK activation by cisplatin compared to the corresponding sensitive one. In contrast to the report of Wang et al and to results presented in this thesis, Persons et al. (1999) performed similar experiments with SKOV-3 and UCI 101 ovarian cancer cell lines but using PD98059, which increased the sensitivity to cisplatin [87]. In a consecutive study, they showed that in A2780 cells the inhibition of ERK1/2 by PD98059 resulted in the decrease of p53 protein half-life and diminished accumulation of p53 protein during cisplatin exposure [79]. However, the authors did not investigate the correlation between lower p53 accumulation and cisplatin sensitivity.

Although PD98059 and U0126 are both MEK inhibitors, U0126 was reported to have 100-fold higher affinity for MEK than does the PD98059 [144]. Another difference is that, PD98059 is a flavone derivative, which increases glutathione level in rat hepatocyte cells independent of MEK inhibition [145]. In contrast, U0126 did not increase glutathione level in these cells.

Three mechanisms have been proposed for the role of glutathione (GSH) in regulating cisplatin sensitivity that affects its ultimate cell-killing ability, Firstly, GSH may serve as a cofactor in facilitating multidrug resistance protein 2-(MRP2-) mediated cisplatin efflux in mammalian cells [146]. Secondly, GSH may serve as a

redox-regulating cytoprotector supported by the observations that many CDDP-resistant cells overexpress GSH and γ- glutamylcysteine synthesis (γ-GCS), the rate-limiting enzyme for GSH biosynthesis. On the other hand, the third suggested role is that, GSH may function as a copper (Cu) chelator. Elevated GSH expression depletes the cellular bioavailable Cu pool, resulting in upregulation of the high-affinity Cu transporter (hCtr1) which is also a cisplatin transporter. It has been demonstrated that overexpression of GSH by transfection with γ-GCS conferred sensitization to cisplatin [147]. Another copper chelator, tetrathiomolybdate, was shown to enhance cisplatin sensitivity in ovarian cancer animal model through CTR1 induction [148].

In contrast, U0126 was reported to decrease the level of CTR1 in A2780 cells, while the decrease was not statistically significant in A2780cis cells [133]. In this thesis, the expression of CTR1 at protein level was investigated after treatment with U0126 in SKOV-3 cells. But change in CTR1 expression was not statistically significant between untreated and U0126 treated cells. From the western blot figure the decrease in CTR1 level after U0126 treatment was clear (not statistically significant), which implies the fact that the decrease in CTR1 expression may have contributed to a reduction in cisplatin sensitivity. Amrán et al., studied the impact of ERK inhibition by U0126 and PD98059 in human myeloid cells (THP-1, HL-60, NB-4) [91]. PD98059 and U0126 reduced the intracellular accumulation of cisplatin in this study. Moreover, U0126 attenuated cisplatin-DNA binding and intracellular peroxide accumulation, which are important regulators of cisplatin cytotoxicity. These results suggest that GSH-independent modulation of drug transport is a major mechanism explaining the anti-apoptotic action of MEK/ERK inhibitors in cisplatin-treated myeloid cells [91].

ERK1 and ERK2 were both activated by cisplatin exposure in A2780 and A2780cis cells, the extent of ERK1 and ERK2 phosphorylation was, however, different. U0126 inhibits the activation of both ERK1 and ERK2. Guégan et al. (2013), demonstrated that ERK1 played a predominant role over ERK2 in cisplatin-induced death in human hepatocellular carcinoma cells Huh-7 and knock-out mice [94]. Our results also showed that ERK1 was activated more than ERK2 in sensitive A2780 cells and ERK2 was activated to a higher extent than ERK1 in the cisplatin-resistant A2780cis cells. This let us presuppose that ERK1 may have a distinct pro-apoptotic function and thereby may sensitize the cells to cisplatin. Therefore, to investigate the role of ERK1 and ERK2 each in cisplatin sensitivity, siRNA-mediated silencing of ERK1 and ERK2 separately was performed. However, the results of both ERK1 and ERK2 knockdown showed an increase in cisplatin resistance in resistant A2780cis cells. This indicates that

both ERK1 and ERK2 are required for cisplatin-induced cell death in cisplatin-resistant A2780cis cells. This is in agreement with the negative impact of U0126 on cisplatin sensitivity in this cell line. In sensitive A2780 cells, both ERK1 and ERK2 knockdown did not show any influence on cisplatin sensitivity, which may be due to different factors. ERK1 knockdown was not enough in A2780 cells, although a very high concentration of ERK1 siRNA was used. A2780 cells are generally considered to be hard to transfect [149]. In the case of ERK2 knockdown, ERK1 could have taken over the apoptotic function. However, it remains unclear why cisplatin-resistant cells behave differently.

The downstream genes of ERK1/2 were not investigated further as the sensitivity did not improve or decreased after the knockdown of ERK1 and ERK2. Interestingly, the study of Guégan et al. (2013) also demonstrated that the selective suppression of either ERK1 or ERK2 activity significantly protected the Huh-7 cells from the toxic effects of high cisplatin concentrations (20-30 µg/ml), which conforms with our results. But at the concentration of 5 µg/ml of cisplatin, ERK2 silencing sensitized Huh-7 cells, whereas ERK1 knockdown seemed to have no impact on low-dose cisplatin cytotoxicity. In our study, the sudden increase of cisplatin sensitivity was not observed for cisplatin-resistant A2780cis cells.

The use of a chemical inhibitor for a certain protein is a common practice of studying the function of a protein. The advantage of using chemical inhibitors is that their effect on the target protein is very strong. The function of the target protein can be completely inhibited by a chemical inhibitor. The disadvantage of this process is that most chemical inhibitors influence other proteins/ signaling pathways, which were not supposed to be affected. For example, the MEK1/2 inhibitor U0126 initiates the activation of AMP-activated protein kinase and enhances the activation of its downstream target acetyl-CoA carboxylase in HEK293 cells [130], impeding the possibility of studying the sole effect of ERK1/2 inhibition on cisplatin sensitivity. Therefore, siRNA knockdown is an alternative and milder way of studying the function of a protein. RNA interference is a very specific process, as the siRNA targets only the target mRNA sequence of a protein. However, this technique also has some drawbacks. As the effect of U0126 on cisplatin sensitivity was much stronger than that of a ERK1 and ERK2 knockdown, one may speculate that a knockdown to just below 50% of the basal level may be insufficient to remarkably limit the protein function and affect cytotoxicity.

The inhibition of ERK1 and ERK2 individually as well as the chemical inhibition of ERK1/2 activation showed that ERK1/2 is actually required for cell death in ovarian

cancer cells. ERK1/2 exerts its cellular survival functions after translocation to nucleus upon activation. ERK1/2 also has targets in the cytoplasm. Cytosolic retention of ERK1/2 denies access to transcriptional factors that are required for mitogenic function. In addition, cytosolic ERK1/2 besides inhibiting the proliferative signal in nucleus potentiates the catalytic activity of proapoptotic proteins like death-associated protein kinase (DAPK) in the cytoplasm [150]. Therefore, we hypothesized that the subcellular localization of the ERK1/2 may determine the cell fate.

5.2 Effect of PEA-15 protein on cisplatin sensitivity in SKOV-3 cells

Scaffold proteins play a pivotal role in spatial and temporal regulation of the ERK1/2 signaling. PEA-15 is a cytoplasmic anchor protein that binds to and sequesters ERK1/2 [151] in the cytoplasm. Both ERK1/2 and phosphorylated ERK1/2 bind to PEA-15 with equal affinity [108]. The crystal structures of PEA-15 bound to three different ERK2 phospho-conformers revealed that PEA-15 uses a bipartite binding mode occupying two key docking sites of ERK2. PEA-15 efficiently binds the ERK2 activation loop in the critical Thr-X-Tyr region in different phosphorylation states. PEA-15 binding stimulates an allosteric conduit in dually phosphorylated ERK2, disrupting key features of active ERK2. At the same time PEA-15 binding protects ERK2 from dephosphorylation, thus facilitating the immediate ERK activity upon its release from the PEA-15 inhibitory complex [152]. PEA-15 is almost exclusively confined to cytoplasm as it contains a nuclear export signal [76]. For these reasons, PEA-15 was used in order to investigate the relationship between subcellular localization of ERK1/2 and cisplatin sensitivity.

PEA-15 binding to ERK and its other functions are regulated by two serine residues at 104 and 116 positions. PEA-15 cannot bind to ERK when these serine residues are phosphorylated. Therefore, more ERK can translocate to nucleus and activate the downstream genes responsible for cellular survival or apoptosis. Two mutated forms of PEA-15 were generated by replacing the two serine residues with alanine and aspartic acid to create non-phosphorylatable (PEA-15AA) and phosphomimetic form (PEA-15DD) of PEA-15, respectively [120]. Bisphosphorylated PEA-15DD sensitized the ovarian cancer cells SKOV3.ip1, OVTOKO and HEY to paclitaxel, while the non-phosphorylatable PEA-15AA decreased sensitivity to this drug [121]. Paclitaxel kills tumor cells by increasing microtubule polymerization via binding to the β-subunit in preformed microtubules [153] and by stabilizing the microtubule network via direct interaction with microtubules [154]. SCLIP (SCG10-like protein), belongs to the

stathmin/OP18 family. The stathmin/OP18 family proteins prevent microtubule polymerization by sequestering soluble tubulin heterodimers [155, 156] and promote microtubule depolymerisation by increasing microtubule catastrophe rate [157, 158]. PEA-15DD impairs the microtubule-destabilizing activity of SCLIP, thereby enhancing the effects of paclitaxel on microtubule assembly, mitosis, and apoptosis and sensitizing cells to paclitaxel [121].

In contrast to the case of paclitaxel, the study conducted within this thesis showed that the sensitization of SKOV-3 cells to cisplatin can be achieved by the non-phosphorylatable PEA-15AA. This is likely due to the difference in the mechanism of action of these two drugs. Paclitaxel kills tumor cell by targeting the microtubule assembly, while cisplatin directly binds to DNA and damaged DNA activates downstream apoptotic pathways. In the latter phase, PEA-15AA may contribute either by influencing the localization of ERK/2 signaling or by intervening the Nrf2/ARE axis as shown by the experiments in this thesis.

The effect of PEA-15 protein on cisplatin sensitivity was investigated on colorectal carcinoma cell line [119] where the overexpression of the PEA-15 protein increased cisplatin resistance and knockdown of PEA-15 was found to enhance sensitivity to cisplatin. This agrees with our results on PEA-15 knockdown, where the sensitivity to cisplatin increased after PEA-15 silencing. This result does not allow to make conclusions about the relevance of ERK1/2 spatial regulation. But in this case, the wild type PEA-15 was overexpressed, where the two regulatory serine residues (104 and 116) were open to be phosphorylated. Inside the cell, these two regulatory serine residues can be phosphorylated by protein kinase C (PKC), Akt or Calmoduline Kinase II, the interactions of so many kinases are beyond control. Therefore, the induction of resistance cannot be attributed to a single factor i.e. overexpression of PEA-15. To be precise about the contribution of the phosphorylation status of PEA-15 on cisplatin resistance, two mutated versions of PEA-15 were used in this study, where both serine residues were replaced either with two alanine (non-phosphorylatable) or two aspartate (phosphomimetic) residues. In another study by Lee et al., (2012), the mutated unphosphorylatable PEA-15AA was found to inhibit ovarian cancer tumorigenicity and progression by blocking beta-catenin [120]. They also found that tissues from patients with ovarian cancer were significantly more likely than the adjacent normal tissues to express PEA-15 phosphorylated at both sites. Eckert et al. (2008) revealed that phosphorylated PEA-15 (Ser116) renders glioblastoma cells resistant to glucose-deprivation mediated cell death [159]. Also, siRNA mediated knockdown of PEA-15 in

U87MG glioblastoma cells abolished tumorigenicity. Another study reported that PEA-15 also modulates the JNK (c-Jun N-terminal kinase) in addition to the ERK signaling pathway. PEA-15 overexpressing glioma cells showed increased signs of autophagy in response to ionizing radiation, rapamycin treatment or serum deprivation. But nonphosphorylatable mutants of PEA-15 were not capable of promoting autophagy in these cells [118].

5.3 Transcriptome analysis of SKOV-3 cells after PEA-15 transfection

Due to the diverse functions of PEA-15, a microarray was warranted for this study to investigate the underlying key players of sensitizing the SKOV-3 cells to cisplatin by PEA-15AA expression.

The results of the array showed differential gene expression in differently transfected cells. The number of differentially expressed genes induced by cisplatin treatment was much higher compared to the number of differentially expressed genes between different transfected cells. This is likely due to the fact that only different forms of the same protein were overexpressed in the same SKOV-3 cells. The genes which were differentially expressed exclusively in cisplatin-treated SKOV-3-AA (444 genes) cells were of interest in this study as the overexpression of PEA-15AA sensitized the cells to cisplatin. The pathways to which these 444 genes belong were investigated by WikiPathways.

5.3.1 Glucuronidation

UGT1A superfamily of genes was downregulated within significantly affected pathways in PEA-15AA transfected cells in response to cisplatin treatment as detected by the array. UGTs, a representative member of the phase II drug detoxification enzymes, include two families: UGT1 and UGT2 [160]. UGTs catalyze the addition of a β-glucuronic acid moiety to a variety of nucleophilic sites of xenobiotic and endogenous compounds. UGTs are involved in the metabolism of bilirubin, steroids, bile acids, and drugs. In addition, they metabolize carcinogens, an important process for the bioinactivation and subsequent excretion of these toxic compounds [138]. UGTs have been linked to drug toxicity and cancer drug resistance. These enzyme's action represent an intrinsic mechanism of resistance to the DNA topoisomerase I inhibitors 7-ethyl-10-hydroxycamptothecin and NU/ICRF 505 in human colon cancer cells [161]. Moreover, due to its structure cisplatin cannot be metabolized by UGTs. However, there is no report about the influence of UGTs on cisplatin sensitivity till now. The downregulation of UGT1A enzymes upon cisplatin exposure could be, therefore, a

consequence of suppression of the upstream gene of the UGT1A. Many phase II enzymes including UGT1A isoforms are activated through the transcription factor Nrf2 (Nuclear factor Erythroid-2 related factor) [162]

Nrf2 is a 66-kDa ubiquitous protein. It is kept in the cytoplasm by Keap1 protein, which acts as a negative regulator of Nrf2 by facilitating the ubiquitination and proteasomal degradation. Upon oxidative stress, Keap1 dissociates from Nrf2, facilitating Nrf2 migration to the nucleus. In the nucleus, Nrf2 binds to the antioxidant response elements (ARE) and functions as a strong transcriptional activator of selected anti-oxidant genes, e.g. γ-GCS, HO-1, UGT1A (Figure 27).

Nrf2 activation is related to cisplatin resistance. Loss of Nrf2 or inhibition by siRNA was reported to increase cisplatin sensitivity in SKOV-3 cells [163]. Ohta et al. (2008) reported that loss of Keap1 function activated Nrf2, causing cells to become more resistant to cisplatin [164].

Nrf2 itself was not differentially regulated after exposure to cisplatin in SKOV-3-AA, rather some downstream genes of Nrf2 were differentially regulated as shown by the microarray data. The WikiPathways of the microarray showed that beside UGT1A, also other genes as described in section 4.5.5.3 were also affected.

In order to investigate whether the PEA-15AA-mediated Nrf2 regulation led to the cisplatin sensitivity in SKOV-3 cells, and thereby to validate the relevance of Nrf2 pathway for the effect, retinoic acid, an inhibitor of Nrf2 pathway was investigated.

There are many inhibitors available for the Nrf2/ARE pathway. Among them retinoic acid was especially chosen due to the fact that retinoic acid was not reported to show any contradictory effect on cells. Another potent chemical inhibitor of Nrf2/ARE pathway is brusatol, which was not used as it is deactivated within an hour [165]. The effect of retinoic acid on Nrf2 is long-lasting (24 hours). Retinoic acid increased the sensitivity to cisplatin in SKOV-3 cells. This implies that the overexpression of PEA-15AA in SKOV-3 cells increased the sensitivity to cisplatin through interference with the Nrf2/ARE signaling.

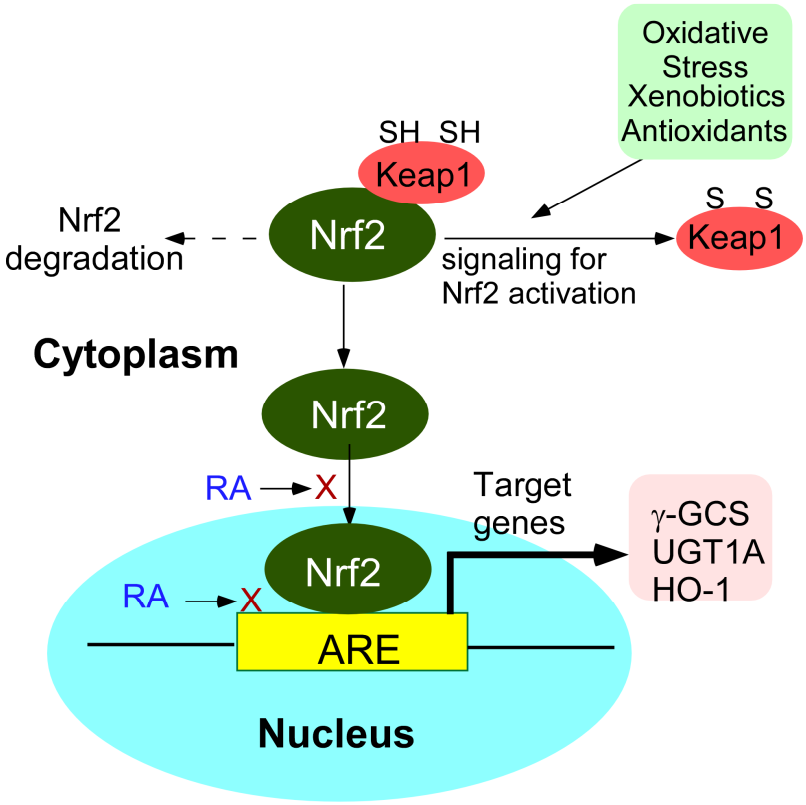

Figure 27: Nrf2-ARE activation pathway in response to oxidative stimuli. Oxidative stress (xenobiotics, antioxidants) activates Nrf2 by dissociating the Keap1 protein from Nrf2, which leads to proteasomal degradation of Nrf2. Retinoic acid inhibits Nrf2 induction both by inhibiting the translocation to nucleus and binding of Nrf2 to the ARE element (modified from Shin et al., 2012) [166].

Similar results were also reported by Whitworth et al. They investigated the combination effect of carboplatin and retinoic acid in A2780 cells. The results of their study revealed that the combination treatment reduced cell viability, cancer stem cell (CSC) marker expression and tumorigenicity compared to the treatment with carboplatin alone. One of the retinoids, called 9cUAB30, has already been approved by the National Cancer Institute for a breast cancer chemoprevention trial [167]. A coffee alkaloid trigonelin, acts as an inhibitor of Nrf2/ARE pathway. Trigonelin was shown to enhance the sensitivity of pancreatic carcinoma cells to anticancer drugs by augmenting TRAIL-induced apoptosis [168].

The Western blot analysis of the SKOV-3-AA cells of Nrf2 expression after cisplatin treatment did not reveal any significant change in the expression level. This could be due to a number of reasons including the time point of measurement (incubation period), possible effect of cisplatin on nuclear Nrf2 translocation or on Nrf2 binding to

ARE. Therefore, the expression of the downstream gene UGT1A was analyzed as the final proof of Nrf2 inhibition.

Also there was no significant decrease of Nrf2 expression after retinoic acid treatment. However, there was a significant decrease in UGT1A expression after retinoic acid treatment. This is due to the fact that retinoic acid reduces the nuclear translocation of Nrf2 and the binding of Nrf2 to ARE elements [169], therefore, the amount of Nrf2 is not affected in this case.

5.3.2 GPCR downstream signaling

The second most significantly affected pathway in cisplatin-treated SKOV-3-AA cells was the GPCR downstream signaling. The gene which was significantly downregulated within this pathway was Guanine Nucleotide Binding Protein β1 (GNβ1 or GNB1). GNB1 was found to be involved in the mammalian target of rapamycin (mTOR) mediated anti-apoptotic pathway. GNB1 mRNA level is positively correlated with mTOR and was found to be a potential target in the treatment of breast cancer [139]. GNB1 protein expression analysis in cisplatin treated SKOV-3-AA cells did not reveal any significant change in GNB1 level after cisplatin treatment. Frequent lack of correlation between mRNA and protein data was discussed in detail by Maier et al. (2009) [170]. Several mechanisms are responsible for this discrepancy between transcriptome and proteome. Among them post-transcriptional parameters, post-translational parameters and noise and experimental errors are of significant importance. Transcription and translation do not have a linear relationship. Cis-acting and trans-acting elements enhance or repress the synthesis of protein from a certain copy number of mRNA molecules. The individual half-life of proteins is the major post-translational factor influencing mRNA-protein correlation. Protein half-lives are highly variable, ranging from a few seconds to several days and depend on several factors like: intrinsic protein stability, the first amino-terminal amino acid (N-end rule), posttranslational processing, such as phosphorylation, and ubiquitination, and on the localization of the respective protein. Meaningful conclusions from comparative studies on large data-sets can only be drawn upon establishment of solid statistical methods embedded in a larger framework.

5.3.3 Other genes affected by PEA-15AA transfection in SKOV-3 cells

UGT1As are the genes involved in most of the significantly affected pathway in SKOV-3-AA cells. These include codeine and morphine metabolism, estrogen

metabolism, constitutive androstane receptor pathway, aryl hydrocarbon receptor pathway, Pregnane X receptor pathway, metapathway biotransformation phase I and II, Irinotecan pathway, nicotine metabolism, Nrf2 pathway.

Other pathways which were significantly affected upon cisplatin treatment in SKOV-3-AA cells, were investigated for the underlying genes which were up- or down-regulated. The differentially regulated genes were explored by literature search to find a relevance to cisplatin sensitivity. The pathways containing differentially regulated genes, which were found to be linked to cisplatin sensitivity are discussed below. The genes are of worth exploring to find their relevance to PEA-15AA-mediated increase in cisplatin cytotoxicity.

GPCR ligand binding was found to be a significantly affected pathway in cisplatin-exposed SKOV-3-AA cells, the underlying differentially expressed genes were: free fatty acid receptor 3 (FFAR3), and endothelin converting enzyme 1 (ECE1). The relevance of these genes to drug resistance, cancer and cell death pathways is discussed below.

FFAR3 was found to be upregulated in cisplatin-treated SKOV-3-AA cells. FFAR3 is a G-protein-coupled receptor (GPCR) which is activated by short chain fatty acids (two to six carbon in length). Propionate, a ligand for FFAR3 was shown to inhibit proliferation and promote apoptosis in several cancer cell types [171, 172]. FFAR3 inhibits MAPK signaling in breast cancer cells (MDA-MB-231), thereby decreases actin polymerization and the invasive property of metastatic cells [173]. The expression of this gene is of potential interest to be investigated further at protein level in SKOV-3-AA cells.

ECE1 gene was found significantly downregulated in cisplatin-treated SKOV-3-AA cells. Previous studies suggested that silencing ECE1 reduced the invasive phenotype in OVCAR 3 and ES2 ovarian cancer cells [174]. Therefore, a further investigation of this gene in the context of cisplatin sensitivity is warranted.

Our study delineates an important role for non-phosphorylated PEA-15 in regulating chemosensitivity to cisplatin in ovarian cancer cells. In addition, our results suggest that phosphorylation status of PEA-15 could be used as a biomarker to predict the responsiveness of ovarian tumors to cisplatin treatment and that patients with ovarian tumors expressing high levels of unphosphorylated PEA-15 would be more likely to benefit from cisplatin treatment than other patients. In future studies, the association between PEA-15 phosphorylation status and the pathologic grade of ovarian tumors and

evaluation of the in vivo impact of PEA-15 phosphorylation status on the effectiveness of cisplatin in human ovarian carcinoma xenograft would be worth o examination.

PEA-15 was already evaluated for treating advanced breast cancer in mice. To target PEA-15 in advanced breast tumors, Xie et al. (2015) developed a breast cancer-specific construct (T-VISA) composed of the human telomerase reverse transcriptase (hTERT; T) promoter and a versatile transgene amplification vector VISA (VP16-GAL4-WPRE integrated systemic amplifier). T-VISA-PEA-15 was found to be highly specific, selectively express PEA-15 in breast cancer cells, and induce cancer-cell killing in vitro and in vivo without affecting normal cells [175]. A similar construct with PEA-15AA would be of interest for ovarian cancer in order to investigate if the efficiency of the cisplatin can be improved.

6. Conclusions and outlook

The results of this thesis unveil the impact of ERK1/2 signaling in the context of cisplatin sensitivity. The major findings are as follows:

1. In A2780, A2780cis and SKOV-3 cells, ERK1/2 activation appears to be required for cisplatin-induced cell death as chemical inhibition of the pathway hindered cisplatin sensitivity. Silencing ERK1 and ERK2 individually diminish the sensitivity to the drug in A2780cis cells but had no effect in A2780 cells.
2. Unphosphorylatable PEA-15 (PEA-15AA), which binds ERK1/2, positively influences the sensitivity to cisplatin, that is susceptibility to cisplatin increased in SKOV-3 cells. The microarray revealed UGT1A as the most significantly affected gene responsible for enhanced cisplatin cytotoxicity of PEA-15AA-overexpressing SKOV-3 cells. Further experimental evaluation divulged that inhibition of Nrf2/ARE pathway is responsible for mediating the increase in cisplatin activity in PEA-15AA-overexpressed cells. However, other mechanisms may also be involved, therefore, further investigations of the affected genes in PEA-15AA-overexpressing cells are warranted.

Some other open issues, which need to be addressed, are as below:

1. siRNA-mediated silencing of UGT1A and investigating its influence on cisplatin sensitivity, as there has been no previous report about glucuronidation and cisplatin resistance, this will help to clarify whether UGT1A itself is important or its downregulation is only a consequence of upstream events
2. Exploring the function of the GNB1 and other genes (discussed in section 5.3.3) in respect to cisplatin action by silencing the genes by siRNA
3. Exploring possible relationship between ERK1/2 localization and Nrf2/ARE signaling to understand how PEA-15AA affects Nrf2/ARE
4. Including more ovarian cancer cells in the study, if possible including patient's samples, which will consolidate the findings observed in this thesis
5. Examining patient's sample at different stages of the ovarian cancer for PEA-15 phosphorylation status and finding correlation of these data with cisplatin response

7. Summary

The efficiency of the anticancer drug cisplatin in ovarian cancer is often hindered by the development of cisplatin resistance. Cisplatin activates a plethora of DNA damage-related signaling pathways, which regulate the cell fate by initiating or inhibiting the cell death machineries. Understanding the functions of the activated pathways is important to combat the resistance. Among the MAPK pathways, ERK signaling was found to be activated by cisplatin in most of the ovarian cancer cells. However, different ovarian cancer cell types showed diverse response to cisplatin upon ERK inhibition. Therefore, in this thesis ERK1/2 signaling pathway was investigated regarding its influence on cisplatin sensitivity. For this purpose, modulation of the pathway with a chemical inhibitor, and siRNA-mediated silencing of ERK1 and ERK2 independently, and altering the localization of the ERK1/2 by overexpression of a scaffold protein PEA-15 were employed.

ERK1/2 was activated in sensitive A2780, cisplatin-resistant A2780cis and SKOV-3 cells when exposed to cisplatin. Inhibition of ERK1/2 activation by the MEK1/2 inhibitor U0126 diminished sensitivity to cisplatin in all of the three cell lines. To study if ERK1 has a predominant role over ERK2 or vice versa in determining cell death or survival, ERK1 and ERK2 were silenced independently in A2780 and A2780cis cells. This enhanced resistance to cisplatin in A2780cis cells, while A2780 cells did not show any change of cisplatin action. ERK1 silencing did not show any effect on cisplatin potency in A2780 cells. The combined results of chemical inhibition and silencing of the ERK1 and ERK2 indicated that ERK1/2 is actually required for cisplatin-mediated cell death in A2780, A2780cis and SKOV-3 cells.

PEA-15 is a ubiquitously expressed protein, which retains ERK1/2 in cytoplasm, inhibiting its translocation to nucleus. The regulation of the PEA-15 function is predominantly controlled by its phosphorylation status. The influence of PEA-15 phosphorylation status was examined in respect to cisplatin cytotoxicity in SKOV-3 cells. Two mutated versions of PEA-15: phosphomimetic (PEA-15DD) and non-phosphorylatable (PEA-15AA), were employed for this purpose. The results indicated that PEA-15AA sensitized the SKOV-3 cells to cisplatin, while PEA-15DD did not have any effect on cisplatin sensitivity. As PEA-15 has many other functions within the cell beside its influence on ERK1/2 localization, a microarray was performed to detect the underlying set of genes accounting for sensitization to cisplatin. The results of the microarray revealed UGT1A family as the most significantly affected genes. UGT1A is

one of the downstream genes of Nrf2 pathway. Therefore, retinoic acid (an inhibitor of Nrf2 pathway) was used to downregulate UGT1A genes via Nrf2/ARE axis, which in turn, sensitized the SKOV-3 cells to cisplatin. This result indicates the fact that PEA-15AA sensitized the cells to cisplatin by interfering with the Nrf2/ARE axis. The results of the phosphorylation status of PEA-15 as a biomarker of cisplatin sensitivity and PEA-15AA as a new therapeutic approach for treating ovarian cancer cells with platinum drugs warrant further investigation.

References

1. Ferlay J, Shin HR, Bray F, Forman D, Mathers C, Parkin DM (2010) Estimates of worldwide burden of cancer in 2008: GLOBOCAN 2008. Int J Cancer 127: 2893-2917
2. Berkenblit A, Cannistra SA (2005) Advances in the management of epithelial ovarian cancer. J Reprod Med 50: 426-438
3. Bast RC Jr, Feeney M, Lazarus H, Nadler LM, Colvin RB, Knapp RC (1981) Reactivity of a monoclonal antibody with human ovarian carcinoma. J Clin Invest 68: 1331-1337
4. McGuire WP, Hoskins WJ, Brady MF, Kucera PR, Partridge EE, Look KY, Clarke-Pearson DL, Davidson M (1996) Cyclophosphamide and cisplatin compared with paclitaxel and cisplatin in patients with stage III and stage IV ovarian cancer. N Engl J Med 334: 1-6
5. Ozols RF, Bundy BN, Greer BE, Fowler JM, Clarke-Pearson D, Burger RA, Mannel RS, DeGeest K, Hartenbach EM, Baergen R; Gynecologic Oncology Group (2003) Phase III trial of carboplatin and paclitaxel compared with cisplatin and paclitaxel in patients with optimally resected stage III ovarian cancer: a gynecologic oncology group study. J Clin Oncol 21: 3194-3200
6. du Bois A, Luck HJ, Meier W, Adams HP, Möbus V, Costa S, Bauknecht T, Richter B, Warm M, Schröder W, Olbricht S, Nitz U, Jackisch C, Emons G, Wagner U, Kuhn W, Pfisterer J (2003) A randomized clinical trial of cisplatin/ paclitaxel versus carboplatin/paclitaxel as first-line treatment of ovarian cancer. J Natl Cancer I 95: 1320-1329
7. Steffensen KD, Alvero AB, Yang Y, Waldstrom M, Hui P, Holmberg JC, Silasi DA, Jakobsen A, Rutherford T, Mor G (2011) Prevalence of epithelial ovarian cancer stem cells correlates with recurrence in early-stage ovarian cancer. J Oncol 2011: 620523
8. Dilruba S, Kalayda GV (2016) Platinum-based drugs: past, present and future. Cancer Chemother Pharmacol 77: 1103-1124
9. Siddik ZH (2003) Cisplatin: mode of cytotoxic action and molecular basis of resistance. Oncogene 22: 7265-7279
10. Galluzzi L, Senovilla L, Vitale I, Michels J, Martins I, Kepp O, Castedo M, Kroemer G (2012) Molecular mechanisms of cisplatin resistance. Oncogene 31: 1869-1883
11. Kalayda GV, Wagner CH, Jaehde U (2012) Relevance of copper transporter 1 for cisplatin resistance in human ovarian carcinoma cells. J Inorg Biochem 116: 1-10
12. Safaei R (2006) Role of copper transporters in the uptake and efflux of platinum containing drugs. Cancer Lett 234: 34-39
13. Holzer AK, Manorek GH, Howell SB (2006) Contribution of the major copper influx transporter CTR1 to the cellular accumulation of cisplatin, carboplatin, and oxaliplatin. Mol Pharmacol 70: 1390-1394.
14. Zisowsky J, Koegel S, Leyers S, Devarakonda K, Kassack MU, Osmak M, Jaehde U (2007) Relevance of drug uptake and efflux for cisplatin sensitivity of tumor cells. Biochem Pharmacol 73: 298-307
15. Yang T, Chen M, Chen T, Thakur A (2015) Expression of the copper transporters hCtr1, ATP7A and ATP7B is associated with the response to chemotherapy and

survival time in patients with resected non-small cell lung cancer. Oncol Lett 10: 2584-2590

16. Kalayda GV, Wagner CH, Buss I, Reedijk J, Jaehde U (2008) Altered localisation of the copper efflux transporters ATP7A and ATP7B associated with cisplatin resistance in human ovarian carcinoma cells. BMC Cancer 8: 175
17. Samimi G, Safaei R, Katano K, Holzer AK, Rochdi M, Tomioka M, Goodman M, Howell SB (2004) Increased expression of the copper efflux transporter ATP7A mediates resistance to cisplatin, carboplatin, and oxaliplatin in ovarian cancer cells. Clin Cancer Res 10: 4661-4669
18. Nakayama K, Kanzaki A, Terada K, Mutoh M, Ogawa K, Sugiyama T, Takenoshita S, Itoh K, Yaegashi N, Miyazaki K, Neamati N, Takebayashi Y (2004) Prognostic value of the Cu transporting ATPase in ovarian carcinoma patients receiving cisplatin-based chemotherapy. Clin Cancer Res 10: 2804-2811
19. Schneider V, Krieger ML, Bendas G, Jaehde U, Kalayda GV (2013) Contribution of intracellular ATP to cisplatin resistance of tumor cells. J Biol Inorg Chem 18: 165-174
20. Planells-Cases R, Lutter D, Guyader C, Gerhards NM, Ullrich F, Elger DA, Kucukosmanoglu A, Xu G, Voss FK, Reincke SM, Stauber T, Blomen VA, Vis DJ, Wessels LF, Brummelkamp TR, Borst P, Rottenberg S, Jentsch TJ (2015) Subunit composition of VRAC channels determines substrate specificity and cellular resistance to Pt-based anti-cancer drugs. EMBO J 34: 2993-3008
21. Wheate NJ, Walker S, Craig GE, Oun R (2010) The status of platinum anticancer drugs in the clinic and in clinical trials. Dalton T 39: 8113-8127
22. Borst P, Evers R, Kool M, Wijnholds J (2000) A family of drug transporters: the multidrug resistance-associated proteins. J Natl Cancer I 92: 1295-1302
23. Takahara PM, Rosenzweig AC, Frederick CA, Lippard SJ (1995) Crystal structure of double-stranded DNA containing the major adduct of the anticancer drug cisplatin. Nature 377: 649-652
24. Brown SJ, Kellett PJ, Lippard SJ (1993) Ixr1, a yeast protein that binds to platinated DNA and confers sensitivity to cisplatin. Science 261: 603-605
25. Huang JC, Zamble DB, Reardon JT, Lippard SJ, Sancar A (1994) HMG-domain proteins specifically inhibit the repair of the major DNA adduct of the anticancer drug cisplatin by human excision nuclease. Proc Natl Acad Sci USA 91: 10394-10398
26. Furuta T, Ueda T, Aune G, Sarasin A, Kraemer KH, Pommier Y (2002) Transcription-coupled nucleotide excision repair as a determinant of cisplatin sensitivity of human cells. Cancer Res 62: 4899-4902
27. Vaisman A, Varchenko M, Umar A, Kunkel TA, Risinger JI, Barrett JC, Hamilton TC, Chaney SG (1998) The role of hMLH1, hMSH3, and hMSH6 defects in cisplatin and oxaliplatin resistance: correlation with replicative bypass of platinum-DNA adducts. Cancer Res 58: 3579-3585.
28. Michels J, Vitale I, Senovilla L, Enot DP, Garcia P, Lissa D, Olaussen KA, Brenner C, Soria J, Castedo M, Kroemer G (2013) Synergistic interaction between cisplatin and PARP inhibitors in non-small cell lung cancer. Cell Cycle 12: 877-883
29. Chang L, Karin M (2001) Mammalian MAP kinase signalling cascades. Nature 410: 37-40

30. Johnson GL, Lapadat R (2002) Mitogen-activated protein kinase pathways mediated by ERK, JNK, and p38 protein kinases. Science 298: 1911-1912
31. Marshall CJ (1995) Specificity of receptor tyrosine kinase signaling: transient versus sustained extracellular signal-regulated kinase activation. Cell 80: 179-185
32. Kirsch DG, Kastan MB (1998) Tumor-suppressor p53: implications for tumor development and prognosis. J Clin Oncol 16: 3158–3168
33. Feldman DR, Bosl GJ, Sheinfeld J, Motzer RJ (2008) Medical treatment of advanced testicular cancer. JAMA 299: 672–684
34. Peng HQ, Hogg D, Malkin D, Bailey D, Gallie BL, Bulbul M, Jewett M, Buchanan J, Goss PE (1993) Mutations of the p53 gene do not occur in testis cancer. Cancer Res 53: 3574-3578
35. Cobb MH, Goldsmith EJ (1995) How MAP kinases are regulated. J Biol Chem 270: 14843-14846
36. Geyer M, Wittinghofer A (1997) GEFs, GAPs, GDIs and effectors: taking a closer (3D) look at the regulation of Ras-related GTP-binding proteins. Curr Opin Struct Biol 7: 786-792
37. Moodie SA, Willumsen BM, Weber MJ, Wolfman A (1993) Complexes of Ras GTP with Raf-1 and mitogen-activated protein kinase kinase. Science 260: 1658-1661
38. Vojtek AB, Hollenberg SM, Cooper JA (1993) Mammalian Ras interacts directly with the serine/threonine kinase Raf. Cell 74: 205-214
39. Zhang XF, Settleman J, Kyriakis JM, Takeuchi-Suzuki E, Elledge SJ, Marshall MS, Bruder JT, Rapp UR, Avruch J (1993) Normal and oncogenic p21ras proteins bind to the amino-terminal regulatory domain of c-Raf-1. Nature 364: 308-313
40. Kyriakis JM, App H, Zhang XF, Banerjee P, Brautigan DL, Rapp UR, Avruch J (1992) Raf-1 activates MAP kinase-kinase. Nature 358: 417-421
41. Dent P, Haser W, Haystead TA, Vincent LA, Roberts TM, Sturgill TW (1992) Activation of mitogen-activated protein kinase kinase by v-Raf in NIH 3T3 cells and in vitro. Science 257: 1404-1407
42. Zheng CF, Guan KL (1993) Dephosphorylation and inactivation of the mitogen-activated protein kinase by a mitogen-induced Thr/Tyr protein phosphatase. J Biol Chem 268: 16116-16119
43. Robinson MJ, Cheng M, Khokhlatchev A, Ebert D, Ahn N, Guan KL, Stein B, Goldsmith E, Cobb MH (1996) Contributions of the mitogen-activated protein (MAP) kinase backbone and phosphorylation loop to MEK specificity. J Biol Chem 271: 29734-29739
44. Sturgill TW, Ray LB, Erikson E, Maller JL (1988) Insulin-stimulated MAP-2 kinase phosphorylates and activates ribosomal protein S6 kinase II. Nature 334: 715-718
45. Pulverer BJ, Kyriakis JM, Avruch J, Nikolakaki E, Woodgett JR (1991) Phosphorylation of c-jun mediated by MAP kinases. Nature 353: 670-674
46. Gille H, Sharrocks AD, Shaw PE (1992) Phosphorylation of transcription factor p62TCF by MAP kinase stimulates ternary complex formation at c-fos promoter. Nature 358: 414-417
47. Boulton TG, Nye SH, Robbins DJ, Ip NY, Radziejewska E, Morgenbesser SD, DePinho RA, Panayotatos N, Cobb MH, Yancopoulos GD (1991) ERKs: a family of protein-serine/threonine kinases that are activated and tyrosine phosphorylated in response to insulin and NGF. Cell 65: 663-675

48. Boulton TG, Yancopoulos GD, Gregory JS, Slaughter C, Moomaw C, Hsu J, Cobb MH (1990) An insulin-stimulated protein kinase similar to yeast kinases involved in cell cycle control. Science 249: 64-67
49. Miyata Y, Nishida E (1999) Distantly related cousins of MAP kinase: biochemical properties and possible physiological functions. Biochem Biophys Res Commun 266: 291-295
50. Raman M, Chen W, Cobb MH (2007) Differential regulation and properties of MAPKs. Oncogene 26: 3100-3112
51. Shaul YD, Seger R (2007) The MEK/ERK cascade: from signaling specificity to diverse functions. Biochim. Biophys. Acta Mol. Cell Res 1773: 1213-1226
52. Giroux S, Tremblay M, Bernard D, Cardin-Girard JF, Aubry S, Larouche L, Rousseau S, Huot J, Landry J, Jeannotte L, Charron J (1999) Embryonic death of Mek1-deficient mice reveals a role for this kinase in angiogenesis in the labyrinthine region of the placenta. Curr. Biol 9: 369-372
53. Saba-El-Leil MK, FDJ Vella, Vernay B, Voisin L, Chen L, Labrecque N, Ang SL, Meloche S (2003) An essential function of the mitogen-activated protein kinase Erk2 in mouse trophoblast development. EMBO Rep 4: 964-968
54. Pages G, Guérin S, Grall D, Bonino F, Smith A, Anjuere F, Auberger P, Pouysségur J (1999) Defective thymocyte maturation in p44 MAP kinase (Erk 1) knockout mice. Science 286: 1374-1377
55. Belanger LF, Roy S, Tremblay M, Brott B, Steff AM, Mourad W, Hugo P, Erikson R, Charron J (2003) Mek2 is dispensable for mouse growth and development. Mol Cell Biol 23: 4778-4787
56. Bessard A, Frémin C, Ezan F, Fautrel A, Gailhouste L, Baffet G (2008) RNAi-mediated ERK2 knockdown inhibits growth of tumor cells in vitro and in vivo. Oncogene 27: 5315-5325
57. Shama, J, Garcia-Medina R, Pouysségur J, Vial E (2008) Major contribution of MEK1 to the activation ERK1/ERK2 and to the growth of LS174T colon carcinoma cells. Biochem Biophys Res Commun 372: 845-849
58. Scholl FA, Dumesic PA, Barragan DI, Harada K, Charron J, Khavari PA (2009) Selective role for Mek1 but not Mek2 in the induction of epidermal neoplasia. Cancer Res 69: 3772-3778
59. Lloyd AC (2006) Distinct functions for ERKs? J Biol 5: 13
60. Lefloch R, Pouysségur J, Lenormand P (2007) Single and combined silencing of ERK1 and ERK2 reveals their positive contribution to growth signaling depending on their expression levels. Mol. Cell. Biol 28: 511-527
61. Voisin L, Saba-El-Leil MK, Julien C, Frémin C, Meloche S (2010) Genetic demonstration of a redundant role of extracellular signal-regulated kinase 1 (ERK1) and ERK2 mitogen-activated protein kinases in promoting fibroblast proliferation. Mol Cell Biol 30: 2918-2932
62. Lefloch R, Pouysségur J, Lenormand P (2009) Total ERK1/2 activity regulates cell proliferation. Cell Cycle 8: 705-711
63. Fukuda M, Gotoh Y, Nishida E (1997) Interaction of MAP kinase with MAP kinase kinase: its possible role in the control of nucleocytoplasmic transport of MAP kinase. EMBO J 16: 1901-1908

64. Reszka AA, Seger R, Diltz CD, Krebs EG, Fischer EH (1995) Association of mitogen-activated protein kinase with the microtubule cytoskeleton. Proc Natl Acad Sci USA 92: 8881-8885
65. Karlsson M, Mathers J, Dickinson RJ, Mandl M, Keyse SM (2004) Both nuclear-cytoplasmic shuttling of the dual specificity phosphatase MKP-3 and its ability to anchor MAP kinase in the cytoplasm are mediated by a conserved nuclear export signal. J Biol Chem 279: 41882-41891
66. Adachi M, Fukuda M, Nishida E (1999) Two co-existing mechanisms for nuclear import of MAP kinase: passive diffusion of a monomer and active transport of a dimer. EMBO J 18: 534
67. Whitehurst AW, Wilsbacher JL, You Y, Luby-Phelps K, Moore MS, Cobb MH (2002) ERK2 enters the nucleus by a carrier-independent mechanism. Proc Natl Acad Sci USA 99: 7496-7501
68. Matsubayashi Y, Fukuda M, Nishida E (2001) Evidence for existence of a nuclear pore complex-mediated, cytosol-independent pathway of nuclear translocation of ERK MAP kinase in permeabilized cells. J Biol Chem 276: 41755-41760
69. Khokhlatchev AV, Canagarajah B, Wilsbacher J, Robinson M, Atkinson M, Goldsmith E, Cobb MH (1998) Phosphorylation of the MAP kinase ERK2 promotes its homodimerization and nuclear translocation. Cell 93: 605-615
70. Kondoh K, Torii S, Nishida E (2005) Control of MAP kinase signaling to the nucleus. Chromosoma 114: 86-91
71. Lenormand P, Sardet C, Pages G, L'Allemain G, Brunet A, Pouyssegur J (1993) Growth factors induce nuclear translocation of MAP kinases (p42mapk and p44mapk) but not of their activator MAP kinase kinase (p45mapkk) in fibroblasts. J Cell Biol 122: 1079-1088
72. Chen RH, Sarnecki C, Blenis J (1992) Nuclear localization and regulation of erk- and rskencoded protein kinases. Mol Cell Biol 12: 915-927
73. Zhao J, Yuan X, Frodin M, Grummt I (2003) ERK-dependent phosphorylation of the transcription initiation factor TIF-IA is required for RNA polymerase I transcription and cell growth. Mol Cell 11: 405-413
74. Marais R, Wynne J, Treisman R (1993) The SRF accessory protein Elk-1 contains a growth factor-regulated transcriptional activation domain. Cell 73: 381-393
75. Torii S, Nakayama K, Yamamoto T, Nishida E (2004) Regulatory mechanisms and function of ERK MAP kinases. J Biochem 136: 557-561
76. Formstecher E, Ramos JW, Fauquet M, Calderwood DA, Hsieh JC, Canton B, Nguyen XT, Barnier JV, Camonis J, Ginsberg MH, Chneiweiss H (2001) PEA-15 mediates cytoplasmic sequestration of ERK MAP kinase. Dev Cell 1: 239-250
77. Deiss LP, Feinstein E, Berissi H, Cohen O, Kimchi A (1995) Identification of a novel serine/ threonine kinase and a novel 15-kD protein as potential mediators of the gamma interferon-induced cell death. Genes Dev 9: 15-30
78. Chen CH, Wang WJ, Kuo JC, Tsai HC, Lin JR, Chang ZF, Chen RH (2005) Bidirectional signals transduced by DAPK-ERK interaction promote the apoptotic effect of DAPK. EMBO J 24: 294-304
79. Persons DL, Yazlovitskaya EM, Pelling JC (2000) Effect of extracellular signal-regulated kinase on p53 accumulation in response to cisplatin. J Biol Chem 275: 35778-35785

80. Lee JC, Kumar S, Griswold DE, Underwood DC, Votta BJ, Adams JL (2000) Inhibition of p38 MAP kinase as a therapeutic strategy. Immunopharmacology 47: 185-201
81. Tang D, Wu D, Hirao A, Lahti JM, Liu L, Mazza B, Kidd VJ, Mak TW, Ingram AJ (2002) ERK activation mediates cell cycle arrest and apoptosis after DNA damage independently of p53. J Biol Chem 277: 12710-12717
82. Tang MKS, Zhou HY, Yam JWP, Wong AST (2010) c-Met overexpression contributes to the acquired apoptotic resistance of nonadherent ovarian cancer cells through a cross talk mediated by phosphatidylinositol 3-kinase and extracellular signal-regulated kinase ½. Neoplasia 12: 128-138
83. Wang X, Martindale JL, Holbrook NJ (2000) Requirement for ERK activation in cisplatin-induced apoptosis. J Biol Chem 275: 39435-39443
84. Yeh PY, Chuang SE, Yeh KH, Song YC, Ea CK, Cheng AL (2002) Increase of the resistance of human cervical carcinoma cells to cisplatin by inhibition of the MEK to ERK signaling pathway partly via enhancement of anticancer drug-induced NFκB activation. Biochem Pharmacol 63: 1423-1430
85. Nowak G (2002) Protein kinase C-α and ERK1/2 mediate mitochondrial dysfunction, decreases in active Na+ transport, and cisplatin-induced apoptosis in renal cells. J Biol Chem 277: 43377-43388
86. Hayakawa J, Ohmichi M, Kurachi H, Ikegami H, Kimura A, Matsuoka T, Jikihara H, Mercola D, Murata Y (1999) Inhibition of extracellular signal-regulated protein kinase or c-Jun N-terminal protein kinase cascade, differentially activated by cisplatin, sensitizes human ovarian cancer cell line. J Biol Chem 274: 31648-31654
87. Persons DL, Yazlovitskaya EM, Cui W, Pelling JC (1999) Cisplatin-induced activation of mitogen-activated protein kinases in ovarian carcinoma cells: Inhibition of extracellular signal-regulated kinase activity increases sensitivity to cisplatin. Clin Cancer Res 5: 1007-1014
88. Basu A, Tu H (2005) Activation of ERK during DNA damage induced apoptosis involves protein kinase Cdelta. Biochem Bioph Res Co 334: 1068-1073
89. Mandic A, Viktorsson K, Heiden T, Hansson J, Shoshan MC (2001) The MEK1 inhibitor PD98059 sensitizes C8161 melanoma cells to cisplatin-induced apoptosis. Melanoma Res 11: 11-19
90. Yeh PY, Yeh KH, Chuang SE, Song YC, Cheng AL (2004) Suppression of MEK/ERK signaling pathway enhances cisplatin-induced NF-κB activation by protein phosphatase 4-mediated NF-κB p 65 Thr dephosphorylation. J Biol Chem 279: 26143-26148
91. Amrán D, Sancho P, Fernández C, Esteban D, Ramos AM, de Blas E, Gómez M, Palacios MA, Aller P (2005) Pharmacological inhibitors of extracellular signal-regulated protein kinases attenuate the apoptotic action of cisplatin in human myeloid leukemia cells via glutathione-independent reduction in intracellular drug accumulation. Biochim Biophys Acta 1743: 269-279
92. Zhang Y, Qu X, Jing W, Hu X, Yang X, Hou K, Teng Y, Zhang J, Liu Y (2009) GSTP1 determines cisplatinum cytotoxicity in gastric adenocarcinoma MGC803 cells: regulation by promoter methylation and extracellular regulated kinase signaling. Anti-Cancer Drug 20: 208-214

93. Lee S, Yoon S, Kim DH (2007) A high nuclear basal level of ERK2 phosphorylation contributes to the resistance of cisplatin-resistant human ovarian cancer cells. Gynecol Oncol 104: 338–344
94. Guégan J-P, Ezan F, Théret N, Langouët S, Baffet G (2013) MAPK signaling in cisplatin-induced death: predominant role of ERK1 over ERK2 in human hepatocellular carcinoma cells. Carcinogenesis. 34: 38-47
95. Danziger N, Yokoyama M, Jay T, Cordier J, Glowinski J, Chneiweiss H (1995) Cellular expression, developmental regulation, and phylogenic conservation of PEA-15, the astrocytic major phosphoprotein and protein kinase C substrate. J Neurochem 64: 1016-1025
96. Estelles A, Yokoyama M, Nothias, F, Vincent JD, Glowinski J, Vernier P (1996) Themajor astrocytic phosphoprotein PEA-15 is encoded by two mRNAs conserved on their full length in mouse and human. J Biol Chem 271: 14800-14806
97. Ramos JW, Kojima TK, Hughes PE, Fenczik CA, Ginsberg MH (1998) The death effector domain of PEA-15 is involved in its regulation of integrin activation. J Biol Chem 273: 33897-33900
98. Fiory F, Formisano P, Perruolo G, Beguinot F (2009) PED/PEA-15, a multifunctional protein controlling cell survival and glucose metabolism. Am J Physiol Endocrinol Metab 297: E592-E601
99. Renault F, Formstecher E, Callebaut I, Junier MP, Chneiweiss H (2003) The multifunctional protein PEA-15 is involved in the control of apoptosis and cell cycle in Astrocytes. Biochem Pharmacol 66: 1581-1588
100. Stassi G, Garofalo M, Zerilli M, Ricci-Vitiani L, Zanca C, Todaro M, Aragona F, Limite G, Petrella G, Condorelli G (2005) PED mediates AKT-dependent chemoresistance in human breast cancer cells. Cancer Res 65: 6668-6675
101. Condorelli G, Vigliotta G, Iavarone C, Caruso M, Tocchetti CG, Andreozzi F, Cafieri A, Tecce MF, Formisano P, Beguinot L, Beguinot F (1998) PED/PEA-15 gene controls glucose transport and is overexpressed in type 2 diabetes mellitus. EMBO J 17: 3858-3866
102. Hao C, Beguinot F, Condorelli G, Trencia A, Van Meir EG, Yong VW, Parney IF, Roa WH, Petruk KC (2001) Induction and intracellular regulation of tumor necrosis factor-related apoptosis-inducing ligand (TRAIL) mediated apoptosis in human malignant glioma cells. Cancer Res 61: 1162-1170
103. Glading A, Koziol, JA, Krueger J, Ginsberg MH (2007) PEA-15 inhibits tumor cell invasion by binding to extracellular signal-regulated kinase 1/2. Cancer Res 67: 1536-1544
104. Formisano P, Perruolo G, Libertini S, Santopietro S, Troncone G, Raciti GA, Oriente F, Portella G, Miele C, Beguinot F (2005) Raised expression of the antiapoptotic protein ped/pea-15 increases susceptibility to chemically induced skin tumor development. Oncogene 24: 7012-7021
105. Sulzmaier F, Opoku-Ansah J, Ramos JW (2012) Phosphorylation is the switch that turns PEA-15 from tumor suppressor to tumor promoter. Small GTPases 3: 173-177
106. Araujo H, Danziger N, Cordier J, Glowinski J, Chneiweiss H (1993) Characterization of PEA-15, a major substrate for protein kinase C in astrocytes. J Biol Chem 268: 5911-5920

107. Kubes M, Cordier J, Glowinski J, Girault JA, Chneiweiss H (1998) Endothelin induces a calcium-dependent phosphorylation of PEA-15 in intact astrocytes: identification of Ser104 and Ser116 phosphorylated, respectively, by protein kinase C and calcium/calmodulin kinase II in vitro. J Neurochem 71: 1307-1314
108. Callaway K, Abramczyk O, Martin L, Dalby K N (2007) The anti-apoptotic protein PEA-15 is a tight binding inhibitor of ERK1 and ERK2, which blocks docking interactions at the D-recruitment site. Biochemistry 46: 9187-9198
109. Condorelli G, Vigliotta G, Cafieri A, Trencia A, Andalo P, Oriente F (1999) PED/PEA-15: an anti-apoptotic molecule that regulates FAS/TNFR1-induced apoptosis. Oncogene 18: 4409-4415
110. Kitsberg D, Formstecher E, Fauquet M, Kubes M, Cordier J, Canton B, Pan G, Rolli M, Glowinski J, Chneiweiss H (1999) Knock-out of the neural death effector domain protein PEA-15 demonstrates that its expression protects astrocytes from TNF-α induced apoptosis. J Neurosci 19: 8244-8251
111. Xiao C, Yang BF, Asadi N, Beguinot F, Hao C (2002) Tumor necrosis factor-related apoptosis-inducing ligand-induced death-inducing signaling complex and its modulation by c-FLIP and PED/PEA-15 in glioma cells. J Biol Chem 277: 25020-25025
112. Renganathan H, Vaidyanathan H, Knapinska A, Ramos JW (2005) Phosphorylation of PEA-15 switches its binding specificity from ERK/MAPK to FADD. Biochem J 3907: 729-735
113. Peacock JW, Palmer J, Fink D, Ip S, Pietras E, Mui AL, Chung SW, Gleave ME, Cox ME, Parsons R, Peter ME, Ong CJ (2009) PTEN loss promotes mitochondrially dependent type II Fas-induced apoptosis via PEA-15. Mol Cell Biol 29: 1222-1234
114. Greig FH, Nixon GF (2014) Phosphoprotein enriched in astrocytes (PEA)-15: A potential therapeutic target in multiple disease states. Pharmacol Ther 143: 265-274
115. Bartholomeusz C, Itamochi H, Nitt M, Saya H, Ginsberg MH, Ueno NT (2006) Antitumor effect of E1A in ovarian cancer by cytoplasmic sequestration of activated ERK by PEA-15. Oncogene 25: 79-90
116. Bartholomeusz C, Rosen D, Wei C, Kazansky A, Yamasaki F, Takahashi T, Itamochi H, Kondo S, Liu J, Ueno NT (2008) PEA-15 induces autophagy in human ovarian cancer cells and is associated with prolonged overall survival. Cancer Res 68: 9302-9310
117. Bartholomeusz C, Oishi T, Saso H, Akar U, Liu P, Kondo K, Kazansky A, Krishnamurthy S, Lee J, Esteva FJ, Kigawa J, Ueno NT (2011) MEK1/2 inhibitor Selumetinib (AZD6244) inhibits growth of ovarian clear cell carcinoma in a PEA-15-dependent manner in a mouse xenograft model. Mol Cancer Ther 11: 360-369
118. Böck BC, Tagscherer KE, Fassl A, Krämer A, Oehme I, Zentgraf H-W, Keith M, Roth W (2010) The PEA-15 Protein Regulates Autophagy via Activation of JNK. J Biol Chem 285: 21644-21654
119. Funke V, Lehmann-Koch J, Bickeböller M, Benner A, Tagscherer KE, Grund K, Pfeifer M, Herpel E, Schirmacher P, Chang-Claude J, Brenner H, Hoffmeister M,

Roth W (2013) The PEA-15/PED protein regulates cellular survival and invasiveness in colorectal carcinomas. Cancer Lett 335: 431-440

120. Lee J, Bartholomeusz C, Krishnamurthy S, Liu P, Saso H, LaFortune TA, Hortobagyi GN, Ueno NT (2012) PEA-15 unphosphorylated at both serine 104 and serine 116 inhibits ovarian cancer cell tumorigenicity and progression through blocking β-catenin. Oncogenesis 1: 1-11
121. Xie X, Bartholomeusz C, Ahmed AA, Kazansky A, Diao L, Baggerly KA, Hortobagyi GN, Ueno NT (2013). Bisphosphorylated PEA-15 sensitizes ovarian cancer cells to Paclitaxel by impairing the microtubule-destabilizing effect of SCLIP. Mol Cancer Ther 12: 1099-1111
122. Mueller H, Kassack MU, Wiese M (2004) Comparison of the usefulness of the MTT, ATP, and calcein assays to predict the potency of cytotoxic agents in various human cancer cell lines. J Biomol Screen 9: 506–515
123. Alley MC, Scudiero DA, Monks A, Hursey ML, Czerwinski MJ, Fine DL, Abbott BJ, Mayo JG, Shoemaker RH, Boyd MR (1988) Feasibility of drug screening with panels of human tumor cell lines using a microculture tetrazolium assay. Cancer Res 48: 589-601
124. Elbashir SM, Harborth J, Lendeckel W, Yalcin A, Weber K, Tuschl T (2001) Duplexes of 21-nucleotide RNAs mediate RNA interference in cultured mammalian cells. Nature 411: 494-498
125. Lau NC, Lim LP, Weinstein EG, Bartel DP (2001) An abundant class of tiny RNAs with probable regulatory roles in Caenorhabditis elegans. Science 294: 858-862
126. Clariom™ S solutions for human, mouse, and rat. Applied Biosystems™. Thermo Fisher Scientific. Available from https://assets.thermofisher.com/TFS-Assets/LSG/brochures/EMI07387-2_DS_Clariom-S_solutions_HMR.pdf
127. Irizarry RA, Hobbs B, Collin F, Beazer-Barclay YD, Antonellis KJ, Scherf U, Speed TP (2003) Exploration, normalization, and summaries of high density oligonucleotide array probe level data. Biostatistics 4: 249-264
128. Ritchie ME, Phipson B, Wu D, Hu Y, Law CW, Shi W, Smyth GK (2015) limma powers differential expression analyses for RNA-sequencing and microarray studies.Nucleic Acids Res 43: e47
129. Motulsky H, Christopoulos A (2004) Fitting models to biological data using linear and non-linear regression, Oxford University Press, New York
130. Dokladda K, Green KA, Pan DA, Hardie DG (2005) PD98059 and U0126 activate AMP-activated protein kinase by increasing the cellular AMP: ATP ratio and not via inhibition of the MAP kinase pathway. FEBS Lett 579: 236-240
131. Howell SB, Safaei R, Larson CA, Sailor MJ (2010) Copper Transporters and the Cellular Pharmacology of the Platinum-Containing Cancer Drugs. Mol Pharmacol 77: 887-894
132. Andrews PA, Mann SC, Huynh HH, Albright KD (1991) Role of the Na,K-ATPase in the accumulation of cis-diammine-dichloroplatinum(II) in human ovarian carcinoma cells. Cancer Res 51: 3677-3681
133. Schneider V, Chaib S, Spanier C, Knapp M, Moscvin V, Scordovillo L, Ewertz A, Jaehde U, Kalayda GV (2017) Transporter-mediated interaction between Platinum drugs and Sorafenib at the cellular level. AAPS J 20: 9

134. Brunet A, Roux D, Lenormand P, Dowd S, Keyse S, Pouyssegur J (1999) Nuclear translocation of p42/p44 mitogen-activated protein kinase is required for growth factor-induced gene expression and cell cycle entry. EMBO J. 18: 664-674
135. Mackenzie PI, Miners JO, McKinnon RA (2000) Polymorphisms in UDP glucuronosyltransferase genes: functional consequences and clinical relevance. Clin Chem Lab Med 38: 889-92
136. Moghrabi N, Sutherland L, Wooster R,Povey S, Boxer M, Burchell B (1992) Chromosomal assignment of human phenol and bilirubin UDPglucuronosyltransferase genes (UGT1A-subfamily). Ann Hum Genet 56: 81-91
137. Furfaro AL, Traverso N, Domenicotti C, Piras S, Moretta L, Marinari UM, Pronzato MA, Nitti M (2016) The Nrf2/HO-1 Axis in Cancer Cell Growth and Chemoresistance. Oxid Med Cell Longev 2016: 1-14
138. Evans WE, Relling MV (1999) Pharmacogenomics: translating functional genomics into rational therapeutics. Science 286: 487-491
139. Wazir U, Jiang WG, Sharma AK, Mokbel K (2013) Guanine Nucleotide Binding Protein β1: A Novel Transduction Protein with a Possible Role in Human Breast Cancer. Cancer Genom Proteom 10: 69-74
140. Soprano DR, Qin P, Soprano KJ (2004) Retinoic acid receptors and cancers. Annu Rev Nutr 24: 201-221
141. Atencia R, Garcia-Sanz M, Unda F, Arechaga J (1994) Apoptosis during retinoic acid-induced differentiation of F9 embryonal carcinoma cells. Exp Cell Res 214: 663-667
142. Herget T, Specht H, Esdar C, Oehrlein SA, Maelicke A (1998) Retinoic acid induces apoptosis-associated neural differentiation of a murine teratocarcinoma cell line. J Neurochem 70: 47-58
143. Valenzuela M, Glorieux C, Stockis J, Sid B, Sandoval JM, Felipe KB, Kviecinski MR, Verrax J, Calderon PB (2014) Retinoic acid synergizes ATO-mediated cytotoxicity by precluding Nrf2 activity in AML cells. Brit J Cancer 111: 874-882
144. Favata MF, Horiuchi KY, Manos EJ, Daulerio AJ, Stradley DA, Feeser WS, Van Dyk DE, Pitts WJ, Earl RA, Hobbs F, Copeland RA, Magolda RL, Scherle PA, Trzaskos JM (1998) Identification of a novel inhibitor of mitogen-activated protein kinase kinase. J Biol Chem 273: 18623-18632
145. Kim SK, Abdelmegeed MA, Novak RF (2006) The Mitogen-activated protein kinase kinase (MEK) inhibitor PD98059 elevates primary cultured rat hepatocyte glutathione levels independent of inhibiting MEK. Drug Metab Disp 34: 683-689
146. Paulusma CC, van Geer MA, Evers R, Heijn M, Ottenhoff R, Borst P, Oude Elferink RP (1999) Canalicular multispecific organic anion transporter/multidrug resistance protein 2 mediates low-affinity transport of reduced glutathione. Biochem J 338: 393-401
147. Chen HH, Song IS, Hossain A, Choi MK, Yamane Y, Liang ZD, Lu J, Wu LY, Siddik ZH, Klomp LW, Savaraj N, Kuo MT (2008) Elevated glutathione levels confer cellular sensitization to cisplatin toxicity by up-regulation of copper transporter hCtr1. Molecular Pharmacology 74: 697–704

148. Ishida S, McCormick F, Smith-McCune K, Hanahan D (2010) Enhancing tumor-specific uptake of the anticancer drug cisplatin with a copper chelator. Cancer Cells 17: 574-583
149. Tanyi JL, Morris AJ, Wolf JK, Fang X, Hasegawa Y, Lapushin R, Auersperg N, Sigal YJ, Newman RA, Felix EA, Atkinson EN, Mills GB (2003) The human lipid phosphate phosphatase-3 decreases the growth, survival, and tumorigenesis of ovarian cancer cells: validation of the lysophosphatidic acid signaling cascade as a target for therapy in ovarian cancer. Cancer Res 63: 1073-1082
150. Mebratu Y, Tesfaigzi Y (2009) How ERK1/2 activation controls cell proliferation and cell death is subcellular localization the answer? Cell Cycle 8: 1168-1175
151. Roskoski R Jr (2012) ERK1/2 MAP kinases: structure, function, and regulation. Pharmacol Res 66: 105–143
152. Mace PD, Wallez Y, Egger MF, Dobaczewska MK, Robinson H, Pasquale EB, Riedl SJ (2013) Structure of ERK2 bound to PEA-15 reveals a mechanism for rapid release of activated MAPK. Nat Commun 4: 1681
153. Xiao H, Verdier-Pinard P, Fernandez-Fuentes N, Burd B, Angeletti R, Fiser A, Horwitz SB, Orr GA (2006) Insights into the mechanism of microtubule stabilization by Taxol. Proc Natl Acad Sci USA 103: 10166-10173
154. Parness J, Horwitz SB (1981) Taxol binds to polymerized tubulin in vitro. J Cell Biol 91: 479-487
155. Cassimeris L (2002) The oncoprotein 18/stathmin family of microtubule destabilizers. Curr Opin Cell Biol 14: 18-24
156. Charbaut E, Curmi PA, Ozon S, Lachkar S, Redeker V, Sobel A (2001) Stathmin family proteins display specific molecular and tubulin binding properties. J Biol Chem 276: 16146-16154
157. Belmont LD, Mitchison TJ (1996) Identification of a protein that interacts with tubulin dimers and increases the catastrophe rate of microtubules. Cell 84: 623-631
158. Manna T, Thrower D, Miller HP, Curmi P, Wilson L (2006) Stathmin strongly increases the minus end catastrophe frequency and induces rapid treadmilling of bovine brain microtubules at steady state in vitro. J Biol Chem 281: 2071-2078
159. Eckert A, Böck BC, Tagscherer KE, Haas TL, Grund K, Sykora J, Herold-Mende C, Ehemann V, Hollstein M, Chneiweiss H, Wiestler OD, Walczak H, Roth W (2008) The PEA-15/PED protein protects glioblastoma cells from glucose deprivation-induced apoptosis via the ERK/MAP kinase pathway. Oncogene 27: 1155-1166
160. Burchell B, Brierley CH, Monaghan G, Clarke DJ (1998) The structure and function of the UDP-glucuronosyltransferase gene family. Advances in Pharmacology 42: 335–338
161. Cummings J, Zelcer N, Allen JD, Yao D, Boyd G, Maliepaard M, Friedberg TH, Smyth JF, Jodrell DI (2004) Glucuronidation as a mechanism of intrinsic drug resistance in colon cancer cells: contribution of drug transport proteins. Biochem Pharmacol 67: 31-39
162. Morimitsu Y, Nakagawa Y, Hayashi K, Fujii F, Kumagai T, Nakamura Y, Osawa T, Horio F, Itoh K, Lida K, Yamamoto M, Uchida K (2002) A sulforaphane analogue

that potently activates the Nrf2-dependent detoxification pathway. J Biol Chem 277: 3456-3463

163. Cho JM, Manandhar S, Lee HR, Park HM, Kwak MK (2008) Role of the Nrf2-antioxidant system in cytotoxicity mediated by anticancer cisplatin: implication to cancer cell resistance. Cancer Lett 260: 96-108
164. Ohta T, Iijima K, Miyamoto M, Nakahara I, Tanaka H, Ohtsuji M, Suzuki T, Kobayashi A, Yokota J, Sakiyama T, Shibata T, Yamamoto M, Hirohashi S (2008) Loss of Keap1 function activates Nrf2 and provides advantages for lung cancer cell growth. Cancer Res 68: 1303-1309
165. Ren D, Villeneuve NF, Jiang T, Wu T, Lau A, Toppin HA, Zhang DD (2011) Brusatol enhances the efficacy of chemotherapy by inhibiting the Nrf2-mediated defense mechanism, Proc Natl Acad Sci USA 108: 1433-1438
166. Shin BY, Jin SH, Cho IJ, Ki SH (2012) Nrf2-ARE pathway regulates induction of Sestrin-2 expression. Free Radical Bio Med 53: 834-841
167. Whitworth JM, Londoño-Joshib AI, Sellers JC, Oliver PJ, Muccio DD, Atigadda VR, Straughn Jr JM, Buchsbaum DJ (2012) The impact of novel retinoids in combination with platinum chemotherapy on ovarian cancer stem cells. Gynecol Oncol 125: 226-230
168. Arlt A, Sebens S, Krebs S, Geismann C, Grossmann M, Kruse ML, Schreiber S, Schäfer H (2013) Inhibition of the Nrf2 transcription factor by the alkaloid trigonelline renders pancreatic cancer cells more susceptible to apoptosis through decreased proteasomal gene expression and proteasome activity. Oncogene 32: 4825-4835
169. Wang XJ, Hayes JD, Henderson CJ, Wolf CR (2007) Identification of retinoic acid as an inhibitor of transcription factor Nrf2 through activation of retinoic acid receptor alpha. Proc Natl Acad Sci USA 104: 19589-19594
170. Maier T, Guell M, Serrano L (2009) Correlation of mRNA and protein in complex biological samples. FEBS Lett 583: 3966-3973
171. Tang Y, Chen Y, Jiang H, Nie D (2011) The role of short-chain fatty acids in orchestrating two types of programmed cell death in colon cancer. Autophagy 2: 235-237
172. Bindels LB, Porporato P, Dewulf EM, Verrax J, Neyrinck AM, Martin JC, Scott KP, Buc Calderon P, Feron O, Muccioli GG, Sonveaux P, Cani PD, Delzenne NM (2012) Gut microbiota-derived propionate reduces cancer cell proliferation in the liver. Brit J Cancer 107: 1337-1344
173. Thirunavukkarasan M, Wang C, Rao A, Hind T, Teo YR, Siddiquee AAM, Goghari MAI, Kumar AP, Herr DR (2017) Short-chain fatty acid receptors inhibit invasive phenotypes in breast cancer cells. PloS One 12: 1-16
174. Rayhman O, Klipper E, Muller L, Davidson B, Reich R, Meidan R (2008) Small interfering RNA molecules targeting endothelin-converting enzyme-1 inhibit endothelin-1 Synthesis and the Invasive phenotype of ovarian carcinoma cells. Cancer Res 68: 9265-9273
175. Xie X, Tang H, Liu P, Kong Y, Wu M, Xiao X, Yang L, Gao J, Wei W, Lee J, Bartholomeusz C, Ueno NT, Xie X (2015) Development of PEA-15 using a potent non-viral vector for therapeutic application in breast cancer. Cancer Lett 356: 374-381

Appendix

Appendix A: Relative p-ERK1 expression after cisplatin treatment in A2780 and A2780cis cells

A1: Relative expression of p-ERK1 in A2780 and A2780cis cells after treating with 5 µM cisplatin for 1 hour (h), 6 hours and 12 hours

	A2780				A2780cis		
	1 h	6 h	12 h		1 h	6 h	12 h
	1.742	5.917	3.667		0.730	1.074	1.466
	1.888	10.707	2.278		0.035	0.913	1.773
	2.100	6.733	2.969		1.324	1.091	1.274
		0.855	1.318			2.022	
		0.788	2.072			1.540	
						2.026	
Mean	1.910	5.000	2.460	Mean	1.030	1.440	1.500
SD	0.180	4.220	0.895	SD	0.297	0.495	0.252
SEM	0.104	1.890	0.400	SEM	0.172	0.202	0.145

A2: Relative expression of p-ERK1 in A2780 and A2780cis cells after treating with 10 µM cisplatin for 1 hour (h), 6 hours and 12 hours

	A2780				A2780cis	
	1 h	6 h	12 h	1 h	6 h	12 h
	2.710	7.891	2.423	0.521	0.278	0.625
	3.889	4.526	1.261	0.528	0.229	0.434
	3.535	5.856	2.459	0.757	0.366	0.374
		2.867			0.897	
		1.977			0.961	
					1.042	
					4.330	
					3.864	
Mean	3.380	4.620	2.050	0.602	1.500	0.478
SD	0.605	2.360	0.681	0.134	1.640	0.131
SEM	0.349	1.060	0.393	0.078	0.580	0.076

A3: Relative expression of p-ERK1 in A2780 and A2780cis cells after treating with 30 µM cisplatin for 1 hour (h), 6 hours and 12 hours

A2780				A2780cis			
	1 h	6 h	12 h		1 h	6 h	12 h
	2.569	1.688	6.268		0.722	3.364	3.737
	2.684	2.356	5.886		0.856	3.085	3.593
	2.515	2.399	5.453		0.852	4.402	3.673
		4.195				5.154	
		3.871				4.148	
		14.770					
		9.602					
Mean	2.590	5.550	5.870	Mean	0.810	4.030	3.670
SD	0.086	4.850	0.408	SD	0.076	0.830	0.072
SEM	0.050	1.830	0.235	SEM	0.044	0.371	0.042

A4: Relative expression of p-ERK1 in A2780 and A2780cis cells after treating with 60 µM cisplatin for 1 hour

	A2780		A2780cis
	1 h		1 h
	2.410		0.362
	2.895		0.656
	2.421		0.449
			1.584
			1.264
			1.609
Mean	2.580	Mean	0.987
SD	0.277	SD	0.567
SEM	0.160	SEM	0.232

Appendix B: Relative p-ERK2 expression after cisplatin treatment in A2780 and A2780cis cells

B1: Relative expression of p-ERK2 in A2780 and A2780cis cells after treating with 5 µM cisplatin for 1 hour (h), 6 hours and 12 hours

	A2780				A2780cis		
	1 h	6 h	12 h		1 h	6 h	12 h
	1.088	3.438	0.742		1.289	15.443	1.230
	1.172	5.350	0.434		1.993	6.427	1.464
	1.531	5.942	0.512		1.555	7.405	1.190
		0.460	0.295				
		0.499	0.223				
			0.311				
			0.152				
			0.232				
Mean	1.260	3.140	0.362	Mean	1.610	9.760	1.320
SD	0.235	2.600	9.192	SD	0.356	4.950	0.138
SEM	0.136	1.160	0.068	SEM	0.205	2.860	0.080

B2: Relative p-ERK2 in A2780 and A2780cis cells after treating with 10 µM cisplatin for 1 hour (h), 6 hours and 12 hours

	A2780				A2780cis		
	1 h	6 h	12 h		1 h	6 h	12 h
	1.652	4.511	3.946		1.089	2.349	0.295
	1.645	2.861	6.583		1.224	3.803	0.078
	1.145	3.337	5.722		1.031	4.731	0.029
		0.637	0.375			2.092	
		0.570	0.359			1.129	
			0.412				
			0.656				
			0.417				
			0.829				
Mean	1.480	2.780	2.140	Mean	1.110	2.820	0.134
SD	0.290	2.070	2.550	SD	0.099	1.430	0.142
SEM	0.168	0.925	0.850	SEM	0.057	0.641	0.082

B3: Relative expression of p-ERK2 in A2780 and A2780cis cells after treating with 30 µM cisplatin for 1 hour (h), 6 hours and 12 hours

	A2780				A2780cis		
	1 h	6 h	12 h		1 h	6 h	12 h
	1.373	1.658	0.346		1.755	3.698	2.765
	1.477	2.458	0.255		1.518	14.654	3.611
	1.313	2.286	0.533		2.043	4.084	4.519
		1.512	2.479			20.935	
		1.133	2.397			13.134	
		1.224	1.754				
		2.305					
		2.532					
Mean	1.390	1.890	1.290	Mean	1.770	11.300	3.630
SD	0.083	0.570	1.040	SD	0.263	7.370	0.877
SEM	0.048	0.202	0.424	SEM	0.152	3.300	0.506

B4: Relative expression of p-ERK2 in A2780 and A2780cis cells after treating with 60 µM cisplatin for 1 hour (h), 6 hours and 12 hours

	A2780				A2780cis		
	1 h	6 h	12 h		1 h	6 h	12 h
	2.079	1.929	3.918		7.274	3.281	1.174
	2.235	1.881	1.592		5.566	2.919	1.756
	2.562	2.786	1.065		8.988	3.319	1.010
		0.378	3.560			1.597	
		0.513	0.334			0.886	
			0.299				
Mean	2.290	1.500	1.800	Mean	7.280	2.400	1.310
SD	0.247	1.030	1.590	SD	1.710	1.100	0.392
SEM	0.142	0.459	0.651	SEM	0.988	0.491	0.226

Appendix C: Relative p-ERK1/2 expression upon MEK1/2 inhibitor (U0126) exposure in A2780 and A2780cis cells

Relative p-ERK1/2 expression in A2780 and A2780cis cells before and after MEK1/2 inhibition by 20 µM U0126 (U0126), 33.3 µM cisplatin treatment (Pt) and combination of U0126 and cisplatin (Pt + U0126) measured by densitometric analysis of Western blot

	Relative p-ERK1/2 expression			
	A2780			
	Control	U0126	Pt	U0126 + Pt
	0.582	0.152	1.033	0.236
	0.236	0.012	1.000	0.027
	0.339	0.019	1.229	0.071
Mean	0.386	0.061	1.087	0.112
SD	0.178	0.079	0.124	0.110
SEM	0.103	0.045	0.071	0.064
	A2780cis			
	0.388	0.283	1.033	0.379
	0.229	0.017	1.165	0.019
	0.259	0.015	1.137	0.008
Mean	0.292	0.105	1.110	0.135
SD	0.084	0.154	0.069	0.211
SEM	0.049	0.089	0.040	0.122

Appendix D: Cisplatin cytotoxicity upon combined treatment with cisplatin and U0126 in A2780 and A2780cis cells

Individual pEC_{50} values for cisplatin (Pt) cytotoxicity in A2780 and A2780cis cells without and with co-treatment with 20 µM U0126 (Pt + U0126) (results of individual testing)

	A2780		A2780cis	
	Pt	Pt + U0126	Pt	Pt + U0126
	5.904	5.672	5.051	4.679
	5.910	5.716	5.020	4.651
	5.947	5.674	5.057	4.698
	6.156	5.140	5.079	4.618
	6.142	5.116	5.033	4.631
	6.107	5.170	5.046	4.636
Mean	6.030	5.410	5.050	4.650
SD	0.120	0.300	0.020	0.031
SEM	0.049	0.122	0.008	0.013

Appendix E: Relative p-ERK1/2 expression upon MEK1/2 inhibitor (U0126) exposure in SKOV-3 cells

Relative p-ERK1/2 expression in SKOV-3 cells before (control) and after MEK1/2 inhibition by 20 µM U0126 (U0126), 33.3 µM cisplatin treatment (Pt) and combination of U0126 and cisplatin (Pt + U0126), measured by densitometric analysis of Western blot

	Relative p-ERK1/2 expression			
SKOV-3	Control	U0126	Pt + U0126	Pt + U0126
	0.190	0.305	1.067	0.090
	0.121	0.006	1.000	0.015
	0.386	0.026	2.870	0.017
Mean	0.232	0.113	1.650	0.041
SD	0.137	0.167	1.060	0.043
SEM	0.079	0.097	0.613	0.025

Appendix F: Cytotoxicity of cisplatin and combination of cisplatin and U0126 in SKOV-3 cells

Individual pEC_{50} values for cisplatin cytotoxicity in SKOV-3 cells without (Pt) and with co-treatment with 20 µM U0126 (Pt + U0126) (results of individual testing)

SKOV-3		
	Pt	Pt + U0126
	5.525	4.618
	5.535	4.678
	5.563	4.767
	5.567	4.825
	5.533	4.847
	5.527	4.800
	5.515	4.768
	5.506	4.765
	5.539	4.697
	5.543	4.744
	5.491	4.632
	5.499	4.724
Mean	5.530	4.74
SD	0.023	0.072
SEM	0.007	0.021

Appendix G: Relative CTR1 expression upon U0126 exposure in SKOV-3 cells

Relative CTR1 expression in SKOV-3 cells before and after treatment with 20 µM U0126 (U0126) in SKOV-3 cells

	CTR1 expression	
SKOV-3	Control	U0126
	0.659	0.624
	1.708	0.745
	1.000	0.735
	1.000	0.625
Mean	1.090	0.682
SD	0.441	0.067
SEM	0.221	0.033

Appendix H: Relative ERK1 expression after ERK1 knockdown in A2780 and A2780cis cells

Relative ERK1 expression in A2780 and A2780cis cells after negative knockdown and knockdown with ERK1 siRNA

	A2780		A2780cis	
	Negative knockdown	ERK1 knockdown	Negative knockdown	ERK1 knockdown
	1.064	0.797	1.085	0.393
	1.000	0.509	1.009	0.219
	0.634	1.069	1.000	0.584
		0.308		0.277
Mean	0.899	0.671	1.031	0.368
SD	0.232	0.333	0.047	0.161
SEM	0.134	0.167	0.027	0.081

Appendix I: Cisplatin cytotoxicity after ERK1 knockdown in A2780 and A2780cis cells

pEC_{50} values for cisplatin cytotoxicity in A2780 and A2780cis cells after knockdown of ERK1 and negative knockdown (results of individual experiments)

	A2780		A2780cis	
	Negative knockdown	ERK1 knockdown	Negative knockdown	ERK1 knockdown
	5.545	5.732	4.817	4.276
	5.619	5.595	4.781	4.625
	5.565	5.475	4.791	4.572
Mean	5.576	5.601	4.796	4.491
SD	0.038	0.129	0.019	0.188
SEM	0.022	0.074	0.011	0.109

Appendix J: Relative ERK2 expression after ERK2 knockdown in A2780 and A2780cis cells

Relative ERK2 expression in A2780 and A2780cis cells after negative knockdown and knockdown with ERK2 siRNA

	A2780		A2780cis	
	Negative knockdown	ERK2 knockdown	Negative knockdown	ERK2 knockdown
	0.943	0.384	1.287	0.227
	0.778	0.306	1.120	0.170
	0.771	0.341	0.888	0.220
	0.577	0.493	1.727	0.151
	1.111	0.204	1.312	0.223
	0.730	0.171	1.523	0.314
	0.439	0.260	0.780	0.640
	0.437	0.376	0.676	0.802
	0.361	0.195	1.001	0.586
	1.395	0.210	1.016	0.360
	1.151	0.233	1.159	0.452
	0.926	0.128		0.488
Mean	0.802	0.275	1.136	0.386
SD	0.319	0.107	0.314	0.209
SEM	0.092	0.031	0.095	0.060

Appendix K: Cisplatin cytotoxicity after ERK2 knockdown in A2780 and A2780cis cells

pEC_{50} values for cisplatin cytotoxicity in A2780 and A2780cis cells after knockdown of ERK2 and negative knockdown (results of individual experiments)

	A2780		A2780cis	
	Negative knockdown	ERK2 knockdown	Negative knockdown	ERK2 knockdown
	5.977	6.033	5.000	4.979
	6.146	6.119	5.009	4.961
	6.118	6.194	5.006	4.986
	5.987	6.074	4.996	4.978
	6.019	6.076	5.000	4.998
	6.137	6.072	4.975	5.012
	6.103	5.883	5.018	4.975
	6.105	5.903	5.018	4.941
	6.108	5.865	5.029	5.000
	6.098	5.947	5.013	4.975
	6.097	5.963	5.024	4.981
	6.117	5.982	5.040	4.947
	6.127	6.161	5.030	5.025
	6.073	6.286		5.014
	6.165	6.049		5.028
	6.222	6.111		5.034
	6.214	6.180		4.998
	6.185	6.083		
Mean	6.111	6.055	5.014	4.978
SD	0.067	0.115	0.016	0.021
SEM	0.016	0.027	0.004	0.006

Appendix L: Relative PEA-15 expression after PEA-15 knockdown in SKOV-3 cells

PEA-15 expression in SKOV-3 cells after negative knockdown and knockdown with PEA-15 siRNA

SKOV-3	PEA-15 expression	
	Negative knockdown	PEA-15 knockdown
	0.720	0.490
	1.857	0.187
	1.019	0.929
	0.707	0.230
	1.358	0.056
	1.387	0.076
		0.019
		0.356
		0.046
Mean	1.170	0.266
SD	0.446	0.295
SEM	0.182	0.098

Appendix M: Cisplatin cytotoxicity after PEA-15 knockdown in SKOV-3 cells

Individual pEC_{50} values for cisplatin cytotoxicity in SKOV-3 cells with negative knockdown and with PEA-15 knockdown (results of individual testing)

SKOV-3	Negative knockdown	PEA-15 knockdown
	4.730	4.893
	4.775	4.966
	4.694	4.856
	4.756	4.921
Mean	4.740	4.910
SD	0.035	0.046
SEM	0.017	0.023

Appendix N: Cisplatin cytotoxicity after overexpression of PEA-15AA, PEA-15DD and empty vector

Individual pEC_{50} values for cisplatin cytotoxicity in Empty vector (EV), PEA-15AA and PEA-15DD overexpressed SKOV-3 cells (results of individual testing)

SKOV-3	EV	PEA-15AA	PEA-15DD
	4.752	4.869	4.775
	4.887	4.968	4.903
	4.840	5.053	4.773
	4.817	5.076	4.800
	4.826	5.033	4.803
	4.918	4.988	4.853
	4.763	5.033	4.960
	4.813	4.998	4.891
Mean	4.830	5.000	4.840
SD	0.056	0.065	0.069
SEM	0.020	0.023	0.024

Appendix O: Relative UGT1A expression in empty vector, PEA-15AA and PEA-15DD transfected SKOV-3 cells

Relative UGT1A expression in empty vector(EV), PEA-15AA(AA) and PEA-15DD (DD) transfected SKOV-3 cells before and after cisplatin (Pt) treatment (15 μM, 24 hours)

SKOV-3	UGT1A expression					
	EV	AA	DD	EV + Pt	AA + Pt	DD + Pt
	0.867	0.889	1.010	0.672	0.380	0.341
	0.914	1.098	0.728	0.353	0.209	0.482
	1.086	1.115	1.000	0.570	0.610	0.499
Mean	0.956	1.030	0.912	0.532	0.400	0.441
SD	0.116	0.126	0.160	0.163	0.201	0.087
SEM	0.067	0.073	0.093	0.094	0.116	0.050

Appendix P: Relative UGT1A expression in empty vector, PEA-15AA and PEA-15DD transfected SKOV-3 cells upon exposure to cisplatin

Relative GNB1 expression in empty vector (EV), PEA-15AA (AA) and PEA-15DD (DD) transfected SKOV-3 cells before and after cisplatin (Pt) treatment (15 μM, 24 hours)

SKOV-3	GNB1 expression					
	EV	AA	DD	EV + Pt	AA + Pt	DD + Pt
	0.735	0.825	0.798	0.784	1.138	1.199
	1.088	1.014	0.985	0.959	0.918	0.842
	0.992	1.042	1.106	0.992	1.058	1.079
Mean	0.938	0.960	0.963	0.912	1.040	1.040
SD	0.183	0.118	0.155	0.112	0.112	0.182
SEM	0.106	0.068	0.090	0.065	0.064	0.105

Appendix Q: Relative Nrf2 expression in empty vector, PEA-15AA and PEA-15DD transfected SKOV-3 cells upon exposure to cisplatin

Relative Nrf2 expression in empty vector (EV), PEA-15AA (AA) and PEA-15DD (DD) transfected SKOV-3 cells before and after cisplatin (Pt) treatment (15 µM, 24 hours)

SKOV-3	Nrf2 expression					
	EV	AA	DD	EV + Pt	AA + Pt	DD + Pt
	0.719	1.072	1.163	0.525	0.885	0.822
	0.983	0.740	0.829	0.850	1.119	0.899
	1.014	1.162	1.197	0.839	0.890	0.898
Mean	0.905	0.991	1.060	0.738	0.965	0.873
SD	0.162	0.223	0.203	0.184	0.134	0.044
SEM	0.094	0.129	0.117	0.106	0.077	0.025

Appendix R: Relative Nrf2 expression in SKOV-3 cells upon exposure to cisplatin and retinoic acid

Relative Nrf2 expression in control SKOV-3 cells, SKOV-3 cells treated with 15 µM cisplatin (Pt), 20 µM retinoic acid (RA), and combination of cisplatin and retinoic acid (Pt + RA) for 24 hours

SKOV-3	Nrf2 expression			
	Control	Pt	RA	Pt + RA
	0.790	0.718	0.641	0.617
	0.471	0.554	0.942	0.539
	0.935	1.072	0.931	0.656
	0.643	0.709	1.000	0.872
	0.427	0.699	1.046	1.021
Mean	0.653	0.750	0.912	0.741
SD	0.214	0.192	0.158	0.199
SEM	0.096	0.086	0.071	0.089

Appendix S: Relative UGT1A expression in SKOV-3 cells upon exposure to cisplatin and retinoic acid

Relative UGT1A expression in control SKOV-3 cells, SKOV-3 cells treated with 15 µM cisplatin (Pt), 20 µM retinoic acid (RA), and combination of cisplatin and retinoic acid (Pt + RA) for 24 hours

SKOV-3	UGT1A expression			
	Control	Pt	RA	Pt + RA
	0.803	0.764	0.730	0.528
	0.911	0.979	0.541	0.529
	1.221	1.098	0.790	0.628
	1.327	1.088	0.800	1.000
	1.013	1.071	0.771	0.918
	1.292	0.981	0.628	0.436
Mean	1.090	0.997	0.710	0.673
SD	0.217	0.126	0.104	0.231
SEM	0.088	0.051	0.042	0.094

Appendix T: Cisplatin cytotoxicity upon exposure to cisplatin, and combination of cisplatin and retinoic acid

Cytotoxicity (pEC_{50} values) of cisplatin alone (Pt), and upon co-incubation with 20 µM retinoic acid (Pt + RA) (results of individual experiments)

	SKOV-3	
	Pt	Pt + RA
	4.364	4.821
	4.315	4.838
	4.408	4.747
	4.163	4.763
	4.518	4.891
	4.580	4.923
	4.658	4.748
	4.595	5.020
	4.783	5.028
		4.773
Mean	4.487	4.855
SD	0.192	0.107
SEM	0.064	0.034